SURFACE INTERACTIONS BETWEEN BITUMEN AND MINERAL FILLERS AND THEIR EFFECTS ON THE RHEOLOGY OF BITUMEN-FILLER MASTICS

Richard Taylor, BSc (Hons)

Thesis submitted to the University of Nottingham

for the degree of Doctor of Philosophy

July 2007

ABSTRACT

A study has been carried out of the rheological behaviour of ten fillers in three different bitumen types. The fillers were laboratory manufactured from clean single-sized aggregates and were grouped according to their broad petrologic type. Five of the fillers were produced from aggregates, which had calcium carbonate as the principal mineral, and five fillers were manufactured from aggregates that contained significant quantities of silica. The bitumens chosen for the study were 40/60 penetration grade and 10/20 penetration grade bitmens manufactured from a Venezuelan crude source and a synthetic polymer-modified resin.

An extensive characterisation of the fillers was undertaken to account for particle size distribution, particle shape, bulk volume, surface area (by laser diffraction and BET method) and surface energy measured employing a Dynamic Vapour Sorption technique. The bitumens where rheologically characterised using standard penetration and softening point tests and more complex creep compliance testing using a Dynamic Shear Rheometer. Additionally, the bitumens in the study were characterised for surface energy using a Sessile Drop technique allowing calculations of the bond energy, $\Delta G_{12,}$ to be made for the bitumen-filler combinations.

A series of rheological tests were carried out on mastics produced using combinations of the bitumens and fillers, commencing with simple Delta Ring and Ball tests and leading to creep compliance testing of mastics over a range of solid volume fractions (φ). The relative creep compliance was derived for each of the mastics using the ratio of the creep compliance of the pure bitumen to the creep compliance of the mastic.

The maximum packing fraction (φ_{max}) was determined for each bitumen-filler combination using a simple two-point projection technique based on the reciprocal relative creep compliance. Three rheological models, those originally proposed by Krieger & Dougherty, Mooney and Chong were examined and the applicability of such models to describe the behaviour of bitumen-filler mastics was assessed. The intrinsic viscosity of each filler type was derived in each bitumen type and this in turn compared to the index properties obtained during the classification of the materials. The most appropriate model found to describe the rheological behaviour of bitumen-filler mastics was the Krieger-Dougherty model.

The product of intrinsic viscosity and maximum packing fraction in the Krieger-Dougherty equation is reported as having a value of 2 and is referred to as the Marron-Pirece-Kitano (MPK) Coefficient. The MPK Coefficient describes the stiffening effects in the mastic in addition to the bulk volume filling relationship, φ/φ_{max}.

For each mastic, the MPK Coefficient was derived and compared with the bond energy of the mastics, $\Delta G_{12,}$ calculated based on the surface energy determinations of the fillers and bitumens. The bond energy of the mastics was found to relate closely to the MPK Coefficient for the majority of the combinations examined. Additionally, bond energy (a physio-chemical property of the mastics) of the bitumen-filler combinations for the fillers containing a proportion of silica was found to relate to the maximum packing fraction in addition to the MPK Coefficient. Conversely, the bond energy of the calcium carbonate based mastics related only to the intrinsic viscosity and not to the maximum packing fraction, highlighting an important insight into significant differences between the behaviour of calcium carbonate in bitumen and silica based aggregates.

ACKNOWLEDGEMENTS

I would like to thank everyone involved in giving his or her time and resources to this work. In particular, I would like to thank Lafarge Aggregates (UK), Lafarge Laboratories Central De Recherché (Lyon, France) and Shell Bitumen for their support during this work, and Dr Gordon Airey who has supervised my work over the last few years.

I am very grateful to Mr Benedict Duggan and M. Nicolas Richard of Lafarge for their technical support during my studies and to Mr Robert Gossling and M. Bruno Espinosa for their financial support and encouragement.

Finally, the biggest thanks go to my wife for all of the times I have locked my self away and left her to tend to the children, and for all of the times when I have not listened to a single word she has said to me because I had been thinking about fillers and bitumen.

Page

CONTENTS

LIST OF FIGURES

LIST OF TABLES

CHAPTER I

INTRODUCTION

BACKGROUND

Fillers modify the properties, increase the performance of, and provide improved durability to composites, polymers, rubbers, adhesives, coatings and construction materials (such as concrete and asphalt). Fillers are used to lower the cost of materials, increase rigidity and give special properties to a material (such as colour or fire retardancy). The filler properties have considerable effects on the processing characteristics of materials such as mixing, pumping and compacting. The effects of fillers are therefore of vital importance.

Fillers are typically fine powders with a particle size distribution in the range of 0-100µm. They can be naturally occurring materials such as calcium carbonate, manufactured fillers for example carbon black, or derived from industrial wastes such as fly ash from power stations. Other common fillers include silica, kaolin ("China Clay"), mica, feldspar and diatomite.

Filler can be defined as *"solid material capable of changing the physical and chemical properties of materials by surface interaction or its lack thereof and by its own physical characteristics"*. A comprehensive list of definitions can be found elsewhere (Wypych, 1999).

The above definition implies the existence of two ways in which fillers modify a system. Firstly, the ways in which the filler's shape, particle size and particle size distribution affect the system through filling of the liquid with solid particles. Secondly, the way in which interactions between the solid and liquid phases of the mixture affects the material. The second interactions can vary from strong chemical bonds or physical interactions leading to strongly reinforced materials, to almost no interaction at all.

Asphalt is an essential construction material. The majority of roads are constructed or surfaced with asphalt. In 2003, close to 300 million tonnes of asphalt were produced in Europe and 500 million tonnes in the United States (EAPA, 2004). As an engineering material, asphalt is typically designed to provide stiffness and bearing capacity, and resist the repeated loading experienced by a pavement under traffic. The effect of repeated loading manifests itself in two ways, permanent deformation, commonly referred to as "rutting", and "cracking" through fatigue of the asphalt.

Asphalt is a material comprised of three principal components; aggregate, bitumen and filler. The different ratios between these components gives rise to a family of asphalt mixtures with different properties. Asphalts typically include a proportion of air, which is often considered as the fourth component. Minimizing the quantity of air through proper mixture design and adequate compaction during placement of the asphalt is essential for ensuring a durable product. Additionally, too little air, as a result of overfilling the aggregate structure, can lead to rutting.

The most frequently used filler in asphalt is limestone (calcium carbonate), which is derived from the consolidation of minute micro-organisms during the formation of the earth's crust. Limestone is the general term for rocks where calcite, a form of calcium carbonate, is

the predominant mineral. Limestone may also contain a proportion of magnesium carbonate, silica, clays, iron oxides and organic material.

Other materials commonly used as fillers in asphalt include Portland Cement and hydrated lime, which possesses well documented properties with regard to mixture durability and increased resistance to moisture damage in asphalt (Little and Epps, 2001). Additionally, recycled fillers in the form of so-called "baghouse" fines have also been frequently used in asphalt. The performance of baghouse fines was the subject of several key studies on the behaviour of fillers in asphalt following changes in the Clean Air Act 1970 in the United States. (Kandhal, 1980; Anderson et al., 1982)

When bitumen is combined with mineral filler, a mastic is formed. This mastic can be viewed as the component of the asphalt mixture that binds the aggregates together and also the component of the asphalt that undergoes deformation when the pavement is stressed under traffic loading. The characteristics of the filler can significantly influence the properties of the mastic, and thus the filler properties can have significant effects on asphalt mixture performance.

The importance of fillers, and the resulting mastics, has been studied for a century (Richardson, 1907). Arguably, the key advance in the understanding of asphalt fillers was made shortly after the Second World War when researchers in the UK (Rigden, 1947) proposed that the volume of fixed bitumen that a filler could accommodate in its compacted state influenced the stiffening behaviour of fillers in mastics. Rigden also proposed that the volume of "fixed bitumen" that the system could accommodate scaled the effects of a given volume of filler. Since that time, several other researchers have found Rigden's approach reasonably successful in predicting the stiffening effect of various filler types in a given

bitumen type (Heukelom and Wijga, 1971; Kandhal, 1980; Anderson et al., 1992a, 1992b; Kavussi and Hicks, 1997; Kandhal et al., 1998; Cooley et al., 1998).

Mastics can be considered as suspensions of solid filler particles in a liquid, bitumen. A model to describe the rheological behaviour of dilute solid in liquid suspensions was first proposed over a century ago (Einstein, 1906). Relative viscosity (η_{rel}) describes the increase in viscosity of the suspension as a ratio to the viscosity of the liquid phase. The Einstein model predicts a linear change in relative viscosity with regard to increases in solid concentration (φ). As solid volume fraction increases, the magnitude of the surface area and particle-particle contacts increase and effects in addition to simple volume filling become more prevalent.

Thus, in reality, increasing additions of solid particles leads to exponentially increasing relative viscosity. The solid volume fraction at the asymptote of this exponential increase is termed the *maximum packing fraction* (φ_{max}) and alongside relative viscosity, is a key term used in modelling and understanding the behaviour of suspensions. In line with Rigden's observations relating to voids within compacted filler, the effects of solid volume on viscosity are scaled by φ_{max} and this ratio is an important variable controlling the rheology of suspensions. Later models developed to describe the behaviour of suspensions (Mooney, 1957; Krieger and Dougherty, 1959; Chong, 1971) include the term φ/φ_{max} and predict exponentially increasing stiffening as the solid volume fraction, φ, approaches φ_{max}. At low filler concentrations, such models tend to reduce to the Einstein equation (Barnes, 2000).

A further variable featured in rheological models used to describe the behaviour of suspensions is *intrinsic viscosity*, $[\eta]$, of the filler. Intrinsic viscosity is not a true viscosity but represents the level of interaction between the solid particles and the liquid at a

theoretical concentration of zero. Einstein calculated the intrinsic viscosity of spheres to be 2.5 (dimensionless), which is sometimes referred to, in the context of suspensions, as the Einstein Coefficient.

Intrinsic viscosity is typically attributed to shape, but encompasses effects experienced by the suspension additional to the bulk filling relationship of φ/φ_{max}. Interaction at the solid liquid interface would be included in the term intrinsic viscosity according to the models used to describe the rheology of suspensions.

The product of intrinsic viscosity and maximum packing fraction found in the Krieger-Dougherty Equation is reported as being close to the value of 2 for a variety of filled systems (Kitano et al., 1981; Barnes, 2000) and this coefficient is referred to as the Marron-Pierce-Kitano Coefficient (MPK). (Kitano et al., 1981; Rides, 2005)

For asphalt-filler mastics the typical approach to research has been to consider the change in penetration, softening point or viscosity of the bitumen (Heukelom and Wijga, 1971; Anderson et al., 1982; Kandhal, 1980, 1998). Later researchers have examined change in complex modulus of bitumen when adding different filler types to a single bitumen type (Cooley et al., 1998; Harris and Stuart, 1998). These types of measurements, for example relative complex modulus, are akin to the relative viscosity component of rheological models used to describe the behaviour of suspensions.

For asphalt fillers, the relative viscosity, or related term, has been compared to several index properties of fillers, typically particle size distribution, particle shape, surface activity and the void content of filler in its compacted state. Most researchers have found that the voids in the compacted filler is the property of the filler most suited to predicting the relative viscosity (or other relative rheological measures) of bitumen-filler mastics (Heukelom and

Wijga, 1971; Kandhal, 1980; Anderson et al., 1992a, 1992b; Kavussi and Hicks, 1997; Kandhal et al., 1998; Cooley et al., 1998;). As the maximum packing fraction is related to the voids in the compacted filler and the effects of solid volume fraction, as proposed in the rheological models outlined previously are scaled by the maximum packing fraction, this conclusion appears reasonable.

Several researchers have noted however that different fillers stiffen different bitumen types to a different extent (Dukatz and Anderson, 1980; Anderson et al., 1982; Shashidar and Romero, 1998) and this has been a limitation to the approach of measuring the filler properties in air. Extreme cases have been noted such as hydrated lime where stiffening massively exceeds the potential estimated by voids in the mineral filler (Shashidar and Romero 1998).

Crucially, voids in the compacted filler are measured in air and do not account for interactions between the bitumen and the filler in the mastic. Interactions of fillers in different bitumen types may lead to changes in different ways. For example φ_{max} may differ in different bitumens as a result of different levels of dispersion of the filler, or alternatively the filler may cause changes in the viscosity of the liquid phase as a result of restructuring, physio-chemical changes or other such effects.

Differences in the level of interaction between filler and bitumen can be quantified using a surface free energy approach. The free energy of adhesion between two materials, such as between filler and bitumen, is given by the Dupré equation (Dupré, 1869).

$$\Delta G_{12} = \gamma_{12} - \gamma_1 - \gamma_2 \quad (1)$$

Where

ΔG_{12} is the free energy of adhesion,

γ is the surface energy (or surface tension) of materials 1 and 2, and

γ_{12} is the free energy of interaction between materials 1 and 2.

In the case of bitumen-filler mastics, γ_1 represents the surface free energy of the filler, γ_2 represents the surface free energy of the bitumen and γ_{12} represents the free energy of adhesion between the bitumen and the filler.

In recent years there has been a significant interest in the measurement and use of surface energy characteristics of the components used in asphalt (Cheng, 2002; Hefer, 2004; Bhasin, 2006). Such techniques allow for the calculation of the adhesive energy between two or more materials using the Dupré equation, and this approach has been used to quantity the level of bond between aggregate and bitumen and additionally the likelihood of the retention of this bond in the presence of water using a three component system – aggregate, bitumen and water.

In summary, the importance of bitumen-filler mastics has been known for over a century and several studies have been carried out with the intention of describing the characteristics of the fillers which best describe the behaviour of the resulting mastics. Voids in the filler in its compacted state, referred to as “Rigden Voids”, has consistently been found to be the best single property of the filler which relates to the increase in stiffness, or reduction in flow, of the mastic when filler is added.

Rheological models have been used to describe the behaviour of solid particles in a liquid since the early part of the twentieth century and Einstein's model of 1906. Later models include the term maximum packing fraction, which relates closely to Rigden Voids. Rigden Voids are measured in air and do not account for the interaction between the filler and the bitumen. Researchers have noted that fillers stiffen different bitumens to different extents and that the level of interaction between the two phases is important. In rheological models, this property would be captured in the term "intrinsic viscosity" and the MPK Coefficient (the product of maximum packing fraction and intrinsic viscosity), which describe the effects on the suspension in addition to those of the simple volume filling relationship φ/φ_{max}.

There has been a significant interest in characterisation of surface energy of materials used to produce asphalt and several methods have been adapted to measure surface energy of aggregates, fillers and bitumens. Knowledge of the surface energy of the bitumen and the filler enables the level of adhesion between the two phases to be quantified. This knowledge has not been applied to the understanding of the rheological behaviour of bitumen-filler mastics.

PROBLEM STATEMENT

Bitumen-filler mastics make an important contribution to the overall behaviour of asphalt mixtures. Although this has long been recognized by researchers in the field of asphalt technology, developments in the characterization of bitumen-filler mastics has tended to focus on increasingly sophisticated evaluation of the fillers, and the relative rheological measurement employed. For example, surface area by gas sorption (Anderson, 1992b) and laser diffraction (Harris and Stuart, 1998) have replaced air permeability techniques (Kandhal, 1980) for measuring of surface area whilst change in complex modulus of bitumen, measured by Dynamic Shear Rheometer (DSR) has replaced change in penetration or softening point as the relative rheological measure used to describe the stiffening of the mastics (Cooley et al., 1998; Harris and Stuart, 1998)

Despite the increase in sophistication of measurement, the same technique is typically employed, a set of fillers with varying properties, are examined in a single bitumen and properties of the mastic are related to index properties of the filler. This approach leads invariably to the conclusion that the effects of stiffening are primarily a result of the ratio between the solid volume fraction and the maximum packing fraction, with the voids in compacted filler being used as a proxy for the maximum packing fraction (Rigden 1947, 1954; Craus et al. 1978, 1981; Ishai et al., 1980).

Although several researchers have commented on the importance of surface interactions in bitumen-filler mastics (Anderson and Goetz, 1973; Anderson et al. 1982; Craus et al. 1978, 1981; Ishai et al., 1980) these effects have not been dealt with in isolation from the bulk filling effects associated with the magnitude of the maximum packing fraction. The extent to which the surface interactions between the filler and the bitumen affect the overall level of stiffening of the bitumen-filler mastic is therefore not clear.

In order to examine this effect, a suitable model to describe the rheological behaviour of the mastic is required which allows a separation between the solid filling relation and other effects. Following the selection of an appropriate model, the importance of the surface effects can be assessed.

RESEARCH SCOPE AND OBJECTIVE

This thesis is intended to examine the effects of bitumen-filler interactions on the rheological characteristics of mastics. In order to examine these effects it is first necessary to choose an appropriate model to describe the rheological behaviour of the mastics in order to separate the bulk filling effects from the other effects at work, such as shape and solid-liquid interaction.

To this end it was necessary to:

- Characterise the fillers and bitumens used in the study, in particular the measurement of surface energy and the use of this data to calculate the level of interaction between fillers and the bitumen of the mastics.
- Devise an experimental programme to determine the rheological properties of mastics produced with various combinations of bitumens and fillers, including the determination of maximum packing fraction of filler in different bitumen types.
- Choose an appropriate model to describe the rheological behaviour of the mastics.
- Determine the extent to which physio-chemical interactions between bitumen and filler affect the mastic properties.

ORGANISATION OF THE DISSERTATION

This dissertation is organised into seven chapters. Chapter I has provided a background to research on bitumen-filler mastics, and describes the problem statement, scope and objectives of the study. Chapter II reviews the available literature relating to the characterisation of fillers and their role in the behaviour of bitumen and asphalt mixtures. Chapter III describes the manufacture and characterisation of the fillers used in this study and describes the experimental plan developed.

Chapter IV provides an overview of the testing carried out on the mastics and reviews the test results obtained. The term relative creep compliance is introduced and discussed and the maximum packing fraction is derived for the mastic using a two-point projection technique. Chapter V discusses the applicability of rheological models to the bitumen-filler mixtures outlined in Chapter VI and the intrinsic viscosity and MPK Coefficient derived for bitumen-filler mastics.

Chapter VI proposes a relationship between the non-solid volume filling effects and the bond energy between the bitumen and fillers in the mastic. Finally, Chapter VII provides the conclusion of this research and makes recommendations for future research.

CHAPTER II

REVIEW OF LITERATURE

ASPHALT PAVEMENTS

General

Asphalt is an essential construction material. The majority of roads are constructed or surfaced with asphalt. In 2003, close to 300 million tonnes of asphalt were produced in Europe and 500 million tonnes in the United States (EAPA, 2004). As an engineering material, asphalt is typically designed to provide stiffness and bearing capacity, and resist repeated loading as experienced by a road under traffic. The effect of repeated loading manifests itself in two ways; permanent deformation, commonly referred to as "rutting", and "cracking", as a result of fatigue.

Additionally, asphalt mixtures are designed to minimise the effects of water on the system by either making the mixture dense and relatively impenetrable to moisture, for example in the case of asphaltic concrete, or by adding sufficient bitumen to the mixture to provide a thick coating of bitumen on the aggregates (referred to as "bitumen film thickness") as in the case of porous asphalt and thin wearing course mixtures.

Road pavements are typically constructed in layers, with each layer of the pavement fulfilling a slightly different function. The surface layers of the road are subjected to the highest stresses in the pavement as they are in direct contact with vehicle tyres, and additionally the surface is exposed to the elements which results in the surface of the pavement reaching the highest temperatures and are subject to the highest stresses.

Typically surfacing layers are made from the highest quality components and require excellent resistance to permanent deformation. This uppermost layer of the pavement provides the running surface for the vehicles, hence, ride quality and skid resistance are key properties of this layer.

Below the surfacing layer is the main structural layer(s) of the road. This layer, referred to simply as the "base", is designed to spread the vehicle loading to a level that can be withstood by the platform of the road pavement, which is typically constructed of unbound aggregates or consists of the naturally occurring ground conditions.

Asphalt is a material comprised of three principal components; aggregate, bitumen and filler. Air is also present in asphalt mixtures to varying extents. The different ratios between these components gives rise to a family of asphalt mixtures with different properties. Very, broadly speaking there are four types of asphalt mixtures used in road construction:

- "Asphaltic Concrete", referred to in the UK as "Macadam", has a maximum aggregate particle size of around 30mm and a continuous particle size distribution (a wide range of particle sizes, well distributed). Asphaltic Concrete is typically used for the structural base layers of a road, although they are also used for the surfacing layers.
- "Stone Mastic Asphalt" (SMA) or "Thin Wearing Courses" (TWC), have very high quantities of aggregate larger than 2mm in size (circa 75% by mass). These types of material are typically used for the surfacing of the pavement.

- "Hot Rolled Asphalt" (HRA) was used extensively in the UK for several decades but usage has reduced dramatically in recent years due to introduction of "Stone Mastic Asphalt" type materials referred to above. SMA type materials provide superior resistance to permanent deformation and lower noise under traffic due to the high coarse aggregate content. HRA is typically used for the surfacing of a road but can also be used for the base layers. The coarse aggregate content of HRA can vary according to the application, but for surfacing layers, around 30% of the aggregate is greater than 2mm in size. This makes HRA the inverse, in terms of particle size distribution, of SMA type mixtures.
- "Porous Asphalt" is a surfacing material designed to achieve a high air void content to allow water to pass through the material and reduce spray under trafficking. The high void content is achieved by limiting the amount of fine aggregate in the mixture. Typically, the air void content of porous asphalt is around 20%.

A summary of the typical components of the four main groups of asphalt is given in Table 2-1 below.

Table 2-1: The main types of asphalt mixtures used in road pavements and a summary of their components.

Mixture Type	Coarse Aggregate PSD type/ %>2mm particle size	Bitumen Content by mass (%)	Filler Content by mass (%)	Air content (%)
Aspaltic Concrete	Continuous, 65%	4-5	2-10	3-6
Stone Mastic Asphalt	Discontinuous, 75%	5-6	6-8	2-6
Hot Rolled Asphalt	Discontinuous, 35-50%	7-8	10-12	2-6
Porous Asphalt	Single size, 90%	4-5	2-4	18-25

Principal components in asphalts

As stated previously asphalt is composed of three principle constituents; aggregates, bitumen and filler. Each component will be discussed in turn.

Aggregates

Aggregate is the term used to describe mineral materials such as gravel, sand and crushed rock. Simplistically, aggregates can be considered as the solid particles in an asphalt mixture. Aggregates provide a structural skeleton to asphalt mixtures and it is this structure that provides mechanical strength to the asphalt. Additionally, because the aggregate constitutes the solid surface of the asphalt mixture, and this surface largely governs the durability of the mixture in the presence of water, aggregate type is very important when considering the durability of asphalt mixtures (Cheng, 2002; Hefer 2004; Choi, 2005; Bhasin, 2006)

An aggregate for use in asphalt needs to possess several fundamental properties:

- Hardness, toughness
- Resistance to abrasion
- Resistance to polishing to provide skidding resistance (for surface aggregates)
- Durability with regard to frost action and de-icing salts used on road surfaces
- Good affinity to bitumen

The requirements for aggregates and the test methods used to characterize aggregates used in asphalt have been standardised in Europe (BS EN 13043, 2002). Aggregates commonly used in asphalt include limestone, granites, amphibolites, diorites, basalt and gneiss. Additionally, recycled aggregates such as crushed glass and secondary aggregates, such as slag from iron or steel production, are also commonly used.

Bitumen

Bitumen is defined in the Oxford English Dictionary as "a tar-like mixture of hydrocarbons derived from petroleum naturally or by distillation". Bitumen acts as a binder in asphalt and binds, or "cements", the aggregate particles together. There are several types of bitumen and the rheological properties of the bitumen reflect:

- the source of the bitumen (the type of crude from which the bitumen is manufactured)
- the manufacturing process of the bitumen
- the addition of polymers or additives

Bitumen is a complex mixture of components and as a result, bitumen is considered a material with a complex response to stress. The response of a bitumen to stress is dependent on both loading time (frequency) and temperature, and it is this behaviour which characterises the mechanical behaviour of asphalt mixtures (Read and Whiteoak, 2003).

In order to discuss the rheological behaviour of bitumen it is necessary to first briefly discuss the rheology of liquids. Rheology describes the interrelation between force, deformation (flow) and time. Flow is typically described in two forms, *shear flow* and *extensional flow* (see Figure 2-1). In shear flow the molecules within a liquid can be considered as flowing over and past each other, whereas in extensional flow the molecules can be thought of as flowing apart (Barnes, 2000).

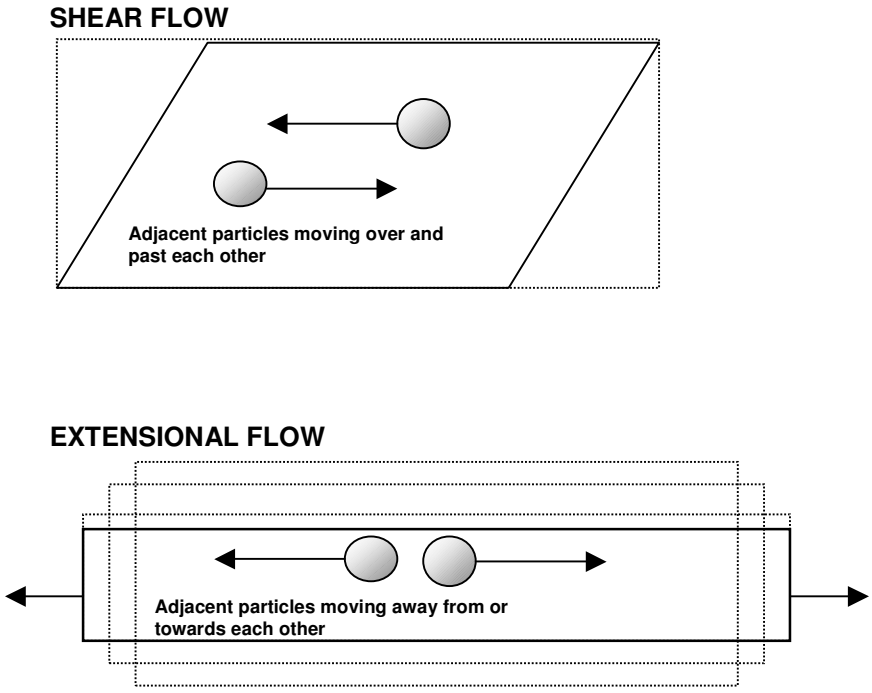

Figure 2-1: Shear Flow and Extensional Flow (After Barnes, 2000)

Viscosity is the term used to describe the resistance of a liquid to flow. To make a liquid flow a force must be applied. For shear flows, the rate at which this force is applied to the liquid is termed the *shear rate* and the magnitude of the shear referred to as the *shear stress*. Liquids are considered "Newtonian" when the viscosity remains constant over

changes in shear stress. This means that the viscosity remains constant, regardless of the applied shear stress. Whereas, liquids that exhibit a change in viscosity with a change in the shear rate are known as "Non-Newtonian" fluids. These terms, frequently used in rheology, are given in Table 2-2.

Table 2-2: Common rheological quantities and their units (After Barnes, 2000)

Quantity	Symbol	Units
Shear strain	γ	-
Shear rate (dγ/dt)	$\dot{\gamma}$	s^{-1}
Shear stress (Force/Area)	σ	Pa
Shear viscosity ($\sigma/\dot{\gamma}$)	η	Pa.s

At high temperatures, (>80°C) bitumen behaves as a liquid and is typically characterised by viscosity and the viscosity governs the acceptable temperatures for manufacture and placing of asphalt mixtures. At low temperatures (<-5°C), bitumen behaves essentially as a solid material. Tests for low temperature behaviour typically assess cracking or ductility. At intermediate temperatures (-5°C to 80°C), which covers the range in which asphalt pavements is under traffic, bitumen behaves as a "visco-elastic" solid and has properties between that of an ideal solid and a liquid.

Several methods have been developed to measure the intermediate temperature behaviour of bitumen and these range from simple index tests, carried out at single temperatures, to complex detailed analysis of the bitumen behaviour over a range of loading frequencies and temperatures.

Historically, two empirical tests dominate the simple characterisation of bitumen, Needle Penetration (BS EN 1426:2000) and Ring and Ball Softening Point (BS EN 1427:2000). Since the 1990's, the Dynamic Shear Rheometer (DSR) has rose to prominence in the fundamental rheological characterisation of bituminous bitumens. (Kennedy et al., 1990).

The penetration test is probably the most commonly used quality control test for bitumen in the world. This test involves the penetration of bitumen by a needle of known load and dimensions, at a fixed temperature (25°C) and loading time (5 seconds). The result is reported in units of tenths of a millimetre (dmm). Soft bitumen has high values of penetration, whereas hard bitumens have low values. Road paving bitumen can be thought of as intermediate in terms of penetration value. These bitumens typically have a penetration between 50 and 200dmm, although both harder and softer grades are used according to the climate. For example, in France and the United Kingdom, hard 10/20dmm penetration bitumens are used (Sanders and Nunn, 2005), whereas in cold countries such as Canada much softer grades are commonly employed to resist the effects of the very cold climate.

The softening point test consists of the placing of a steel ball of mass 3.5g onto a brass ring filled with bitumen. The test specimens are then suspended in water, or glycerol, and heated at a rate of 5°C per minute. At the moment the ball drops through the ring and hits a plate 25mm below the ring, the temperature is noted and reported as the softening point of the bitumen.

As previously stated, bitumen is a complex material with a complex response to loading time and temperature, and at normal pavement temperatures the bitumen has properties that are in the visco-elastic region. There has been a considerable increase in more complex assessment of bitumen with the aim of better characterizing the rheological behaviour of bitumen and the resulting behaviour of the asphalt mixture. Much of this change was bought about by the climate and loading condition based "Performance Grade" classification of bitumen resulting from the US Strategic Highway Research Program (SHRP) of the 1990's (Kennedy et al., 1990).

SHRP introduced the Dynamic Shear Rheometer (DSR) as a key tool in the Dynamic Mechanical Analysis (DMA) of bitumens. Various testing geometries, such as cone and plate, parallel plates and cup and plate, can be used in dynamic mechanical testing. For many materials cone and plate geometry is preferred as shear stress and shear rate are constant over the entire area of the plate, thereby simplifying calculations and giving accurate fundamental rheological properties. However, for bitumen testing parallel plate geometry is almost invariably used to avoid the very small gap present at the centre of the cone and plate geometry.

In general, two testing (plate) geometries are commonly used with the DSR, namely an 8 mm diameter spindle with a 1 or 2 mm testing gap and a 25 mm diameter spindle with 1 mm testing gap. The selection of the testing geometry is based on the operational conditions with the 8 mm plate geometry generally being used at lower temperatures (-5°C to 20°C) and the 25 mm geometry at intermediate to high temperatures (20°C to 80°C). However, it is possible to use the same testing geometry over a wide temperature range, although the

precision of the results may be limited as a result of compliance errors and the reduction in precision with which the torque can be measured at low stress levels.

Small-strain oscillatory measurements and creep compliance tests can both be carried out using a DSR but assess different characteristics of the bitumen. Oscillatory tests are typically carried out in the linear visco-elastic region of the bitumen and represent the bitumen behaviour when the bitumen is subjected to small strains. A test for measuring the behaviour of bitumen in the linear visco-elastic region over a range of temperatures and frequency has been standardised in Europe (EN 14770, 2005). This method produces a master curve, using the time-temperature superposition principle, of the bitumen's response to small strains as measured in the linear visco-elastic region.

A DSR can also perform creep tests and the rheological behaviour of bitumen can also be defined in terms of its creep compliance. At the surface of the road, especially at high ambient temperatures, higher strains are experienced and creep compliance tests may be better representative of the conditions under which the bitumen is loaded than small strain oscillatory tests (Delgadillo et al. 2006).

To determine creep properties, material is subjected to prolonged loading and creep compliance is obtained by applying a constant stress and measuring the resulting time-dependent strain.

Compliance is defined as:

$$J(t) = \frac{\gamma(t)}{\sigma_0} \quad (2)$$

Where

$J(t)$ = creep compliance, a function of time and temperature

$\gamma(t)$ = time dependent strain

σ_0 = constant stress

There has been an increase in interest in the United States and Europe in the measurement of creep and recovery characteristics of bitumen, and its relationship to permanent deformation characteristics of asphalt mixtures, and standard procedures to measure such properties have been developed. (NCHRP Publication 459, 2002; Collop et al., 2002; Taherkani and Collop, 2006; Delgadillo et al. 2006).

In summary, at high temperatures, (>80°C) bitumen behaves as a liquid and typically is characterised by viscosity whereas at low temperatures (<-5°C), bitumen behaves essentially as a solid material. The intermediate temperatures (-5°C to 80°C), represent the temperatures at which the bitumen in asphalt pavements is under traffic, and at these temperatures bitumen behaves as a "visco-elastic" solid and has properties between that of an ideal solid and a liquid.

Several methods have been developed to measure the intermediate temperature behaviour of bitumen. These range from simple index tests carried out at single temperatures up to complex detailed analysis of the bitumen behaviour over a range of frequencies and temperatures.

Asphalt fillers

Fillers modify the properties, increase the performance of, and provide improved durability to composites, polymers, rubbers, adhesives, coatings and construction materials. Fillers are used to lower the cost of materials, change processing characteristics and increase rigidity. Additionally, fillers can be used to give special properties to a material such as fire retardancy, electrical or magnetic properties. Fillers are used for cost reduction, density, colour, surface properties (such as controlling stickiness) and thermal properties (for example conductivity).

In general terms, fillers are typically fine powders with a particle size distribution in the range of 0 - 100µm. They can be naturally occurring materials such as calcium carbonate (limestone), manufactured fillers, for example carbon black, or derived from industrial wastes such as fly ash from power stations. Other common fillers include silica, kaolin ("China Clay"), mica, feldspar and diatomite.

Fillers in asphalt can be defined as *"finely divided mineral matter such as rock dust, slag dust, hydrated lime, hydraulic cement, fly ash or other suitable matter"* and typically this definition refers to the size fraction smaller than 75µm or 63µm. Fillers in asphalt are used to obtain increased stiffness or rigidity, reducing creep (permanent deformation), increase density and lower the cost of asphalt mixtures. Too much filler in asphalt mixtures can lead to cracking or fatigue problems as the stiffness is increased. Too little can lead to "bleeding" of bitumen from the mixture (Kandhal, 1980; Anderson et al. 1982).

The most frequently used filler in asphalt is limestone (calcium carbonate), which is derived from the consolidation of minute micro-organisms during the formation of the earth's crust. Limestone is the general term for rocks where calcite, a form of calcium carbonate, is

the predominant mineral. Limestone may also contain a proportion of magnesium carbonate, dolomite, silica, clays, iron oxides and organic material.

Other materials commonly used as fillers in asphalt include Portland Cement and hydrated lime, which possesses well documented properties with regard to mixture durability and reduced potential for moisture damage in asphalt (Little and Epps, 2001). Additionally, recycled fillers in the form of so-called "baghouse" fines are frequently used. The performance of baghouse fines was the subject of several key studies (Kandhal, 1980; Anderson et al., 1982) on the behaviour of filler in asphalt.

Kavussi and Hicks (1997) proposed that in order to provide satisfactory properties in the finished asphalt, filler should:

- Not have adverse chemical reactions with bitumen
- Not possess hydrophilic surfaces to ensure good adhesion
- Not possess high porous particles which may lead to excessive stiffening through selective adsorption
- Contain a dense (well graded) Particle Size Distribution

With regard to the specification of fillers, each European country has its own specifications and National Guidance Documents that list the requirements, test methods and acceptable limits. In the UK, the asphalt mixture specifications BS 4987 and BS 594, together with the National Guidance Document, PD 6682-2, Aggregates for asphalt and chippings, and contract specifications, such as the Highways Agency, Specification for Highway Works, are used to specify properties for mineral fillers.

In Europe the following tests are specified:

Geometrical properties

- Particle size distribution (Air-jet sieving) (EN 933-10)
- Requirement for harmful fines - Methylene blue value (EN 933-9)

Physical and Mechanical

- Water content (EN 1097-5)
- Particle density (EN 1097-7)
- Stiffening properties - Voids of dry compacted filler (Rigden voids) (EN 1097-4)
- Stiffening properties - “Delta Ring and Ball” (EN 13179-1)
- “Bitumen number” (EN 13179-2)
- Loose bulk density in kerosene (EN 1097-3)

Chemical

- Water solubility (EN 1744-1:1998)
- Water susceptibility (EN 1744-4:2001)
- Calcium carbonate content of limestone filler (EN 196-21)
- Calcium hydroxide (hydrated lime) content of mixed filler (EN 459-2)
- Loss on ignition of coal fly ash (EN 1744-1:1998)
- Loss on ignition of blast-furnace slags (EN 196-2:1994)

Surface area - fineness

- Blaine test (Blain specific surface) (EN 196-6)

Although several test methods are specified, the performance level for each test is a National concern and EU member states have National Guidance Documents that outline the requirements for the asphalt filler. In the UK, the specification for fillers is not onerous and consists of minimal requirements, namely particle size distribution and filler type is specified, for example Limestone or Portland Cement are permitted.

Summary – Asphalt pavements and asphalt constituents

Asphalt pavements are typically constructed in layers, with each layer of the pavement fulfilling a slightly different key function. Asphalt is an essential construction material comprising three key components, aggregate, bitumen and filler. The bitumen and filler combined constitute the true binder of the asphalt and this mastic is the part of the asphalt, which undergoes deformation under traffic loading. The properties of the filler significantly influence the behaviour of the mastic and hence the overall properties of the asphalt, making the properties of the fillers an important consideration when designing asphalt mixtures.

PHYSICAL PROPERTIES OF FILLERS

General

Each type of filler has different characteristics that influence the end properties of the finished products in which they are used. Aside from their chemical composition, fillers are traditionally characterised by their particle size distribution, shape, particle packing, surface area and surface activity (Wypych, 1999). Some of the key properties of fillers and their means of measurement are discussed in turn in the following section.

Particle Density

The particle density of fillers is typically measured in the classical way by measuring the volume of particles by displacement of water, or other liquids, using Archimedes' principle.

The particle density is then calculated by:

$$\rho_{particle} = \frac{m_{particles}}{v_{particles}} \qquad (g/m^3) \qquad (3)$$

Where: $m_{particles}$ = the mass of particles (g) and $v_{particles}$ = the volume of particles (m^3)

Particle density of fillers in all applications can cover a significant range, from hollow glass or ceramic beads with densities of around 0.1 - 0.2 g/cm^3 up to above 9 g/cm^3 for metal powder based fillers (Wypych, 1999). For asphalt fillers, the range is relatively narrow as

most fillers are derived from natural aggregates. Typically, asphalt fillers have particle densities in the range 2.65 - 2.75 g/cm^3. Fillers used in asphalt that are not derived from natural aggregates have a wider range of particle density, for example Portland Cement 3.15 g/cm^3 and Hydrated Lime, 2.30 g/cm^3.

Particle Size Distribution

Particle size distribution (PSD) describes the range of particles found within a substance. Particle size distribution is typically expressed as a percentage passing a particular size. PSD is normally depicted graphically, either by percentage mass or volume of particles within a particular size range (See Figures 2-2 and 2-3).

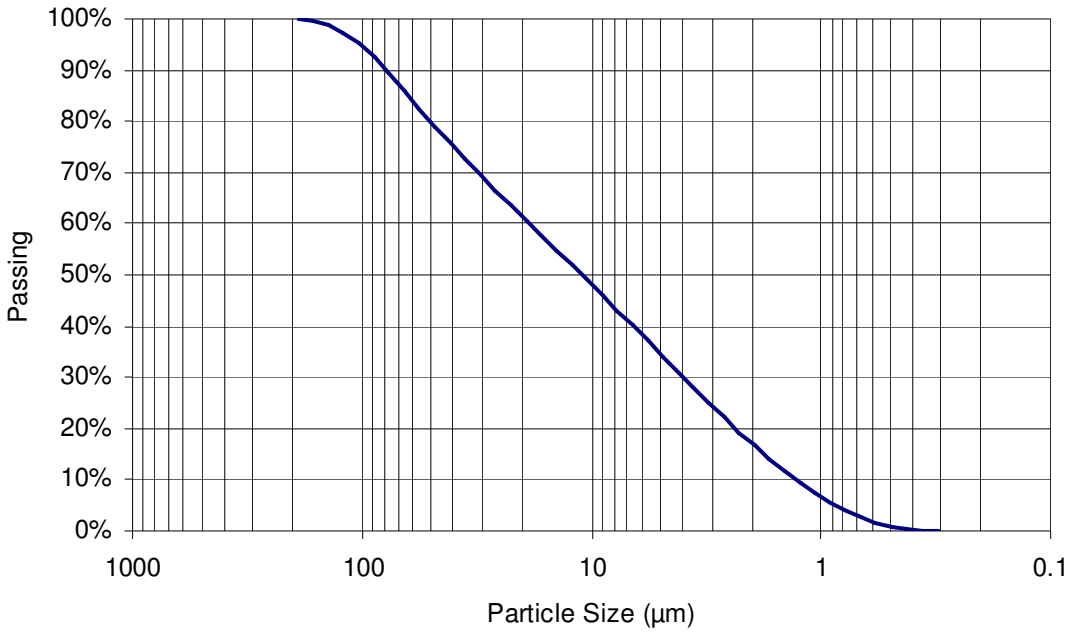

Figure 2-2: A typical particle size distribution curve, represented as % by mass passing a particular particle size

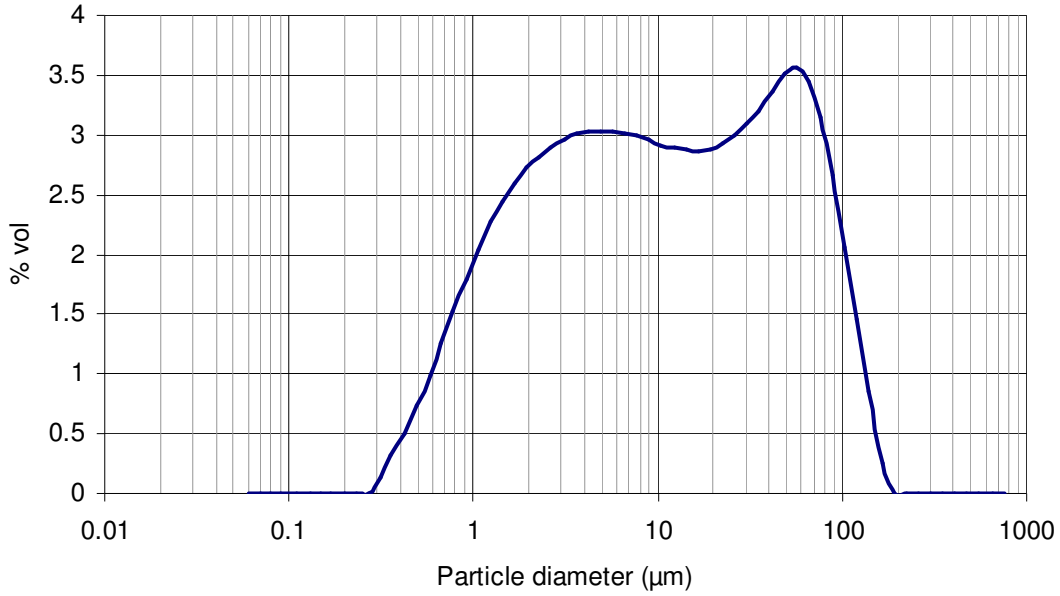

Figure 2-3: Identical data as that in Figure 2-2, presented as volumetric particle size distribution

Volumetric particle size distribution and particle size distribution by mass can be inter-converted by making assumptions of the density and shape of the particles. Typically in such calculations the particles are taken to be spherical.

In order to allow more convenient comparisons between two or more sets of particle size distribution data, mathematical descriptors of PSD curves such as Fineness Modulus and Coefficients of Uniformity are sometimes used. The Coefficient of Uniformity gives an indication of the range of sizes within a particle size distribution. A low coefficient of uniformity indicates a PSD with a small range of particles. It is typically calculated as follows:

$$U_C = \frac{D_{60}}{D_{10}} \tag{4}$$

Where:

U_C = Coefficient of uniformity

D_{60} = the size (μm) at which 60% of particles are smaller than (by mass)

D_{10} = the size (μm) at which 10% of particles are smaller than (by mass)

Fineness modulus is an empirical mathematical description of the fineness of a material and is typically derived by taking the sum of the percentage of material passing different sizes. The higher the value of fineness modulus, the finer the material. This approach has been adopted for asphalt fillers (Kandhal et al., 1998; Harris and Stuart 1998) and the Fineness Modulus of asphalt fillers has been calculated using the following formula:

$$F_M = \frac{P_{75} + P_{50} + P_{30} + P_{20} + P_{10} + P_3 + P_1}{100} \tag{5}$$

Where:

F_M = Fineness Modulus

P_x = the percentage passing diameter size x by mass, where x = μm

There are several methods that can be employed to produce particle size distribution information for fillers. It is important to note that different techniques lead to different results as a result of the test method employed. Additionally, the conditions of the test method may differ from the situation in which the filler is going to be used making the link between particle size distribution and filler performance difficult to make. For example, in laser diffraction measurements, the fillers are typically dispersed in a liquid. The conditions of the filler in the liquid may be very different to the conditions in the product formed when the filler is mixed with the liquid phase of the product. Additionally, mechanical (such as ultrasound) and chemical means of dispersing the filler during testing may lead to better (or worse) dispersion than in real life situations, another factor which makes linking particle size distribution to product performance problematic.

For many materials, sieving is a simple technique for producing PSD data. However, for very fine materials, such as fillers, this method has limitations. When particles become very small the electrostatic interactions between the particles causes agglomerations. Additionally, the particles become attracted to the sieves causing bridging across the apertures known as “blinding” which prevents further particles from passing through the sieve.

Air-jet sieving has been developed to overcome the effects of blinding. This technique can be used to measure the PSD of particles larger than 20µm. The method has been standardised in Europe (BS EN 933-10, 2002). The particles finer than 20µm are a major factor governing the behaviour of fillers as they possess the highest surface area, thus air-jet sieving has a significant limitation in measuring the coarser filler particles distribution only.

A particle size distribution can also be obtained by microscopy. This technique has the additional advantage of allowing a measurement of the particle shape and (at a sufficient magnification) texture. It is an accurate technique for obtaining the particle size but it is a time consuming process and only a relatively small amount of particles can be measured practicably. In a material such as a filler, the number of particles required to obtain an accurate particle size distribution is extremely large and using microscopy to estimate the PSD of fillers can lead to errors.

By assuming the particle density and the shape of the particles (usually as spheres), a particle size distribution expressed as percentage by mass can be derived. Sedimentation can be an inexpensive technique but requires relatively large sample sizes and is a slow test to perform. Additionally, it is not suitable for very fine particles (smaller than 2μm) as these particles tend to float in the sedimentation fluid. Laser diffraction is commonly used to measure the particle size distribution of fine materials. This technique represents a fast, accurate means of obtaining a particle size distribution. Additionally, the technique can measure very small particle sizes, as low as 0.05μm. The laser diffraction technique is based on the phenomenon that particles scatter light in all directions with an intensity pattern that is dependent on particle size. The diffracted patterns are detected and analysed to produce a particle size distribution (See Figure 2-4). The principles of laser diffraction are set out in BS ISO13320-1:1999.

Laser diffraction is a volume-based technique i.e. it reports the volume of particles which have a given particle size. This makes the technique extremely sensitive to the presence of large particles. Although they may be present in a powder in small numbers, they contain a large volume of material compared to finer particles for example; a 1mm diameter

particle has a volume of 0.52ml, which is equivalent to one million particles of 1µm diameter. Hence, the presence of larger particles in the sample can have a significant effect on the volumetric distribution.

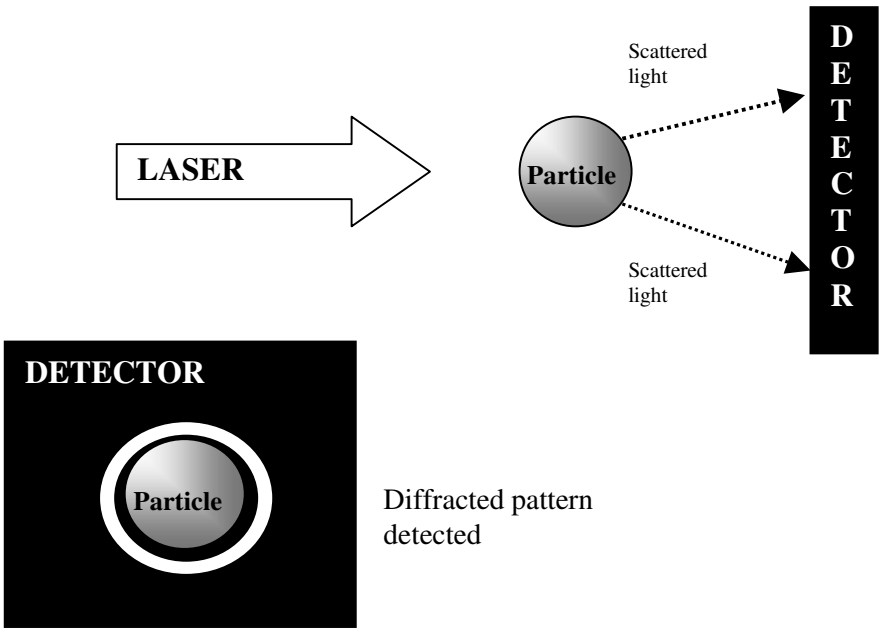

Figure 2-4: Schematic of the principles of particle size distribution by laser diffraction technique

Studies relating to the behaviour of fillers in asphalt mixtures typically include a particle size distribution as a classification test for the fillers. In earlier studies, (Kandhal, 1980; Anderson et al., 1982) the particle size distribution tended to be measured by microscopy or sedimentation techniques, whereas later studies (Harris and Stuart, 1998; Kandhal et al., 1998; Cooley et al., 1998) made use of laser diffraction techniques, as this technique became more widespread.

However, there has been little success in predicting the behaviour of fillers in asphalt based on their particle size distribution. The general observation has been made that finer fillers tend to lead to a higher relative viscosity when mixed with bitumen. Fillers have been separated into individual size fractions and rheological measurements using a sliding plate viscometer taken to study the stiffening effect on bitumen. It was proposed that not only was particle size important, with smaller particle size fillers stiffening the bitumen the most, but the mineralogy of the surface also played a role in modifying the rheology of the mastic (Anderson and Goetz, 1973). In fact, this study could be viewed as producing fillers with different surface areas, as producing fillers of progressively smaller particle size increases the surface area massively.

A study of 30 fillers from 4 countries (US, Sweden, Germany and Switzerland) measured several particle size distribution indicators (Harris and Stuart, 1998)

- Fineness Modulus
- Percentage passing 30µm
- Percentage passing 10µm
- Median particle size
- Coefficient of uniformity

The study reported that particle size descriptors did not adequately account for the behaviour of the mastics and concluded that "Rigden Voids" was the only independent variable of the sixteen analysed which could adequately differentiate between most of the

"good" and "bad" fillers, as experienced in the field. This is consistent with many other studies (Kandhal, 1982; Anderson et al., 1992b; Kandhal et al., 1998; Cooley et al., 1998).

In conclusion, although the general observation has been made that finer fillers produce a greater effect on the stiffening of bitumen, PSD data alone is insufficient to predict the behaviour of the filler in bitumen. Finer fillers possess greater surface area for the same mass of material and this may account for the perceived increase in stiffening. Additionally, several studies examined fillers such as hydrated lime, carbon black and kaolin, (Crauss et al. 1978, 1981; Ishai et al. 1980; Dukatz and Anderson, 1980; Kavussi and Hicks, 1997) which, in addition to having a much finer PSD than mineral fillers derived from natural aggregates, have a much greater surface activity.

Particle Shape

Particle shape of fillers is typically examined using microscopy, due to the very small particle sizes. Particle shape is important as the shape of the filler particles directly affects the maximum packing fraction (discussed in the following section). In asphalt filler studies Scanning Electron Microscopy has been use to examine the particle shapes of fillers (Kandhal, 1980; Anderson et al., 1973). Typically asphalt fillers derived from natural aggregates tend to be described as "grains".

Aspect ratio describes the relationship between the longest to the shortest dimension of a particle, and the aspect ratio of solid particles in suspension has a significant effect on the rheology of suspensions (Barnes, 2000). For asphalt fillers derived from natural aggregates, aspect ratios fall in a relatively small range (See Chapter III). Particle shape does

have a significant effect on the packing characteristics of filler and the value of maximum packing fraction. As the effects of the filler on viscosity of a suspension are scaled by the maximum packing fraction, and particle shape is clearly an important factor.

Maximum packing fraction

The space filler occupies in its compacted state is close to a key term in describing the rheology of suspensions, the maximum packing fraction, φ_{max}. The maximum packing fraction is defined as the solid volume content of a suspension at which the viscosity of the suspension becomes infinite. The combined effects of particle size distribution, particle size, shape and density are encompassed in this key property of fillers.

The packing of a filler can be estimated from the particle size distribution (Barnes, 2000; Wypych, 1999). However, because the relationship between particle size distribution, shape, texture and packing is complicated, it is more convenient to measure bulk density directly than to calculate or correlate from other properties.

"Tap Density" or "Compacted Density" refers to the maximum density filler can attain through repeated tapping, tamping, vibration or other means of compaction. Filler is added to a container of known volume and tapped a prescribed number of times, or alternatively, vibrated for a set time. The filled container is weighed and the bulk density calculated by dividing the mass of filler by the volume of the container.

The percentage voids in the filler ($\%V_{FILLER}$) can then be calculated by:

$$\%V_{FILLER} = 100\left(1 - \frac{\rho_{tap}}{\rho_{particle}}\right) \tag{6}$$

Where:

ρ_{tap} = the "tap density" (bulk volume density)

$\rho_{particle}$ = the particle density

The tap density is the bulk volume of filler and includes the air voids between the particles (See Figure 2-5).

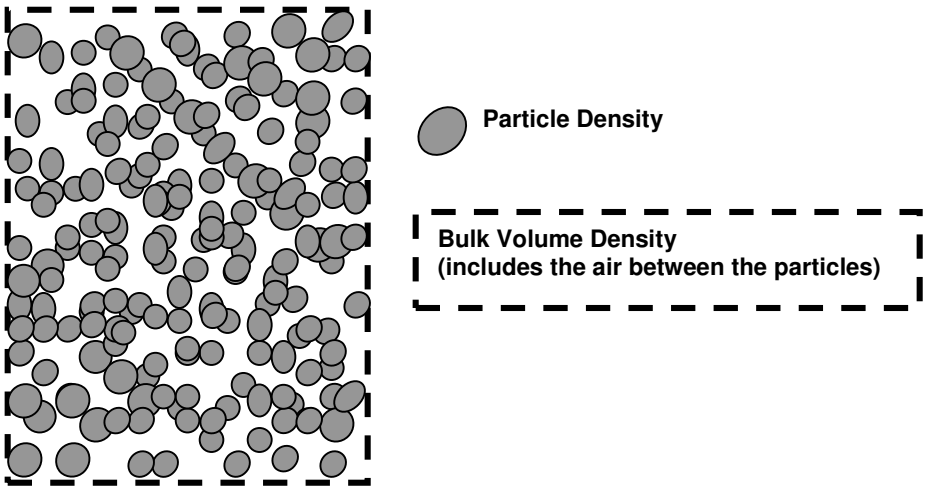

Figure 2-5: Bulk volume density and particle density

The maximum packing fraction can also be estimated using "Oil-Drop" of "Water drop" tests. These tests involve adding a liquid of known density drop-wise to a quantity of filler until a coherent mass is formed during mixing. The quantity of liquid, divided by its

density, determines the level of voids in the filler and hence the solid bulk volume can be estimated. The end point of such drop tests is difficult to judge and is subject to operator error, but this method has the advantage of including the interaction between the filler and a liquid.

Similarly, bulk density of filler under settlement can be used to estimate the maximum packing fraction of filler Typically kerosene is used as the test liquid, but other liquids, such as benzene and toluene have been used (Mitchell and Lee, 1939). Measuring the different levels of bulk density in liquids has been used to provide a measure of surface activity (Craus et al., 1978, 1981).

The maximum packing fraction can also be determined experimentally using rheological tests. As stated previously, in suspensions, the maximum solid packing fraction is the point at which the viscosity of the suspension becomes infinite. Increasing solid volume content produces an exponentially increasing relative viscosity. Carrying out several measurements at different solid volume contents allows the vertical asymptote of the exponential curve to be defined, which gives the maximum packing fraction.

An alternative method using minimal experimentation has been developed to derive the maximum packing fraction of powders in ceramic pastes (Hurysz and Cochrane, 2004). By carrying out measurements of viscosity at two or more concentrations close to the estimated maximum packing fraction and plotting the reciprocal of viscosity against φ (solid volume fraction) extrapolating to zero viscosity obtains a value of φ_{max} (See Figure 2-6).

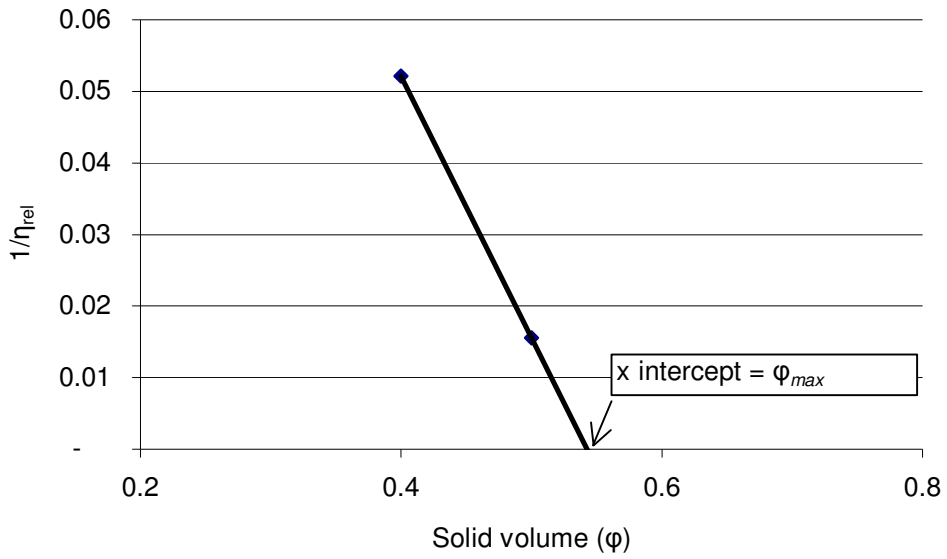

Figure 2-6: Rheological determination of φ_{max} using a two-point projection technique– example data

In this section we have seen how the combined effects of particle density, particle shape and particle size distribution are captured in a single property of fillers, the maximum packing fraction. This property can be estimated in several ways, including examining the packing characteristics of the filler in air. In asphalt technology, this approach is expressed as "Rigden Voids" which is the air void content of the filler obtained under standard test conditions (BS EN 1097-4, 1999) and which relates approximately to 1 – the maximum packing fraction. In the following section, the rheology of suspensions and models to describe the increase in relative viscosity with respect to the ratio of solid volume to maximum packing fraction are discussed.

THE RHEOLOGY OF SUSPENSIONS

Introduction

When solid particles, such as fillers, are added to liquid a suspension is formed. The presence of solid particles increases the viscosity of the suspension and continued additions of the filler will lead to a progressively more viscous suspension. Shearing of the liquid during flow results in shear forces across the axes of the particles which act as couples producing rotation. This absorbs energy and results in an increase in viscosity of the suspension (Barnes, 2000).

Modelling the rheology of suspensions

The first significant model to describe the increase in viscosity caused by increasing quantities of solid particles in suspension was derived by Einstein (1906). Einstein considered the case of dilute solutions of rigid spheres, where the particles are widely spaced, i.e. unaware of each other's existence.

For dilute suspensions the predicted increase in viscosity is given according to Einstein by:

$$\eta = \eta_0 (1 + [\eta]\varphi) \tag{7}$$

Where:

η = the viscosity of the suspension,

η_0 = the viscosity of the liquid phase,

$[\eta]$ = the intrinsic viscosity of the solid phase and

φ = the solid phase volume

The Einstein equation yields a linear relationship with respect to solid volume concentration and the equation does not include the term φ_{max}. Thus, according to the Einstein equation, the viscosity of the suspension can carry on increasing indefinitely, as long as the system is still considered a dilute system.

As the concentration of solid particles is increased there is increasing interaction in the liquid phase close to the surface of neighbouring solid particles and further energy is dissipated. Additionally, inter-particle interactions become increasingly important as the solid phase volume increases (Barnes, 2000).

Several later models (Mooney, 1957; Krieger and Dougherty, 1959; Chong, 1971) introduced the term φ_{max}, the maximum packing fraction, which represents the solid phase volume at which the viscosity of the suspension becomes infinite. These equations have been used to predict the behaviour of suspensions and differ in their predictions of viscosity of suspensions for the same solid fraction volume. Einstein's equation takes no account of extra interactions resulting from the increased concentration of solid particles, whereas the Mooney equation places the greatest emphasis on the effect of increasing concentration and particle-particle interactions.

Figure 2-7 shows the model predictions for an intrinsic viscosity of 2.5 (as proposed by Einstein for spheres), and an assumed φ_{max} of 0.5 and η_0 equal to unity.

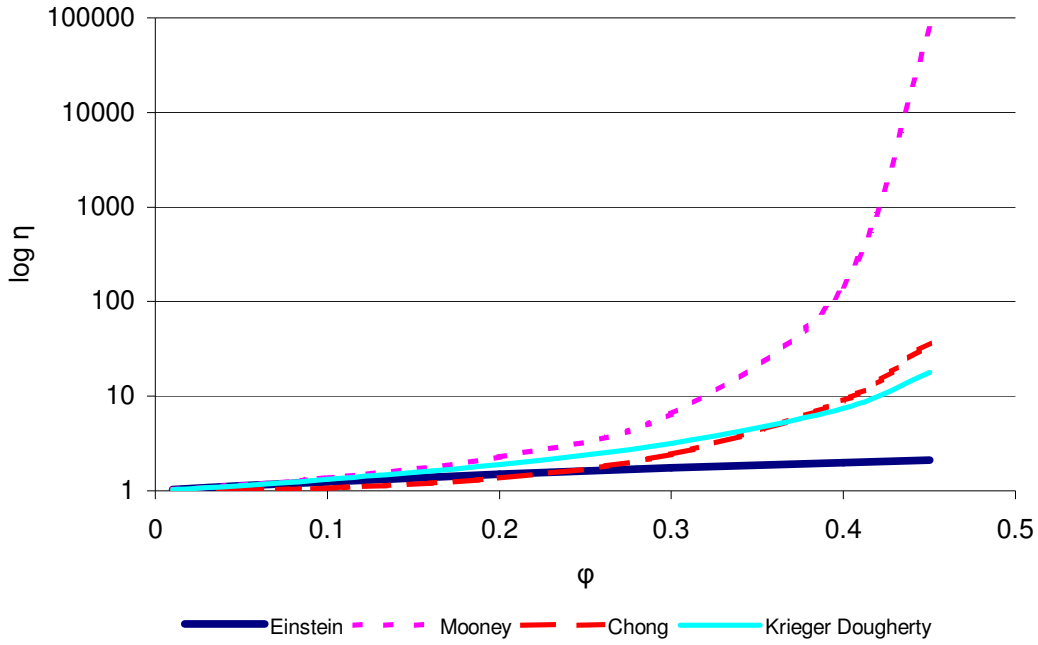

Figure 2-7: A comparison of models to predict the viscosity of suspensions

The Mooney equation (Mooney, 1957) has the form:

$$\eta = \eta_0 \exp\left(\frac{[\eta]\phi}{1-\frac{\phi}{\phi_{\max}}}\right) \tag{8}$$

The Krieger-Dougherty equation (Krieger and Dougherty, 1959) has the form:

$$\eta = \eta_0 \left(1 - \frac{\phi}{\phi_{\max}} \right)^{-[\eta]\phi_{\max}} \tag{9}$$

The Chong equation (Chong, 1971) has the form:

$$\eta = \eta_0 \left[1 + \frac{[\eta]\phi}{2} \left(\frac{\frac{\phi}{\phi_{\max}}}{1 - \frac{\phi}{\phi_{\max}}} \right) \right]^2 \tag{10}$$

Each term used the above equations will be discussed in turn and related to bitumen-filler mastics where appropriate.

The *solid phase volume (φ)* is the volume of solid particles within a suspension. It is expressed as the volumetric ratio of solid volume to the volume of the suspension. For bitumen-filler mastics a ratio by weight has often been employed, with 2:1 ratios of filler to bitumen being commonly employed to investigate the effects of filler in bitumen (Cooley et al., 1998; Harris and Stuart, 1998; Kandhal et al., 1998). In order to model the rheology of the mastic according to the equations above a volumetric calculation is required.

Relative viscosity (η_{rel}) is equal to the viscosity of the suspension divided by the viscosity of the liquid phase (η_0).

$$\eta_{rel} = \frac{\eta}{\eta_0} \quad (11)$$

Where:

η_{rel} = relative viscosity

η = the viscosity of the suspension

η_0= the viscosity of the liquid phase

Several researchers in the field of bituminous mixtures have used similar ratios to describe the behaviour of bitumen-filler mastics. Typically the effects of fillers in bitumen have been assessed using changes in traditional bitumen tests such as Penetration and Softening Point, which is referred to as "Delta Ring and Ball". In the Delta Ring and Ball Test, samples are produced in a fixed volumetric ratio of 0.375: 0.652 filler to bitumen. The softening point of the bitumen is measured and the Delta Ring and Ball value is the increase in softening point recorded in degrees centigrade recorded when the filler is added. A maximum Delta Ring and Ball of 11.5°C has been proposed in the US (Kandhal, 1980) and a maximum of 16^{o}C has recently been proposed in the UK for certain asphalt mixtures (Sanders and Nunn, 2005)

More recent studies (Anderson et al., 1992b) have introduced the term "modular ratio" to describe the relative increase in complex modulus (G*) over the G* of the pure bitumen, measured by the Dynamic Shear Rheometer. Other studies have described the behaviour of mastics using this approach (Anderson and Bahia, 1992; Kavussi and Hicks, 1997; Cooley et al., 1998; Kandhal et al., 1998).

The maximum packing fraction (φ_{max}) is the volume of solid particles at which the viscosity becomes infinite. Methods used to estimated φ_{max} have been discussed previously. The effects of solid phase volume (φ) are scaled by the maximum packing fraction according to Equations 8-10.

The most successful concept typically used to describe the observed effect of fillers in asphalt was established during the 1940's (Rigden, 1947). "Rigden voids" encompasses the effects of particle size distribution, shape and texture in a single value. It was proposed by Rigden that the volume of bitumen a filler can hold in its void structure is related to the stiffening observed in the bitumen-filler mastic (See Figure 2-8). Rigden proposed that fillers can accommodate a fixed volume of bitumen within their void structure. Bitumen in excess of the "fixed voids" is termed free bitumen. Therefore, for a fixed volume of bitumen, the stiffening is a function of the quantity of free bitumen, which is a result of the level of voids within the filler structure.

Essentially, Rigden described the point at which the filler concentration causes changes in the viscous nature of the mastic. By plotting the inverse of viscosity (labelled "fluidity") against filler concentration and projecting this line to "zero fluidity" he located the transition concentration. This point correlated well with the packing characteristics of the fillers. "Rigden Voids Content" of filler is termed a "tap density" and is measured by repeatedly tapping and compacting a cylinder containing filler on a rubber mat. The bulk volume of filler is divided by the specific gravity of the filler to arrive at the void content as described previously in Equation 6.

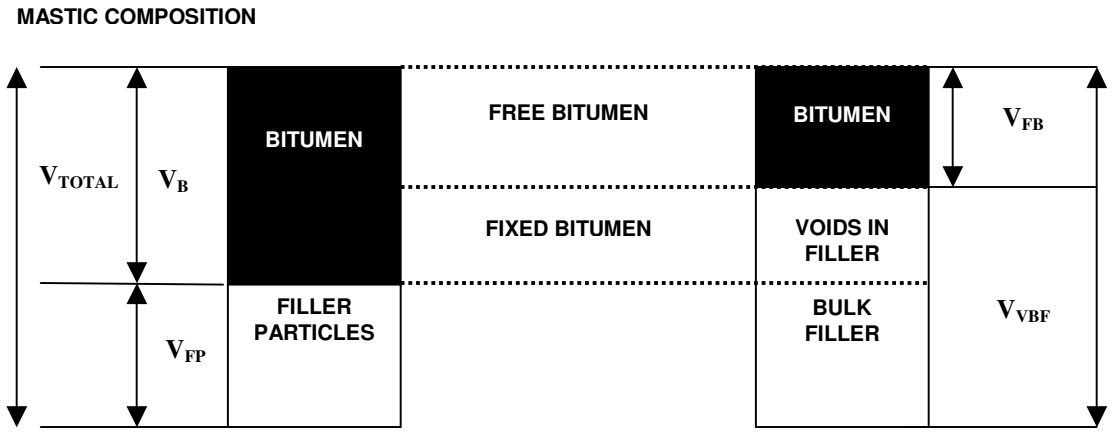

Figure 2-8. Illustration of the concept of "free bitumen", after Rigden (1947)

Where:

V_{TOTAL} = total volume of the mastic

V_{FP} = volume of filler particles

V_B = volume of bitumen

V_{FB} = volume of free bitumen

V_{BF} = bulk volume of filler.

Whilst it has been reported as difficult to correlate the stiffening of bitumen by filler to any single parameter such as particle size distribution or surface area, several researchers over many years have reaffirmed the usefulness of the concept of "Rigden Voids" (Heukelom and Wijga, 1971; Kandhal, 1980; Anderson et al., 1992a, 1992b; Kavussi and Hicks; 1997; Kandhal et al., 1998; Cooley et al., 1998). Thus, in asphalt technology, the so-called "Rigden Voids" are widely accepted as a means of assessing filler for potential stiffening of bitumen.

Some attempts have been made to suggest a maximum Rigden Void value to avoid excessive stiffening of the bitumen by the filler (Kandhal, 1982; Cooley et al., 1998). This is typically set at around the 50% level, i.e. 50% of the compacted volume of the filler can be air voids. In terms of suspension models, this equates to a φ_{max} of 0.5.

Intrinsic viscosity [η] is not a true viscosity but represents the level of interaction between the solid particles and the liquid at a theoretical concentration of zero. Einstein calculated the intrinsic viscosity of spheres to be 2.5 (dimensionless), which is sometimes referred to, in the context of suspensions, as the Einstein Coefficient.

Researchers have proposed (Barnes, 2000), that the intrinsic viscosity is related broadly to the shape of the particles. For a fixed solid phase volume (φ) the viscosity of the suspension decreases in the following order

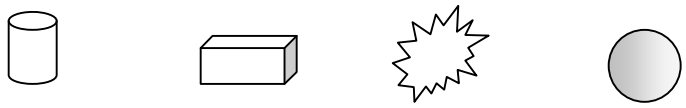

Rods >plates >grains >>spheres.

Figure 2-9: Intrinsic viscosity and its relationship to particle shape

Bitumen-filler mastics, as suspensions

Mineral filler mixed with bitumen can be viewed as a suspension of fine solid incompressible particles (filler) in a liquid (bitumen) matrix. This mixture is typically referred to as "mastic". The behaviour of fillers in different bitumen types is not easy to predict due to the complex nature of the interactions between the two materials. The mastic formed from filler and bitumen in asphalt can be considered the "true binder" of the mixture

and thus the properties of the mastic, and hence the properties of filler are important in an asphalt mixture (Anderson et al., 1992a).

Previously it had been proposed (Tunnicliffe, 1967; Puzinauskas, 1968; Anderson et al., 1982) that if the filler diameter is smaller than the asphalt mixture film thickness then that part of the filler becomes part of the film, and hence forms part of the suspension. If the filler particle is bigger than the film thickness then it can be considered an extension of the aggregate skeleton. These studies considered that a significant part of the filler acts as part of the bitumen. One study (Anderson and Goetz, 1973) concluded that a proportion of the bitumen could be replaced by fine filler (<10μm) but the mixtures produced were very sensitive to changes in the filler type. Later studies by the same researchers have questioned the approach of using film thickness to describe filler behaviour (Anderson et al., 1992b).

Harris and Stuart (1998), studied the effects of fillers in Stone Mastic Asphalt (SMA) mixtures and argued that the gap graded nature of SMA means that coarse aggregate particles dominate the aggregate skeleton. In this instance all of the filler contributes to the mastic formed.

In asphalt research the use of rheological models, such as the Krieger-Dougherty, Chong and Mooney has not been widespread. The Mooney equation has been examined (Heukelom and Wijga, 1971) in the context of fillers in asphalt mixtures, along with empirical models (Eilers, 1941). More recent research has modelled the rheology of suspensions as consisting of a maximum packing fraction, determined from the vertical asymptote of the solid volume concentration versus relative viscosity curve, and proposed a generalized Einstein Coefficient to describe the stiffening rate of the exponential curve (Shashidar and Romero, 1998).

Filler research in the field of asphalt has typically centred on the stiffening role of the filler in bitumen using simple tests such as increase in softening point or viscosity or the decrease in needle penetration at different filler to bitumen ratios by mass. For bitumen-filler mixtures, the change in softening point, expressed as the "delta ring and ball" (BS EN 13179-1:2000, Tests for filler aggregate used in bituminous mixtures – Part 1: Delta Ring and Ball test) has been standardised as a measure of the stiffening potential of filler of bitumen at a fixed volumetric ratio. The increase in softening point of a bitumen-filler mixture of 37.5 volume parts of filler and 62.5 volume parts of 70/100 paving bitumen grade is reported.

More recently, complex rheological testing based on the US SHRP protocols have been used to describe the stiffening of bitumen by fillers at both intermediate and low temperatures (Cooley et al., 1998: Harris and Stuart, 1998)

The most important factors governing the relative viscosity of bitumen-filler suspensions (Heukelom and Wijga, 1971) are the viscosity of the bitumen, the nature of the filler particles, the volume concentration of the particles, the rate of shear and interaction between the solid particles.

Early studies (Rigden, 1947, 1954; Heukelom and Wijga, 1971) of fillers in bitumen, measured viscosity of mastics and found that the filler type affected both the temperature susceptibility and the shear dependency of the mastic. Shear susceptibility is a very important effect of dispersions. Bitumen-filler mixtures exhibit shear thinning behaviour as an increase in shear causes agglomerations of filler particles to break down and increase the degree of peptization of the system (See Figure 2-10). Increasing the degree of peptization can be thought of as a decrease in volume of solid particles caused by the removal of air or the

breaking down of particle arrangements, and as such ties in to the influence of volume concentration (Heukelom and Wijga, 1971).

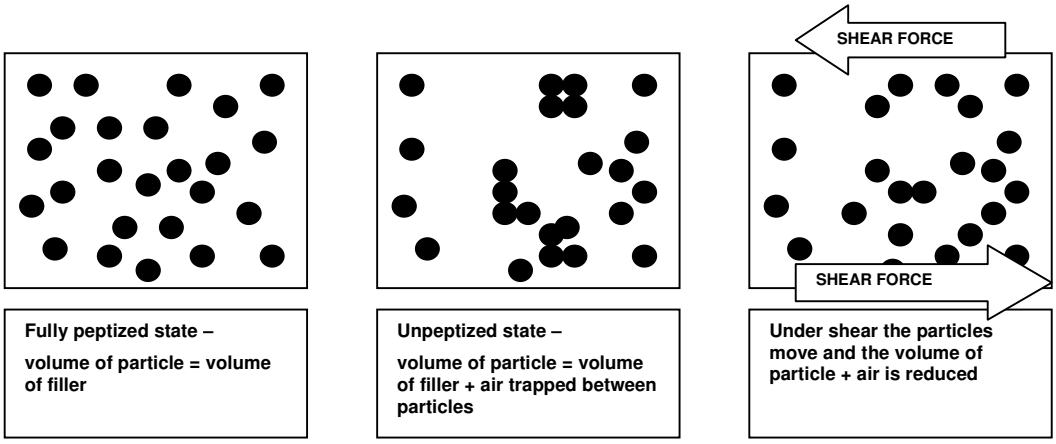

Figure 2-10: Peptization and shear thinning in bitumen-filler mastics

Heukelom and Wijga (1971) proposed a correction factor to take into account the true volume of filler in the system instead of the theoretical volume. They used the degree of peptization as a correction factor to account for the fact that if the filler is not adequately dispersed the volume is larger than the theoretical volume.

There is a general consensus amongst researchers that the effects of fillers in bitumen are a result of two factors – the physical volume concentration of solid particles and interactions between the filler surface and the bitumen (Rigden, 1947, 1954; Heukelom and Wijga, 1971; Anderson et al. 1973, 1982; Shashidar and Romero, 1999). Despite this, the vast majority of filler research has focussed on linking the stiffening effect of different fillers to a simple index property of the filler in air (Crauss et al. 1978, 1981; Dukatz and Anderson, 1980; Harris and Stuart, 1998; Kandhal et al 1998, Cooley et al. 1998).

In the next section the nature of the filler surface and it role in the behaviour of mastics is outlined.

SURFACE CHARACTERISATION OF FILLERS

Specific Surface Area

Specific surface area represents the ratio of a particle's surface area to its mass. Specific surface encompasses the combined effects of particle size, shape and texture in a measurement that is complementary to Particle Size Distribution (PSD). Surface area can be derived from PSD curves, related to air permeability or be derived from gas adsorption experiments. Additionally, specific surface area can be inferred from known thermodynamic properties using techniques such as calorimetry.

The simplest procedure for calculating surface area is using data from particle size distribution tests. Assuming a particle shape (usually, particles are taken to be spherical) it is possible to calculate the surface area of a substance.

Calculating surface area from particle size distribution data does present several difficulties due to the number of assumptions made in the calculation (See Figure 2-11). Additionally, as the particles become finer, and more numerous, the surface becomes larger. This infers more error in the calculation of surface area from an assumed geometry for filler compared with that with coarser materials, such as aggregates or natural sand.

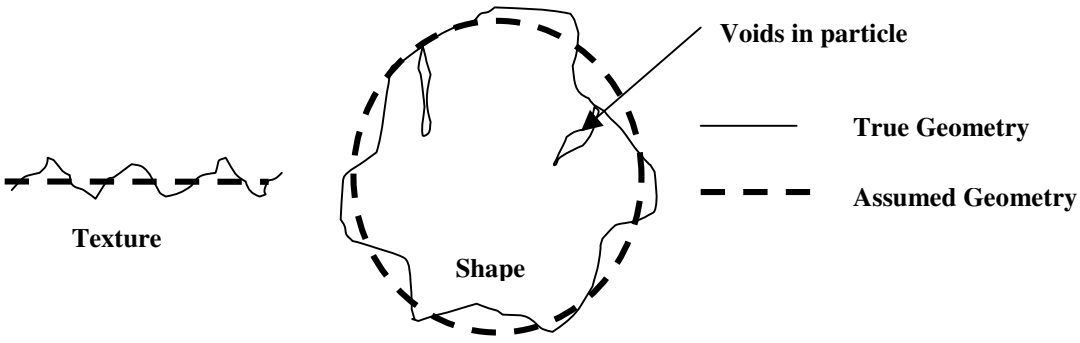

Figure 2-11: Sources of error in calculating surface area using an assumed geometry

Gas sorption measurements are considered to be an accurate means of measuring surface area of very fine materials, such as fillers. This method has the advantage of taking into account the surface texture and shape of the particles. The surface area of the solid includes both the external surface and the internal surface of the pores that are accessible to the gas used in the test, thus the specific surface measured by gas adsorption is biased by the molecular size of the adsorbate gas relative to the size of small pores and crevices (See Figure 2-12).

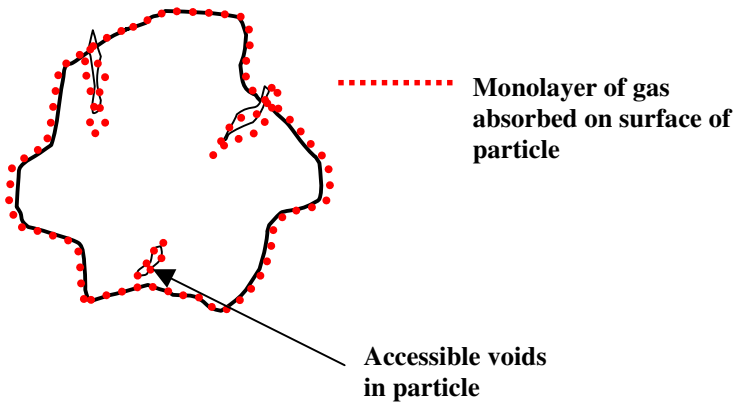

Figure 2-12: Schematic of a filler particle in a gas sorption test

Adsorption of the gas takes place because of the presence of an intrinsic surface energy. When a material is exposed to a gas, an attractive force acts between the exposed surface of the solid and the gas molecules. The result of these forces is characterized as "physio-adsorption".

Gas physio-sorption is considered non-selective, thus filling the surface step by step depending on the available solid surface and the relative pressure. Filling a complete layer enables the measurement of the surface area of the material, because the amount of gas adsorbed when the mono-layer is saturated is proportional to the entire surface area of the sample.

For such tests, nitrogen gas is typically used, but any gas can be used provided it is physically adsorbed by weak bonds (van der Waals) at the surface, and can be desorbed by a decrease in pressure at the same temperature. There are two general methods of obtaining an isotherm. The gravimetric method involves measuring the weight increase of the specimen as the pressure of the sorptive gas is incrementally increased, to determine how much gas is adsorbed. A second method is the volumetric method where the universal gas law is used to

calculate the volume of gas adsorbed at a measured relative pressure. In both methods the end result is a plot of gas adsorbed versus pressure. This plot is referred to as a "sorption isotherm".

The most common means of determining the surface area of a solid from a sorption isotherm is referred to as the "BET" method after its developers Brunauer, Emmet and Teller (1938). This method has subsequently been standardised in Europe (BS EN 4359-1: 1996). By assuming that the heat of adsorption is constant throughout the formation of the first monolayer and that the heat of adsorption for subsequent monolayers is equal to the heat of condensation of the bulk liquid, Brunauer et al. (1938) were able to derive a relationship between the relative pressure of the gas and the volume adsorbed per unit specimen mass.

$$\frac{P}{V_{ads}\,(P_0 - P)} = \frac{1}{V_m c} + \frac{c-1}{V_m c}\frac{P}{P_0} \qquad (13)$$

Where:

P = the equilibrium pressure, (Pa)

P_0 = the saturation pressure, (Pa)

V_{ads} = the volume of gas adsorbed at P/P_0, ($mm^3\ g^{-1}$)

V_m = the volume of adsorbate for one monolayer of surface coverage, (mol g^{-1})

and

c = the BET constant, (Unitless)

Where:

$$c = \exp\left(\frac{E_1 - E_L}{RT}\right) \quad (14)$$

Where:

E_1 = the heat of adsorption for the first layer (kJ mol^{-1})

E_L = the heat of adsorption for the subsequent layers (kJ mol^{-1})

R = the universal gas constant (8.314 J mol^{-1} K^{-1})

T = absolute temperature (K)

Plots of $P/V_{ads}(P_0–P)$ versus P/P_0 yield a straight line, y = a + bx, from which the slope (b) gives the term $(c-1)/(V_m c)$ and intercept (a) gives $(1/V_m c)$. From this V_m, the volume of gas to form a monolayer on the surface is given by:

$$Vm = \frac{1}{a+b} \quad (15)$$

and the BET constant is given by

$$c = \frac{b}{a} + 1 \quad (16)$$

Figure 2-13, below, shows a typical BET plot.

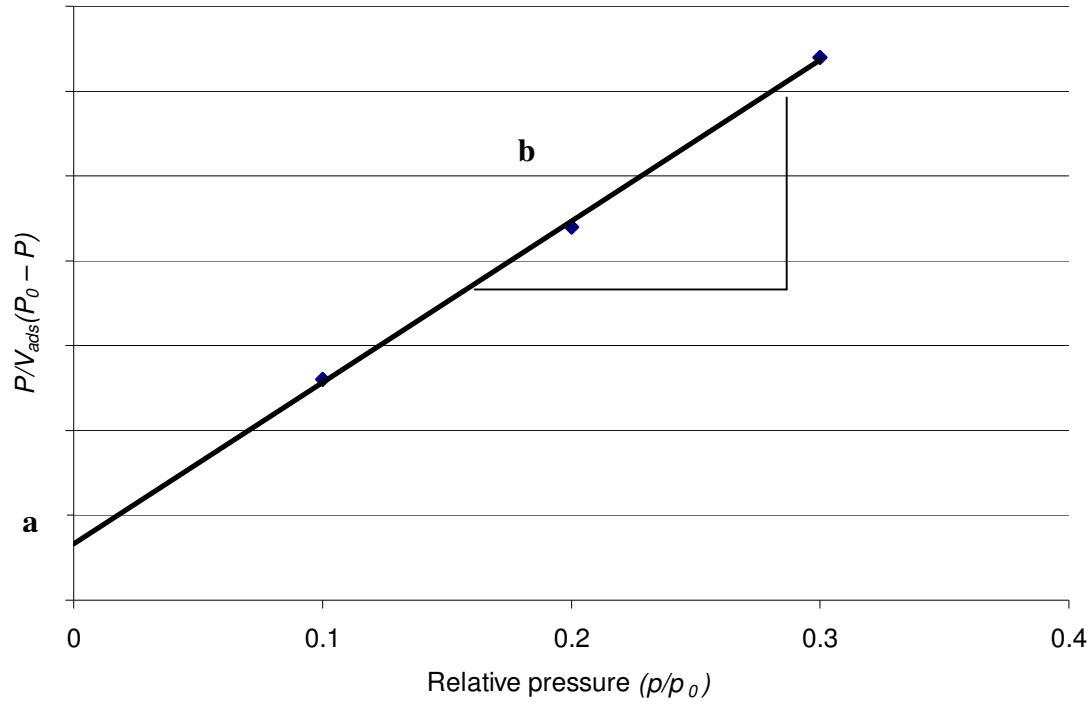

Figure 2-13: A typical BET plot

The surface area A_s of the specimen is given by:

$$A_s = V_m . A_{molecule} . L \qquad (17)$$

Where:

A_s is the total surface area (m²)

V_m is the volume of adsorbate for one monolayer of surface coverage (mol g^{-1})

$A_{molecule}$ is area covered by one molecule of adsorbate (nm²)

L = Avogadro's constant (6.022 x 10^{23} mol^{-1})

The specific surface area, m²/g (SSA) is then calculated from:

$$SSA = \frac{A_s}{M} \quad (18)$$

Where:

M = the mass of the sample (g)

In terms of surface area of asphalt fillers, the Blaine fineness test (BS EN 196-6), an empirical measure of surface area related to the air permeability of a Portland cement, has been used in some studies into the effect of fillers in asphalt (Kandhal, 1980). Later studies have used surface area calculated from laser diffraction data (Kavussi and Hicks, 1997; Harris and Stuart 1998; Kandhal et al., 1998).

Gas sorption and the BET technique have not been used typically for the examination of fillers in asphalt although one study, limited to two filler types, did measure the specific surface area by BET (Anderson et al., 1992a).

Surface Energy

Surface energy is a measure of the work required to increase the surface of a material by a unit area. “Surface tension” is normally the term used to refer to liquids and “surface energy” the term used for solids. The quantity of surface, expressed as specific surface area, is complimented by the surface energy, which can be considered a “quality” aspect of the surface. Knowledge of the surface energies of two (or more) media allows the calculation of

the level of bond energy when the two surfaces are brought together, or conversely the bond energy per unit area required to separate the materials.

There has been a considerable interest in the understanding of the implications of surface energy of bitumen, aggregates and fillers used in asphalt and detailed test methodologies have been developed related specifically to the application of surface energy theory to bituminous materials (Cheng, 2002; Hefer, 2004; Bhasin, 2006).

Surface energy can be related to the process of creating unit area and is equivalent to separating two half units of an identical material. This can be represented by the following equation.

$$\gamma_1 = \frac{G_{11}}{2} \tag{19}$$

Where:

γ_1= surface energy (mN/ m²)

G_{11} = the cohesive energy which is equivalent to $2\gamma_{1,}$ (mN/ m²)

Where two different media are considered, the interfacial energy (solid/liquid), (or interfacial tension (two liquids)), is the free energy required to increase the interfacial area between the two media. This is referred to as γ_{12} and can be represented as:

$$\gamma_{12} = \gamma_1 + \gamma_2 - G_{12} \tag{20}$$

Where:

γ_1 = the surface energy of medium 1 (mN/m²)

γ_2 = the surface energy of medium 2 (mN/m²) and

G_{12} represents the work of adhesion between the two media (mN/m²)

Equation 20 is known as the Dupré equation. The Dupré equation can be rearranged and written to represent the work of adhesion of the bitumen - filler interface of a mastic as

$$\gamma_{FILLER-BITUMEN} = \gamma_{FILLER} + \gamma_{BITUMEN} - G_{FILLER-BITUMEN} \quad (21)$$

To make use of Equation 20 it is necessary to obtain values for the γ_{FILLER}, $\gamma_{BITUMEN}$ and $\gamma_{BITUMEN\text{-}FILLER}$.

Measuring the surface energy (tension) of a liquid (γ_{LIQUID}) is relatively straightforward and surface energy values of liquids can either be obtained from literature, accurately measured by analysis of the shape of drops, or can be determined using force-wetting experiments where well-characterized solids are immersed and removed from the liquid. The "Du Nouy Ring" method and Wilhelmy plate method are well known examples of force wetting methods of measuring surface tension of liquids (Wilhelmy, 1863; Du Nouy, 1919).

Measuring the values of a solid (γ_{SOLID}) is less straightforward as direct measurement of the solid surface energy is not possible. Surface energy measurements of solids are typically determined indirectly and reflect the thermodynamics of a fluid (liquid or gas)/solid interaction. Hence the choice of test liquids (or gases) directly influences the values obtained. Therefore, one has to be careful in the selection of the test liquids (or gases) in order to correctly obtain the surface energy which is an intrinsic property of the materials.

The use of contact angles is the oldest and best known of techniques for measuring the behaviour of a solid liquid interface. This technique was first described two centuries ago (Young, 1805). A contact angle captures the competing tendencies between a solid (S), a liquid (L) and a vapour (V) (Figure 2-14).

When the work of cohesion in a liquid exceeds the work of adhesion between the solid and the liquid, a drop placed on the solid surface will form a finite contact angle. Whereas, when the cohesion of the liquid is lower than the work of adhesion, spreading will occur. The Young equation assumes that the interactions between the solid and the gas phase (or the liquid vapour phase) are so small as to be negligible.

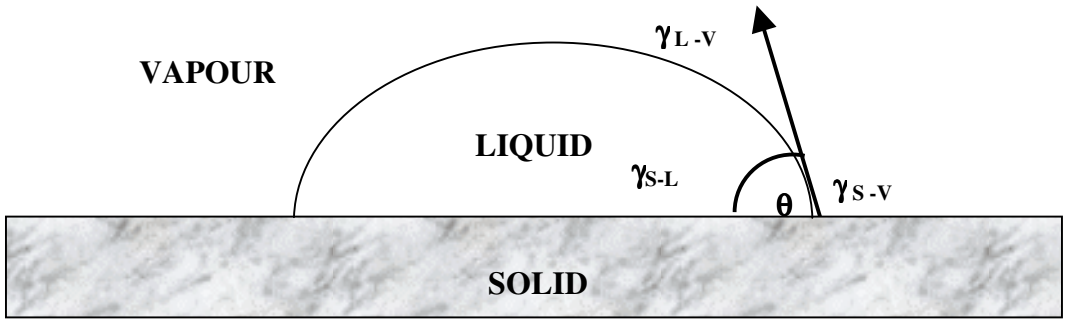

Figure 2-14: Schematic of a contact angle and its relation to the Young Equation

A contact angle given by the three surface tensions (solid, liquid and vapour) is summarised in the Young equation:

$$\gamma_{VAPOUR-SOLID} = \gamma_{LIQUID-VAPOUR}\cos\theta + \gamma_{SOLID-LIQUID} - \pi_e \qquad (22)$$

Where:

$\gamma_{VAPOUR\text{-}SOLID}$ = interfacial energy vapour to solid (mN/m²)

$\gamma_{LIQUID\text{-}VAPOUR}$ = interfacial energy liquid to vapour (mN/m²)

θ = the contact angle (degrees)

$\gamma_{SOLID\text{-}LIQUID}$ = interfacial energy solid to liquid (mN/m²)

π_e = the equilibrium pressure of adsorbed vapour of the liquid on the solid (Pa)

Typically, in measurement of contact angles, π_e is considered to be equal to zero and the Young equation is represented simply as:

$$\gamma_{SOLID} = \gamma_{LIQUID} \cos\theta + \gamma_{SOLID-LIQUID} \quad (23)$$

Combining Equations 20 and 23, the bond energy between two media can be expressed as:

$$G_{12} = \gamma_1(1 + \cos\theta) \quad (24)$$

Equation 24 is known as the Young-Dupré equation and this equation determinations the bond energy between the materials from two experimentally simple terms, the contact angle and the surface tension of the liquid.

Surface energy, γ, has thus far been discussed as a single term, however several different forces are acting at the surface. A comprehensive review of the fundamental forces acting at the surface during adhesion can be found elsewhere (Hefer 2004) but these include dipole-dipole interactions (referred to as Keesom orientation forces), dipole-induced dipole interactions (referred to as Debye induction forces) and induced dipole-induced dipole interactions (known as London dispersion forces)

Several theories exist around the grouping of these forces with regard to surface energy. For example, Fowkes (1964, 1966) proposed that the total surface energy of a media γ^{TOTAL} was the sum of the following types of interaction at the surface.

$$\gamma_{TOTAL} = \gamma^{d} + \gamma^{p} + \gamma^{h} + \gamma^{i} + \gamma^{ab} \quad (25)$$

Where:

γ^{TOTAL} = the total surface energy

γ^{d} = nonpolar dispersive forces (London Forces)

γ^{p} = weak polar forces (Keesom)

γ^{i} = induction forces (Debye Forces)

γ^{h} = hydrogen bonding forces

γ^{ab} = acid base forces

More recently, researchers propose surface energy can be represented by two groups of forces. According to this approach:

$$\gamma^{TOTAL} = \gamma^{LW} + \gamma^{AB} \quad (27)$$

and

$$\gamma_{AB} = 2\left(\gamma^{+}\gamma^{-}\right)^{1/2} \quad (28)$$

Where

γ^{LW} = the Lifshitz - van der Waals component of surface energy

γ^{AB} = the acid-base component of surface energy

Some of the polar forces, for example the Keesom and Debye forces, are weak and as such can be included in the dispersive component and the combination of weak polar forces with the non-polar dispersive forces is termed the "Lifshitz - van der Waals forces" and is identified as γ^{LW} (Good and van Oss, 1992; Good, 1992).

Lifshitz - van der Waals forces act on all molecules, even neutral ones, and can act over long distances (up to 100 Å), and include dispersion, orientation and induction energies.

The contribution of the dispersive forces can be expressed as a geometric mean as outlined in Equation 26 but using the subscript "LW" to denote the grouping of the forces.

$$G_{12}^{LW} = 2\left(\gamma_1^{LW}\gamma_2^{LW}\right)^{1/2} \tag{29}$$

A second group contributes to the surface interactions and is related to the Lewis acid-base interactions and is termed γ^{AB}. These forces are reversible and act over short distances (3Å). Hydrogen bonding is a commonly cited example of this type of interaction.

For the acid-base interactions there are two sets of interactions, those between the base component of medium one with the acid component of medium two and the acid component of medium one with the base component of medium two.

This can be expressed as:

$$G_{12}^{AB} = 2\left(\gamma_1^+ \gamma_2^-\right)^{1/2} + 2\left(\gamma_1^- \gamma_2^+\right)^{1/2} \quad (30)$$

Thus the total work of adhesion of the system can be expressed as the combination of Equations 29 and 30:

$$G_{12} = 2\left(\gamma_1^{LW} \gamma_2^{LW}\right)^{1/2} + 2\left(\gamma_1^+ \gamma_2^-\right)^{1/2} + 2\left(\gamma_1^- \gamma_2^+\right)^{1/2} \quad (31)$$

Referring back to the Equation 24 (the Young Dupré equation), and substituting Equation 31 gives

$$(1+\cos\theta)\gamma_1 = 2\left(\gamma_1^{LW} \gamma_2^{LW}\right)^{1/2} + 2\left(\gamma_1^+ \gamma_2^-\right)^{1/2} + 2\left(\gamma_1^- \gamma_2^+\right)^{1/2} \quad (32)$$

This is referred to as the Van Oss-Chaudhury-Good (OCG Equation) thermodynamic approach to determining the surface energy of solids. This is the approach that has been used recently to characterize bitumen, fillers and aggregates for use in asphalt (Cheng, 2002; Hefer, 2004; Bhasin, 2006).

In order to make use of Equation 32, it necessary to make contact angle measurements with at least three different liquids of known values of γ^{TOTAL}, γ^{LW}, γ^+ and γ^- for the test liquids. Typically, one of test liquids is apolar, (i.e. where $\gamma^{TOTAL} = \gamma^{LW}$) and γ^{LW} of the solid can be determined directly using Equation 33.

$$(1+\cos\theta)\gamma_1 = 2\left(\gamma_1^{LW}\gamma_2^{LW}\right)^{1/2} \quad (33)$$

Contact angle measurements using two further liquids of differing γ+ and γ- are then measured and the terms γ+ and γ- for the solid are calculated by solving a simultaneous equation. Other means of calculation, for example using a matrix, can also be used (See Chapter III).

Having made surface energy measurements of the fillers and bitumen using the approach outlined above, the bond energy can be calculated using Equation 20 (this methodology is further outlined in Chapter VI).

Surface characteristics of fillers in asphalt

As previously stated, whilst a significant effort has been made to understand the packing of fillers and the effect on the rheology of bitumen-filler mastics, far less attention has been paid to the interaction between the bitumen and the surface of the filler. Rigden, whilst focussing much of his work on the packing characteristics of the fillers and their relationship to the visco-plastic transition point in mastic systems acknowledged the importance of the interfacial conditions in the system;

"Although in some systems rheological behaviour is markedly influenced by changes in surface conditions at the solid/liquid interface, in the present work this factor was not considered to be of much importance and has not so far been directly investigated"

(D.J. Rigden, 1947)

Surface activity of fillers in asphalt has been measured in several ways. The Methylene Blue Test (BS EN 933-10, 2002) has been used and was found to correlate with water damage of asphalt mixtures made with different filler types (Kandhal et al., 1998). Typically with regard to aggregates for construction, the Methylene Blue test is associated with detecting the presence of clays which possess very large surface areas and therefore if present in an aggregate in sufficient quantities mask the surface activity of the filler resulting in Methylene Blue Value approximating the quantity of clay present in the aggregate or filler. It is important to note that "pure" fillers, containing no clay, will still record a Methylene blue value due to the surface area and surface activity present.

Differences in bulk density of fillers with liquids of different polarity have been used to assess "surface activity" (Dukatz and Anderson, 1980). Hygroscopic moisture contents can be considered a measure of hydrophobicity/ hydrophilicity of filler. This measure of surface activity has also been used in studies to characterise the filler and propose correlation to mixture properties made with the fillers (Craus et al., 1978, 1981; Kandhal 1980; Ishai et al. 1980). Calorimetric measurements have also been used in the past to describe the activity level of the surface of fillers (Craus et al., 1978, 1981; Ishai et al., 1980).

When water is used as the test liquid, the nature of the surface is referred to as "hydrophobic" or "hydrophilic". Hygroscopic moisture contents, where an oven dry sample of filler absorbs atmospheric moisture and the change in mass is measured over time, are conceptuality similar with high values of hygroscopic moisture indicative of a more hydrophilic material, than low values of hygroscopic moisture. This concept has been used to describe the surface activity of asphalt fillers (Craus et al., 1978,1981).

The surface of filler has not been typically considered as the major factor in the resultant mechanical properties of the mastic, which is typically accounted for by the Rigden Voids approach of "free bitumen". The surface characteristics of fillers are more commonly associated with long-term environmental changes (durability) of asphalt mixtures and several researchers acknowledge that the nature of the filler can have a large effect on the long-term durability of asphalt (Ishai et al., 1980; Craus et al., 1978, 1981; Kandhal et al., 1998).

The level of surface activity has been linked to the durability of asphalt mixtures made using the fillers, but the correlations have not been typically successful (Craus et al. 1978, 1981; Kandhal et al. 1998). Hygroscopic measurements alone could not predict potential for water damage in bitumen-filler mastics. Similarly, pH values did not show a clear trend, despite higher pH being considered to be favourable in reducing stripping tendency in mixture. Neither the activity coefficient, nor the hygroscopic moisture contents predicted the durability of the mixture (Kandhal, 1980).

Calorimetric measurements proved a little more successful in predicting the mixture durability of different filler additions (Craus et al., 1978, 1981), however the different filler types in the study could be considered quite extreme in terms of their chemical composition - glass beads, dolomite, basalt, sandstone, salt, limestone and hydrated lime. The glass bead filler failed the criteria of the study, in immersion tests after less than 24 hours. The next two fillers, termed "non-active" sandstone and basalt failed the immersion test within 4-7 days. The final group were termed "active" fillers, the hydrated lime, dolomite and limestone, which retained their properties during long periods of immersion.

However, a good correlation between specific heat of absorption of the fillers and durability was reported. The higher the specific heat (cal/m²), the better the resulting durability of asphalt mixtures used with this filler type. The specific heat of absorption was used as a "surface activity characteristic" in this work.

It has been observed that fillers stiffen to a different extent with different bitumen types, inferring a level of interaction between filler and bitumen beyond the bulk filling. Additionally, some fillers such as hydrated lime and carbon black have been termed "reinforcing" fillers as the stiffening observed is above that estimated from the Rigden Voids test (Anderson et al., 1992b). In the case of "reinforcing fillers" structural changes to the bitumen may occur and hence a change in the continuous phase (bitumen) viscosity.

Dukatz and Anderson (1980) proposed that two types of bitumen stiffening exist, volume filling and physio-chemical interactions. According to Dukatz and Anderson (1980) the role of volume filling is relatively small and that the physio-chemical interaction between the bitumen and the surface of the mineral filler can lead to 100-1000 fold increases in viscosity.

Ishai et al. (1980) proposed that different fillers have different effects on the same bitumen and these were attributable to the surface activity of the fillers. The study was limited by regard to the range of fillers studied, but found that hydrated lime had both the highest geometrical irregularity and the highest surface activity. These observations were based on hygroscopic measurements.

Similarly, Kavussi and Hicks (1997) in a study of four types of filler - limestone, quartz, fly ash and kaolin - attributed the higher stiffening potential of kaolin to the fineness and the surface affinity to bitumen.

A further study (Anderson and Goetz, 1973) used rheological measurements using a sliding plate viscometer to study the stiffening effect of different fillers, separated into different size fractions. They found that not only is size important, but the mineralogy of the surface also played a role in modifying the rheology of the mastic.

CHAPTER SUMMARY

Asphalt is a material comprised of three principal components; aggregate, bitumen and filler. The different ratios between these components gives rise to a family of asphalt mixtures with different properties. Fillers in asphalt are used to obtain increased stiffness or rigidity, reducing creep (permanent deformation), increasing density and lowering the cost of asphalt mixtures. Too much filler in asphalt mixtures can lead to cracking or fatigue problems as the stiffness is increased. Too little can lead to "bleeding" of bitumen from the mixture.

Fillers in asphalt can be defined as *"finely divided mineral matter such as rock dust, slag dust, hydrated lime, hydraulic cement, fly ash or other suitable matter"* and typically this definition refers to the size fraction smaller than 75µm or 63µm. Aside from their chemical composition, fillers are traditionally characterised by their particle size distribution, shape, particle packing, surface area and surface activity.

When bitumen is combined with filler, mastic is formed. This mastic can be viewed as the component of the asphalt mixture that binds the aggregates together and also the component of the asphalt that undergoes deformation when the pavement is stressed under traffic loading. The characteristics of the filler can significantly influence the properties of the mastic, and thus the filler properties can have significant effects on asphalt mixture performance. The behaviour of fillers in different bitumen types is not easy to predict due to the complex nature of the interactions between the two materials.

Mastics can be considered as suspensions of solid filler particles in liquid bitumen. Models developed to describe the behaviour of suspensions (Mooney, 1957; Krieger and Dougherty, 1959; Chong, 1971) include the term φ/φ_{max} and predict exponentially increasing stiffening as the solid volume fraction, φ, approaches the maximum packing fraction φ_{max}. Effects outside of the solid volume fraction ratio are captured in such models by the intrinsic viscosity of the solid phase, which is often related to the shape of the particles.

Increasing additions of solid particles leads to exponentially increasing relative viscosity up to the point where flow is not possible and relative viscosity becomes infinite. The solid volume fraction at this point is termed the maximum packing fraction, φ_{max}, and alongside relative viscosity, is a key term used in modelling and understanding the behaviour of suspensions.

In line with Rigden's observations relating to voids within compacted filler, the effects of solid volume on viscosity are scaled by φ_{max} and this is an important variable controlling the rheology of suspensions. Most asphalt researchers have found that the voids in the compacted filler, "Rigden Voids", a property related to the maximum packing fraction, is the property of the filler most suited to predicting the relative viscosity of bitumen filler

mastics (Heukelom and Wijga, 1971; Kavussi and Hicks, 1997; Kandhal, 1980; Kandhal et al., 1998; Cooley et al., 1998; Anderson et al., 1992a, 1992b).

Crucially however, voids in the compacted filler are typically measured in air and thus do not account for interactions between the bitumen and the filler in the mastic. Interactions of fillers in different bitumen types may lead to changes in φ_{max} caused by different dispersions of the filler in different bitumens, or alternatively changes in the viscosity of the liquid phase by restructuring, physio-chemical changes or other such effects on the bitumen.

Several researchers have noted that different fillers stiffen different bitumen types to a different extent (Anderson et al., 1982; Dukatz and Anderson, 1980; Shashidar and Romero, 1998) and this has been a limitation to the approach of measuring the filler properties in air. It has been observed that fillers stiffen to a different extent with different bitumen types, inferring a level of interaction between filler and bitumen beyond the bulk filling. There has been a general consensus amongst researchers (Rigden, 1947; Heukelom and Wijga, 1971; Anderson and Goetz, 1973; Shashidar and Romero, 1998) that the effects of fillers in bitumen are a result of two factors – the physical volume concentration of solid particles and interactions between the filler surface and the bitumen.

Extreme cases have been noted such as hydrated lime where stiffening massively exceeds the potential estimated by voids in the mineral filler (Shashidar and Romero, 1998). Despite this, the vast majority of filler research has focussed on linking the stiffening effect of different fillers to a simple index property of the filler in air, namely “Rigden Voids”.

Although several researchers have commented on the importance of surface interactions in bitumen-filler mastics, these effects have not been dealt with in isolation from the bulk filling effects associated with the magnitude of φ_{max}, the maximum packing fraction.

The free energy of adhesion between two materials, such as between filler and bitumen, is given by the equation (Dupré, 1869) using the surface energy of the filler and bitumen that comprise the mastic.

Surface energy, and in particular its application to moisture damage in asphalts has been the subject of much current research giving rise to new methods for quantification of the interaction between the two or more phases (Cheng, 2002; Hefer, 2004; Bhasin, 2006). Knowledge of the surface energy of the bitumen and the filler enables the level of adhesion between the two phases to be quantified and its importance for the rheology of mastics assessed. Such a characterisation has not been applied to the study of asphalt-filler interactions and their implications for the rheology of suspensions.

By choosing an appropriate rheological model to describe the behaviour of the mastics, the stiffening effects outside of the bulk volume filling can be separated from the surface effects and compared to the magnitude of interaction between the two phases, bitumen and filler.

CHAPTER III

EXPERIMENTAL SET UP

INTRODUCTION

In order to investigate the effects of the surface characteristics of bitumen-filler mastics, a detailed experimental plan was required to encompass the requirements of the three rheological models chosen for the study, proposed by Mooney, Krieger-Dougherty and Chong. All three models possess the same factors, solid volume fraction (φ), the maximum packing fraction (φ_{max}), relative viscosity (η_{rel}) and intrinsic viscosity *($[\eta]$).* By way of an example, Equation 9, the Krieger-Dougherty model is outlined below.

$$\eta_{rel} = \left(1 - \frac{\phi}{\phi_{\max}}\right)^{-[\eta]\phi_{\max}} \tag{9}$$

For each mastic, the solid fraction needs to be accurately determined through determination of particle density of the fillers. The maximum packing fraction of the fillers needs to be defined by making tests at different levels of solid volume addition, and a relative viscosity, or related measure is required. Finally, having determined these factors, the intrinsic viscosity can be calculated for each model.

The most appropriate model(s) was to be chosen and the rheological factors compared to the interactive adhesive energy between the bitumen and filler. To calculate the adhesive energy between the two phases of the mastic, the Dupré equation (Equation 20) would be used, necessitating the measurement of surface energy of all bitumens and fillers selected for the study.

During the experimental work, ten fillers were examined in three different bitumen types. The fillers were divided into two sub-sets based on their petrologic type. Five fillers were manufactured from aggregates where calcium carbonate was the principal mineral and five were derived from igneous aggregates containing a significant proportion of silica. The three bitumens were chosen to represent a range of both chemical and rheological types.

The intention was to provide a set of fillers with a relatively small range of physical properties such as particle size distribution and shape, but with variations in surface characteristics. To this end, fillers were ground in the laboratory to produce fillers of essentially the same particle size distribution and particle size.

Following filler manufacture, a series of detailed classification tests were undertaken on the fillers and bitumen used to manufacture the mastics. A summary of the testing carried out is given below.

For the fillers:

PHYSICAL CHARACTERISATION

- Particle Size Distribution using laser diffraction
- Particle Shape – aspect ratio by optical microscopy
- Particle Density
- Water absorption (of parent aggregate)
- Compacted "Tap" Density and estimation of φ_{max}

SURFACE CHARACATERISATION

- Surface area using laser diffraction and the BET Technique
- Methylene Blue Testing
- Surface Energy (Van Oss approach) – Dynamic Vapour Sorption technique.

For the bitumens:

RHEOLOGICAL CHARACTERISATION

- Penetration
- Softening point
- Determination of creep compliance using Dynamic Shear Rheometer, tests carried out over the temperature range 45-69^{o}C

SURFACE CHARACTERISATION

- Determination of surface energy by sessile drop, Van Oss Approach

A series of mastic tests were then carried out on each filler type in the three bitumen types. Firstly simple testing, using change in softening point, "Delta Ring and Ball Tests", was carried out for each bitumen-filler combination. The values of Delta Ring and Ball were compared with the physical and surface characteristics of the fillers. Following this, more complex creep compliance testing was undertaken at three solid volume fractions, 0.3, 0.4 and 0.5 over the temperature range 45^{o}C to 69^{o}C. Hence all rheological measurements were made at high in-service temperatures associated with asphalt pavements. Relative creep compliance was calculated at each temperature and solid volume concentration. The maximum packing fraction $\varphi_{\max}$ was calculated using a two-point projection method.

For the creep testing, the effects of the fillers were examined in two ways. Firstly, the behaviour of the ten fillers in a single bitumen type was modelled rheologically using the three models. Additionally, the changes in the values of φ_{max}, and $[\eta]$ with temperature were derived and discussed in the context of the filler characteristics. This work is outlined in Chapter IV.

Finally, the behaviour of a single filler type was examined in the three different bitumen types, and modelled in the manner described above. Additionally, the bond energy was calculated for each bitumen-filler combination and compared to the rheological model parameters. These results and discussion are presented in Chapter V.

CHARACTERISATION OF REFERENCE MATERIALS

Selection and manufacture of the fillers

According to Wypych (1999), calcium carbonate can be considered "inert" as it does not possess the functional groups at the surface. On the other hand, silica based fillers do possess functional groups of their surface and can form bonds as depicted by Figure 3-1. It follows that there should be differences between the behaviour of fillers derived from calcium carbonate aggregates and fillers derived from siliceous aggregates.

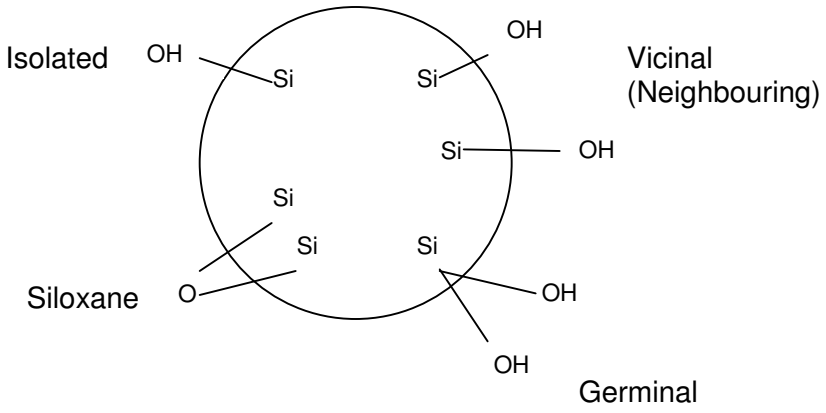

Figure 3-1: Functional groups at the surface of silica (after Wypych, 1999)

For this study, five fillers were manufactured from aggregates where the predominant mineral was calcium carbonate and can be considered "inert", and five fillers were manufactured from aggregates where the predominant mineral was silica which can be considered "active".

The ten fillers were ground in the laboratory from natural aggregates and all fillers had particles substantially smaller than 100µm. Filler samples were laboratory manufactured from clean, very large single pieces of aggregate (>80mm aggregates). The aggregates were ground in a mill to produce samples, as far as was possible, where the particle size distribution of the fillers were similar. Figure 3-2 shows the type of equipment used to produce the fillers.

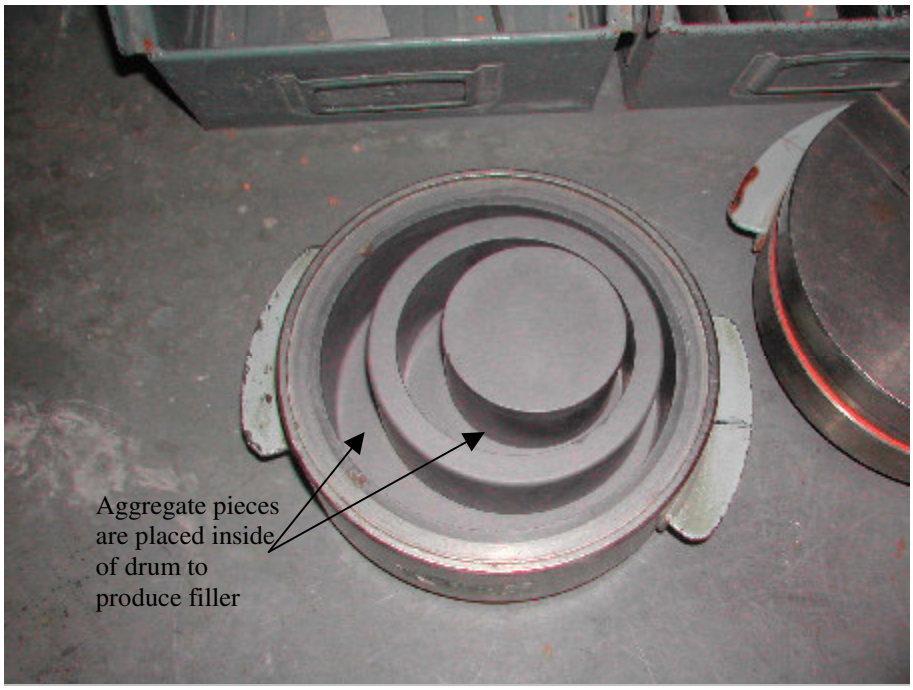

Figure 3-2: Equipment used to produce the filler samples

The aggregate types from which the fillers were made represent many of the major aggregate types used in the production of asphalt. For the calcium carbonate based fillers, C1-5, C1 and C2 were pure calcium carbonate and therefore chemically identical, although derived from different sources of pure calcium carbonate. By "pure", more than 99% of the aggregate was composed of calcium carbonate. Fillers C3 and C4 were dolomitic. A

dolomitic limestone contains magnesium carbonate as well as calcium carbonate and although such materials are considered to be “limestones” they do differ chemically to “pure” limestones such as C1 and C2, as a proportion of the calcium carbonate is replaced by magnesium carbonate. Again, it would be expected that the behaviour of fillers derived from dolomitic limestones would differ from pure limestones.

Finally, Filler C5 was a limestone with a significant proportion of clay within the matrix of the aggregate. The presence of clay minerals in the matrix gives rise to functional groups at the surface and may cause the filler to behave in a way closer to the siliceous Fillers S1-5 than the other limestone fillers.

The second subset is based on aggregates where silica is one of the principle minerals present. These fillers are considered to be active as discussed previously. The petrology of sub-group S1-5 is more complex than for sub-group C1-5. A very brief description of the petrological type of each filler is given below. The following definitions are taken from the US geological survey website (http://geology.usgs.gov/).

Filler S1

Granodiorite: An intrusive igneous rock similar to granite, but contains more plagioclase than potassium feldspar. It usually contains abundant biotite mica and hornblende, giving it a darker appearance than true granite. Mica may be present in well-formed hexagonal crystals, and hornblende may appear as needle-like crystals.

Filler S2

Granite-Gneiss: A foliated crystalline rock composed essentially of silicate minerals with interlocking and visibly granular texture, and in which the foliation is due primarily to alternating layers, regular or irregular, of contrasting mineralogic composition. In general, gneiss is characterized by relatively thick layers as compared with a schist. According to their mineralogic compositions, gneisses may correspond to other rocks of crystalline, visibly granular, interlocking texture, such as those included under the definition of commercial granite, and may then be known as granite gneiss if strongly foliated, or gneissic granite if weakly foliated. Gneisses that are metamorphosed igneous rocks or their equivalent are termed granite gneisses.

Filler S3

Basalt: A hard, black volcanic rock with less than about 52 weight percent silica (SiO_2). Because of basalt's low silica content, it has a low viscosity (resistance to flow). Therefore, basaltic lava can flow quickly and easily move >20 km from a vent. The low viscosity typically allows volcanic gases to escape without generating enormous eruption columns. Basaltic lava fountains and fissure eruptions, however, still form explosive fountains hundreds of meters tall. Common minerals in basalt include olivine, pyroxene, and plagioclase. Basalt is erupted at temperatures between 1100 to 1250°C.

Filler S4

Amphibolite: The name amphibolite usually refers to a type of metamorphic rock, an igneous rock composed dominantly of amphibole. Amphibole refers to the family of silicate minerals forming prism or needlelike crystals. Amphibole minerals generally contain iron, magnesium, calcium and aluminum in varying amounts, along with water. Hornblende always has aluminum and is a most common dark green to black variety of amphibole; it, forms in many igneous and metamorphic rocks. Actinolite has no aluminum; it and is needle-shaped and light green

Filler S5

Gneiss: Gneiss is a common and widely distributed type of rock formed by high-grade regional metamorphic processes from preexisting formations that were originally either igneous or sedimentary rocks. Gneissic rocks are coarsely foliated and largely recrystallized but do not carry large quantities of micas, chlorite or other platy minerals.

A summary of the petrologic type of the fillers is given in Table 3-1 below

Table 3-1: Petrologic type of the fillers manufactured for the study

Limestone Fillers		**Silica Fillers**	
C1	Calcium Carbonate	S1	Granodiorite
C2	Calcium Carbonate	S2	Granite-Gneiss
C3	Dolomitic Limestone	S3	Basalt
C4	Dolomitic Calcite	S4	Amphibolite
C5	Mudstone	S5	Gneiss

Physical characterisation, overview

Each of the fillers were tested for the following physical properties:

- Particle Size Distribution using laser diffraction
- Particle Shape – aspect ratio by optical microscopy
- Particle Density
- Water absorption (of parent aggregate)
- Compacted "Tap" Density and estimation of φ_{max}

Particle Size Distribution

The fillers were tested using a "Malvern Mastersizer S" particle size analyzer, which uses a laser diffraction technique, as outlined previously in Chapter II. The type of equipment used can be seen in Figure 3-3. The fillers were dispersed in ethanol during the test and ultrasonic separation applied for 180 seconds prior to determination of particle size distribution.

Particle size distributions by volume, by mass and specific surface area were calculated, (assuming that particles were spherical). Additionally, several descriptors of the particle size distribution were derived, Fineness Modulus, $D_{10}V$ (diameter at which ten percent by volume of particles are smaller than), and the Uniformity Coefficient D60/10 (the diameter at which 60% by mass of particles are smaller than divided by the diameter at which 10% by mass of particles are smaller than). A summary of the particle size distribution results is given in Table 3-2.

Table 3-2: Particle size distribution data for the fillers data obtained by laser diffraction technique

Filler	Passing 100µm	Passing 60µm	Passing 20µm	D(v,0.90) µm*	D(v,0.50) µm*	D(v,0.10) µm*
C1	94.3	84.1	64.2	79.2	7.8	1.1
C2	97.5	89.0	64.4	63.0	9.9	1.3
C3	97.0	87.6	64.2	66.8	9.5	1.1
C4	96.5	87.9	65.5	66.8	9.5	1.2
C5	96.9	90.1	74.5	59.8	4.5	0.9
S1	91.3	75.3	45.1	95.2	25.0	2.3
S2	88.1	68.9	35.9	106.4	35.0	3.6
S3	95.3	84.2	57.8	76.3	14.1	1.8
S4	92.8	77.1	47.6	89.7	22.5	1.8
S5	93.4	81.3	53.9	85.0	17.0	2.0

*Diameter where x% by volume is smaller.

Figure 3-3: Equipment used for measuring particle size distribution of the fillers - laser diffraction technique

All fillers were substantially finer than 100 microns in particle size. As a general trend, Fillers S1-5 are coarser than Fillers C1-5. Filler C5, which has a significant proportion of clay within its matrix produced the finest particle size distribution of the fillers produced. The greatest variation between the fillers is at the percentage passing 20μm with a range of 35 – 75% for the ten fillers. Fillers C1-4 gave very similar results for the particle size descriptors.

Fineness modulus and coefficient of uniformity

As outlined in Chapter II, Fineness modulus is an empirical mathematical description of the fineness of a material and is typically derived by taking the sum of the percentage of material passing different sizes allowing easier comparisons between materials with different particle size distribution curves.

The coefficient of uniformity gives an indication of the range of sizes within a particle size distribution. A low coefficient of uniformity indicates a PSD with a small range of particles. For each filler, Uniformity Coefficient and Fineness Modulus were calculated and presented in Table 3-3.

Table 3-3: Uniformity coefficient and fineness modulus of the fillers

Fillers	Uniformity Coefficent (D60/D10)	FM
C1	13.1	4.1
C2	12.9	4.1
C3	14.4	4.2
C4	12.5	4.1
C5	7.9	4.9
S1	15.7	3.0
S2	13.0	2.5
S3	12.0	3.6
S4	18.7	3.2
S5	12.9	3.4

The fineness modulus captures the particle size distribution information in a single figure and hence it relates closely to individual points taken from the particle size distribution curve. For example, Figure 3-4 shows the close relationship between fineness modulus and the D60 value. As a result, the fineness modulus was chosen in this study as the single value to represent the particle size distribution information obtained using the laser diffraction tests.

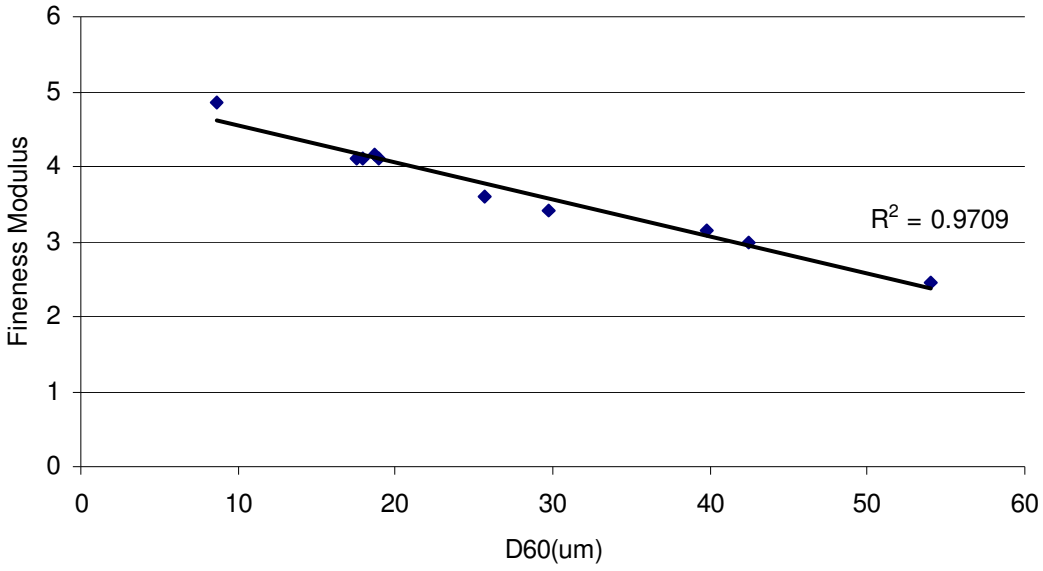

Figure 3-4: Relationship between the D60 and Fineness Modulus of the fillers

Aspect Ratio

A simple characterisation of shape of the filler particles was carried out using optical microscopy. Several digital photographs of the ten fillers were taken under normal light. The average aspect ratio was calculated as the ratio of the longest dimension of the filler particle to the shortest dimension, using 100 particles of each filler type. The results for each filler type are given in Table 3-4.

Table 3-4: Average aspect ratio of the fillers obtained using optical microscopy

Filler	Average Aspect Ratio	Filler	Average Aspect Ratio
C1	1.31	S1	2.14
C2	1.34	S2	1.74
C3	1.35	S3	1.54
C4	1.73	S4	2.34
C5	1.75	S5	2.14

In general filler set C1-5, derived from aggregates where calcium carbonate is the principal mineral have more uniform particles than filler set S1-5, however there is not a clear distinction between the two filler subsets with regard to particle shape. Fillers based on pure calcium carbonate, C1 and C2 produced fillers with the lowest aspect ratio, and conversely the highest aspect ratios were recorded for the siliceous Fillers S1, S4 and S5.

The particle shape of the fillers is quite uniform when put into the context of the wide range of materials available for use as fillers and rheology modifiers. Aspect ratios in the range of 1.3 – 2.3 represent relatively regular particle shapes, when compared to fibres or rod-like particles which can possess aspect ratios as high as 20 (Barnes, 2000).

Particle Density and Water Absorption

The importance of the volumetric properties of a suspension has been outlined in Chapter II, thus before a calculation of the solid volume fraction, φ, can be made, the particle density of the fillers need to be measured. This is a simple procedure based on Archimedes principle and standardised in Europe as BS EN 1097-7:1999.

For each filler, a small sample was oven dried to constant mass at 105°C, weighed and placed in a small pycnometer. The pycnometer was filled with distilled water at 20°C

and the total mass recorded. The pycnometer was then emptied and washed and dried. The volume of water in the pycnometer is then measured by filling with distilled water at 20^{o}C and the density simply calculated as the mass of filler divided by the volume of filler measured by displacement.

The measurement of water absorption of the filler is not as straightforward as the measurement of absorbed water requires the surface drying of the filler to include only the water absorbed by the filler and not excessive surface moisture. As a result the water absorption of the parent rock used to produce the fillers was taken. The range of water absorptions is very low, 0.3-1.4% by mass with most parent aggregates having water absorption less than 1% by mass. For the purpose of this study, the water absorption was considered to be a constant for the ten fillers. Table 3-5 below summarises the particle density and water absorption of the fillers.

Table 3-5: Particle density and water absorption of the fillers

Filler	Specific Gravity (Mg/m^3)	Water Absorption (%) 0/4mm Fraction of parent rock
C1	2.70	0.6
C2	2.70	0.8
C3	2.78	0.8
C4	2.78	0.5
C5	2.65	1.4
S1	2.68	1.0
S2	2.68	0.3
S3	2.67	1.1
S4	3.02	0.4
S5	2.68	0.9

Estimation of maximum packing fraction

Estimations of maximum packing fraction of the fillers were carried out using the following procedure. Filler, weighed to constant mass after oven drying at 105°C, was compacted into a glass vial and repeatedly tapped. More filler was added and further tapped and weighed until a maximum constant mass was achieved to fill the glass vial. The volume of the container was measured using distilled water at 20°C, and the bulk density of the filler calculated. The specific gravity of the fillers, measured using the pyknometer method as outlined in the previous section, was then used to calculate the volume fraction present in the compacted filler. This approach is the inverse of Rigden's approach, where the level of voids is reported (See Chapter II). The results are given in Table 3-6 below.

Table 3-6: Bulk volume properties and estimated φ_{max} for the fillers

Fillers	Tap Density (Mg/m^3)	Estimated φ_{max}
C1	1.073	0.398
C2	1.213	0.449
C3	1.242	0.467
C4	1.628	0.603
C5	1.293	0.482
S1	1.574	0.583
S2	1.383	0.507
S3	1.364	0.513
S4	1.163	0.431
S5	1.730	0.562

The values, 0.4 – 0.6, for the fillers compare well with observations made by other researchers in the field of asphalt (Kandhal, 1980; Cooley et al., 1998; Harris and Stuart, 1998; Anderson et al., 1973,1982). The fillers produced can be thus considered typical of those employed in asphalts with regard to void content of the compacted fillers.

Summary of physical properties

The physical characteristics of the fillers are similar, with a relatively small range of particle densities and shapes and similar particle size distributions. In general, fillers C1-5 are finer and have lower aspect ratios compared to Fillers S1-5. No clear trend was evident in the tap density determinations and calculations of estimated φ_{max} for the ten fillers. In order to simplify the rheological analysis three key factors are taken from the physical characterization to describe the fillers (all unitless). These are summarised in Table 3-7.

Table 3-7: Key physical characteristics of the filler used in the study

Fillers	Estimated ϕmax	Average Aspect Ratio	Fineness modulus
C1	0.398	1.31	4.11
C2	0.449	1.34	4.11
C3	0.467	1.35	4.15
C4	0.603	1.73	4.12
C5	0.482	1.75	4.85
S1	0.583	2.14	2.98
S2	0.507	1.74	2.46
S3	0.513	1.54	3.60
S4	0.431	2.34	3.15
S5	0.562	2.14	3.42

Surface characterisation

Introduction

In addition to the physical characteristics of the filler, several surface properties were measured. Two measures of surface area were made, one derived from the laser diffraction particle size distribution data and a second calculated using the BET equation outlined in the previous chapter. Surface energy measurements were made on the fillers using a dynamic vapour sorption technique. Measurements were made using three gases and the surface

energy components calculated according to the Van Oss Approach. In addition, a further simple measure related to surface area/ surface energy, the Methylene Blue Value was determined for the ten fillers.

Surface area measurements

The first measure of surface area was taken from the laser diffraction determinations of particle size distribution. This technique assumes that the particles are solid and spherical.

The surface area was also measured using the BET technique and the Methylene Blue Value was also recorded. Details of the principle and calculation of the BET surface area are given and outlined in Chapter II. The BET measurements of the fillers used in this study were carried out using octane gas during the surface energy measurements carried out by Surface Measurement Systems UK.

Specific surface area by BET accounts for surface texture, shape and pores accessible to the saturate gas, rather than being based on the assumption in the laser diffraction tests that the particles are spherical solid particles. Therefore the BET value should be more realistic as a value of specific surface area compared to the calculation of surface area based on assumptions of particle shape and porosity.

The Methylene Blue Test (BS EN 933-9 1999) measures the quantity of Methylene Blue dye a sample can absorb onto its surface. Typically, the Methylene Blue Test is used to estimate the quantity of clays present in a fine aggregate. Clays have very large surface areas and relatively small quantities of clays give rise to measurable values for Methylene Blue Value. Some countries, for example in France, specify aggregate cleanliness by Methylene Blue Value.

Increments of a solution of Methylene Blue are added successively to a suspension of the test portion in water. The adsorption of dye solution by the test portion is checked after each addition of solution by carrying out a stain test on filter paper to detect the presence of free dye. When the presence of free dye is confirmed, the Methylene blue value is calculated and expressed as grams of dye adsorbed per kilogram of the size fraction tested.

A summary of the surface area measured by Laser Diffraction and the BET method, plus Methylene Blue Values of the fillers used in this study are summarised in Table 3-8.

Table 3-8: Specific surface area of the fillers measured by laser diffraction and BET Technique and Methylene Blue Values

Fillers	SSA Laser (m^2/g)	SSA BET (m^2/g)	Methylene Blue Value (g/kg)
C1	1.90	1.44	0.8
C2	1.70	1.23	0.6
C3	1.87	0.97	0.2
C4	1.74	1.93	1.8
C5	2.46	8.27	9.2
S1	0.91	0.71	1.1
S2	0.64	0.67	0.9
S3	1.17	2.21	3.4
S4	1.15	0.62	1.4
S5	1.10	1.85	1.4

The values of surface area obtained from laser diffraction testing range from 0.64 – 2.46 m^2/g, whereas the values obtained from the BET procedure range from 0.62 – 8.27 m^2/g. The greater range for the BET values is result of the very high value obtained for Filler C5. Excluding Filler C5, all determinations of specific surface areas from the two techniques range from 0.62 - 2.21 m^2/g. As previously stated, Filler C5 contains a significant amount of clay within the matrix of the aggregate. In several cases, the BET value is lower than the specific surface area measured using laser diffraction. It would be expected that as the BET

technique includes pores accessible to the probe gas, the specific surface areas recorded using this technique should be higher than the values obtained by laser diffraction, which assumes the particles are solid. The lower values of BET could be attributable to the use of octane as the probe gas, which compares to nitrogen that is often used, is a relatively large molecule. This could limit the area accessible to the gas and hence lead to values lower than those obtained using laser diffraction.

The Methylene Blue Values ranged from 0.15 to 9.24g/kg, representing a wide range of values. Once again, Filler C5 is markedly different, having a far higher Methylene blue value than the other fillers. Where other researchers have measured Methylene blue values very similar results were found. A study of characterization tests for fillers examined six filler types – Natural Sand, Limestone, Dolomite, Granite, Blast Furnace Slag and Limerock - and the Methylene blue values ranged from 0.3 – 18.7 (Kandhal et al., 1998). Two fillers derived from natural sand and limerock respectively had values of 9.5g/kg and 18.7g/kg and the lowest recorded value of MBV was filler derived from dolomite. This is consistent with the values obtained in this study, where Filler C3, derived from dolomite, also gave a low result, 0.2g/kg.

Both surface area by laser and fineness modulus are derived from the same particle size distribution data and, as would be expected, there is a very close correlation between the two values, which are essentially mathematical descriptors of the same data. Figure 3-5 below shows the correlation between the two values. Therefore, it is only necessary to consider one of these parameters in any further analysis.

The Methylene Blue test is conceptually similar to a gas sorption test where gas is absorbed onto the surface until “free” gas is measured by changes in the gas pressure in the

test chamber. The values of specific area measured by BET and Methylene Blue Value (MBV) are therefore relatively well correlated, with Filler C5 having the highest BET/MBV compared with the other samples.

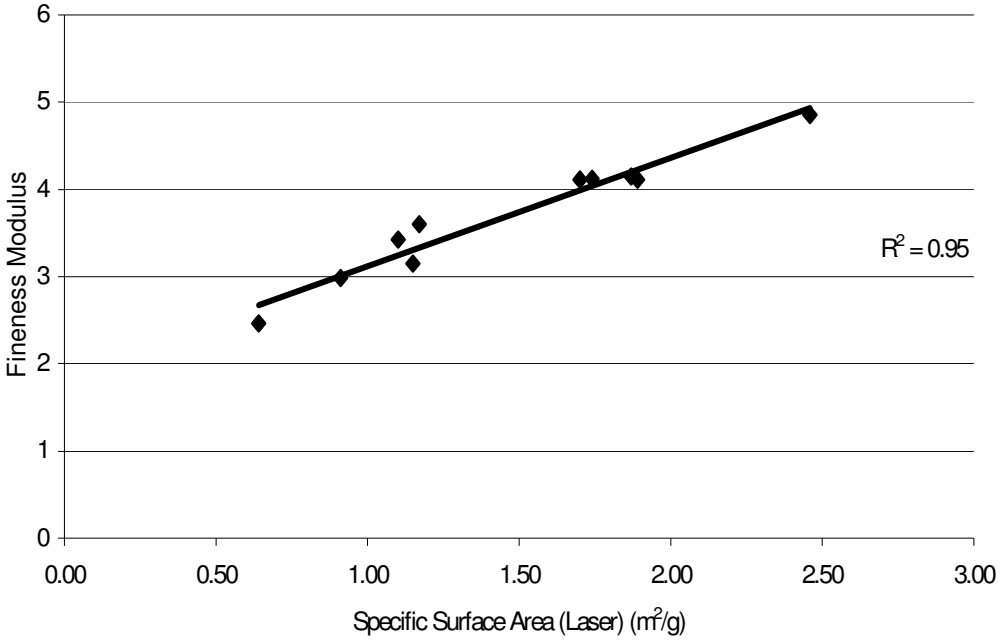

Figure 3-5: Correlation between Fineness Modulus and Specific Surface Area measured by laser diffraction

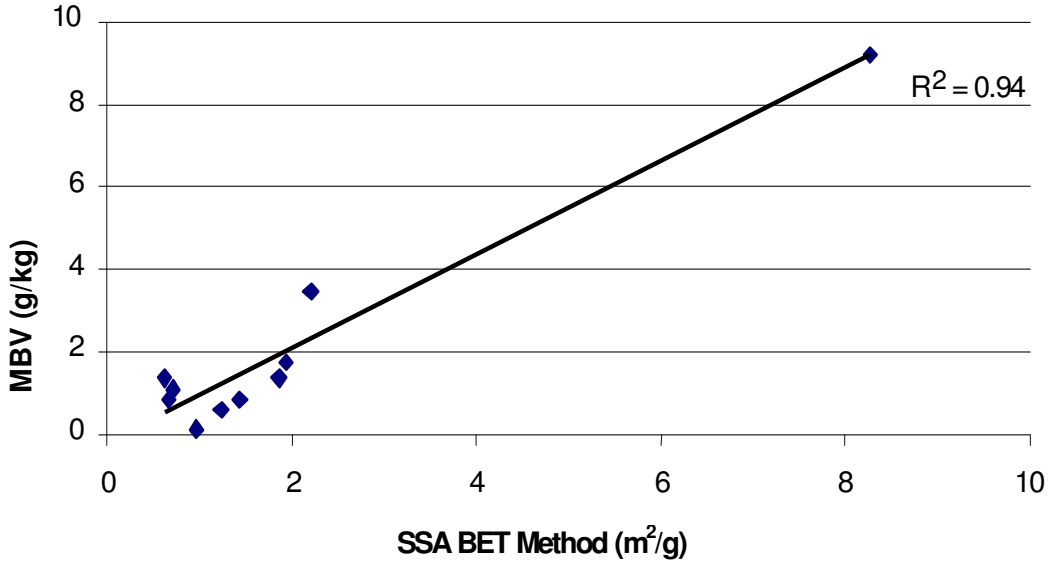

Figure 3-6: Correlation between Methylene Blue Value and Specific Surface Area measured by BET Method

The correlation between the two sorption type determinations and the laser diffraction results are not good, although all three methods show Filler C5 as the filler with the largest surface area. Figure 3-8 below shows the relationship between specific surface area measured by laser and BET techniques.

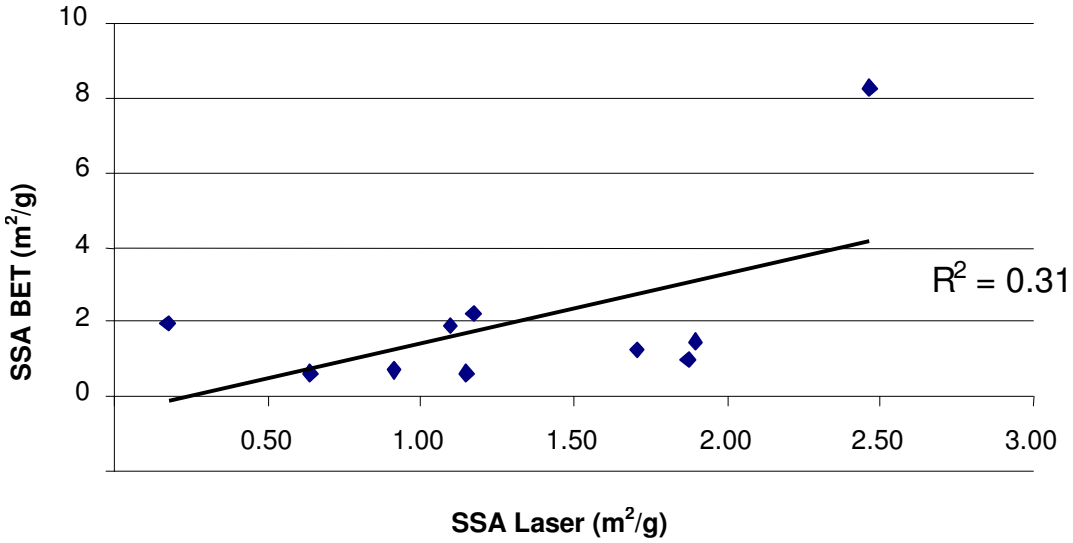

Figure 3-8: Correlation between Specific Surface Area measured by BET Method and Specific Surface Area measured by laser

Surface energy measurements

To quantify the magnitude of adhesive energy between two materials, such as filler and bitumen, using the Dupré equation (Equation 20), it is necessary to measure the surface energy of both components. Chapter II described the theory and use of contact angles to relate the interaction between a solid and a liquid. To measure contact angles directly it is necessary to prepare samples of flat, smooth, non-porous surfaces of solid large enough to place drops of liquid upon. For measuring the surface energy of fine powders, like fillers, Dynamic Vapour Sorption (DVS) testing is a relatively new technique developed to measure the surface energy of high surface area solids, such as fillers (Levoguer et al., 2003). The basic principles of the test are given below.

In the Young Equation (Equation 22) the interaction between the solid and the vapour and the liquid and vapour are assumed to be negligible when a measurable contact angle is

formed. In a vapour sorption measurement the surface tension of the liquid is considerably less than the energy of the solid surface and spreading occurs. The resulting contact angle is zero and the magnitude of the spreading pressure significant. This relationship forms the basis of the vapour sorption approach of measuring surface energy.

The interaction between a solid and a liquid in a vapour sorption test can be described by a derivation of the Young-Dupré equation.

$$W_{SOLID-LIQUID} = \gamma_{LIQUID-VAPOUR}(1+\cos\theta) + \pi_e \qquad (34)$$

Where:

π_e = the equilibrium spreading pressure, which is equal to the reduction in surface energy of a solid surface due to surface adsorption of vapour onto the surface from the adjacent liquid phase.

When the phase angle is zero, Young's equation can be simplified to

$$W_{SOLID-LIQUID} = 2\gamma_{LIQUID-VAPOUR} + \pi_e \qquad (35)$$

The equilibrium spreading pressure, πe,, is defined as the net change in surface energy of a surface resulting from the adsorption of vapour onto the surface. Using Gibbs surface tension equation, the change in surface energy can be written as:

$$d\gamma = -RT\,\Gamma\, d \ln p \qquad (36)$$

Where:

R = the universal gas constant (8.314 J mol^{-1} k^{-1})

T = temperature (K)

Γ = the amount of adsorbate per unit area (mol mm^2)

p = the partial pressure (Pa)

π_e can be calculated from:

$$\pi e = \frac{RT}{\sigma} \int \Theta d \ln p \qquad (37)$$

Where:

Θ is the total amount adsorbed (mm^3 g^{-1})

σ is the specific surface area (m^2 g^{-1})

As the surface energy of the liquid is known from literature, the solid-liquid work of adhesion can be calculated if the spreading pressure is known. By using an apolar gas for one experiment, the dispersive component, γ^{LW} can be determined directly and the use of two (or more) further gases of differing polarity allows the calculation of surface energy components γ^+ and γ^- of the solid according to the approach developed by Van Oss and others (Good, 1992; Good and Van Oss, 1992).

It is important to note that the same probe liquids/gases can not be used effectively in both contact angle and vapour tests. In contact measurements a liquid which does not spread significantly on the substrate is required, whilst in vapour sorption tests a vapour which readily spreads is required. The test liquids, and their surface energy components, used in the vapour sorption tests are given in Table 3-9 below.

Table 3-9: Test liquids used in the vapour sorption tests and their surface energy components

Liquid	γ^{TOTAL} (mN m^2)	γ^{LW} (mN m^2)	γ^+ (mN m^2)	γ^- (mN m^2)
Chloroform	27.32	25.0	3.80	0.00
Octane	21.62	21.62	0	0
Ethyl acetate	23.97	19.60	0.00	19.20

Sub-samples of the fillers were prepared and surface energy measurements determined using the DVS technique as outlined above, the results of the tests are presented in Table 3-10.

Table 3-10: Surface energy components of the fillers

SURFACE ENERGY					
Fillers	γ^{TOTAL}	γ^{LW}	γ^{AB}	**γ+**	**γ-**
C1	88.4	84.0	4.4	10.7	0.4
C2	56.6	54.6	2.1	0.4	3.0
C3	83.3	81.5	1.8	7.3	0.1
C4	80.8	73.8	7.1	7.1	1.8
C5	125.5	70.6	54.9	23.9	31.5
S1	106.3	77.2	29.0	32.5	6.5
S2	82.2	81.2	1.1	4.9	0.1
S3	87.2	61.4	25.9	35.0	4.8
S4	73.0	71.5	1.5	2.6	0.2
S5	84.2	71.6	12.6	5.4	7.4

The values obtained are reasonably consistent with recent results published relating to the surface energy of aggregates for use in asphalt (Hefer, 2004; Bhasin, 2006). The sub-groups C1-5 and S1-5 do not present a clear trend with respect to the levels of the components of surface energy measured. Three of the Fillers, C5, S1 and S3 have significantly higher levels of γ^+ and γ^- than the other fillers.

Summary of the filler characterisation

Ten fillers were laboratory manufactured for the study and an extensive testing programme was undertaken to characterize the fillers. Several properties measured are inter-related and where possible a rationalization was carried out to limit the number of factors to be considered in the rheological evaluation of the mastics.

Data obtained from laser diffraction tests can be presented in several ways, as a particle size distribution curve, a fineness modulus or specific surface area, but essentially all

are derived from the same data and as a result are well correlated. To this end, Fineness Modulus was chosen to represent the characterization of the filler by laser diffraction tests.

Maximum packing fraction, φ_{max}, was estimated by using compacted dry density of the filler as related to the specific gravity, while shape was quantified by optical microscopy and the calculation of aspect ratios.

In addition to physical characterization of the fillers, state-of-the-art tests were carried out to calculate the surface energy components of each filler using dynamic vapour sorption tests. γ^{TOTAL}, γ^{LW}, γ^{AB}, γ^{+} and γ^{-} were derived for each filler. Again, as γ^{AB} is derived directly from γ^{+} and γ^{-}, it was not used in the later rheological analysis. Additionally γ^{TOTAL} is simply the sum of γ^{AB} and γ^{LW}, so this value was also not considered. A summary of the key filler properties is given in Table 3-11.

Table 3-11: Summary of the key index parameters of the fillers examined in the study

FILLERS	PHYSICAL			SURFACE AREA		SURFACE ENERGY (mN/m^2)		
	φ_{max}	Aspect Ratio	Fineness Modulus	BET (m^2/g)	MBV	γ^{LW}	γ +	γ-
C1	0.398	1.31	4.1	1.44	0.83	84.0	10.7	0.4
C2	0.449	1.34	4.1	1.23	0.61	54.6	0.4	3.0
C3	0.467	1.35	4.2	0.97	0.15	81.5	7.3	0.1
C4	0.603	1.73	4.1	1.93	1.78	73.8	7.1	1.8
C5	0.482	1.75	4.9	8.27	9.24	70.6	23.9	31.5
S1	0.583	2.14	3.0	0.71	1.1	77.2	32.5	6.5
S2	0.507	1.74	2.5	0.67	0.87	81.2	4.9	0.1
S3	0.513	1.54	3.6	2.21	3.44	61.4	35.0	4.8
S4	0.431	2.34	3.2	0.62	1.4	71.5	2.6	0.2
S5	0.562	2.14	3.4	1.85	1.35	71.6	5.4	7.4

Selection of bitumens

Three different bitumen types were chosen for the experimental work:

- B1: 40/60 Penetration Grade Venezuelan bitumen
- B2: 10/20 Penetration Grade Venezuelan bitumen
- B3: A polymer-modified synthetic resin

Bitumens B1 and B2 are derived from the same crude oil source and should be chemically similar. Whereas Bitumens B1 and B3 have similar penetration and softening point and are rheologically similar although chemically very different. Bitumens B2 and B3 are dissimilar both chemically and rheologically. An extensive characterization was carried out on the three bitumens prior to the mastic stage of the experiments:

- Penetration
- Softening point
- Creep compliance measurements, DSR tests in temperature range 45-69°C
- Determination of surface energy by sessile drop technique

Rheological characterisation

Penetration (BS EN 1426:2000, BS2000-49,) and Softening Point (BS EN 1427:2000, BS2000-58) values were determined for the three bitumens and presented in Table 3-12.

Table 3-12: Penetration and Softening Point values of bitumens used in the study

Bitumen	Penetration (dmm)	Softening Point (°C)
B1	48	53.0
B2	16	68.0
B3	50	60.0

In the UK one of the most common forms of road failure is permanent deformation (rutting) where material from under the wheel path of a heavy vehicle flows and compacts to form a groove or rut. Permanent deformation in bituminous materials has been shown to be mainly due to shear displacements, although there may also be some densification under initial traffic, particularly for those pavements not adequately compacted during construction (Collop et. al., 1995).

When asphalt mixtures are loaded and unloaded, as occurs under traffic, a small amount of the deformation is not recovered on unloading. The accumulation of these loads can lead to permanent deformation over several years. Additionally, during high ambient temperatures where the asphalt mixture attains high temperatures, permanent deformation can occur very quickly.

In order to better understand the behaviour of bitumen there has been a considerable rise in more complex testing of bitumen with the aim of better characterizing the rheological behaviour of bitumen and the resulting behaviour of the asphalt mixture. Much of this change

was bought about by the climate and loading condition based "Performance Grade" classification of bitumen resulting from the US Strategic Highway Research Program of the 1990's (Kennedy et al., 1990).

Dynamic Shear Rheometers (DSRs) are used to measure the rheological characteristics of bitumens. Typically, dynamic tests are performed and the parameters that are determined are the complex modulus and phase angle from which the viscoelastic properties of the bitumen can be evaluated. The DSR has become an accepted test method for determining the dynamic mechanical properties of bitumen in the linear region (Airey, 1997).

The rheological behaviour of bitumen and mastics can also defined, and be measured using DSR, in terms of its creep compliance. Creep compliance is obtained by applying a constant stress and measuring the resulting time-dependent strain. This area has been subject to much recent research (see Chapter II).

In the UK during the Summer of 2003, very high ambient temperatures were experienced throughout July and August, and during this period there were several instances where newly installed surfacing material experienced loss of surface texture as a result of permanent deformation in the surfacing. Pavement temperatures in this period were in region of $50^{o}C$ - $55^{o}C$.

The bitumens used in the surfacing were polymer-modified and had been assessed previously using small-strain oscillatory testing using a DSR. Such measurements failed to predict the performance of the bitumens at such high ambient temperatures over a prolonged period.

Following this experience, the author developed a methodology based on creep compliance testing to better assess the likely behaviour of the bitumens in early life and/or high ambient temperature scenarios. The test examines the behaviour of the bitumen over the temperature range 45°C to 69°C using a dynamic shear rheometer in creep mode. The creep of the bitumen is measured over 1 second. The stress level used during the test is 2kPa. The bitumens in the study were assessed using this procedure. A summary of the test results is given in Table 3-13 below.

Table 3-13: Creep compliance as a function of temperature for the bitumens used in the study

	Creep Compliance @ 1 second (1/J x 10^6) Pa		
Temperature (°C)	B1	B2	B3
45	255	29	515
49	515	37	1084
53	975	49	2219
57	1770	66	3917
61	3056	90	5691
65	4902	120	7213
69	6035	169	8360

Surface energy measurements

In order to make calculations of adhesive energy of the two phases, γ_{12}, it is necessary to obtain surface energy components from both phases. As outlined in the previous sections, the fillers in the study were measured using Dynamic Vapour Sorption, due to difficulties in preparing non-porous, flat surfaces for direct measurement of contact angles.

For the bitumens, standard glass microscope slides were coated in a thin layer of bitumen and direct measurements of contact angles were made using a GBX Digidrop contact angle measurement system. The basic set up consists of a mechanical syringe for dispensing small drops, typically 5 microlitres, of test liquids, a moveable platform and a

camera and acquisition software for imaging the drops and measuring of the contact angles. As with the DVS procedure three test liquids were used (given in Table 3-14 below) and the surface energy of the bitumens expressed according to the Van Oss approach.

Table 3-14: Test liquids used in contact angle measurements and their surface energy components

Liquid	γTOTAL (mN m^2)	γLW (mN m^2)	γ+ (mN m^2)	γ- (mN m^2)
Water	72.8	21.8	25.5	25.5
Glycerol	64.0	34.0	3.92	57.4
Di-iodomethane	50.8	50.8	0	0

Separate slides were prepared for each test liquid, and onto each slide five drops of liquid were placed and measured, one at a time. The contact angle was recorded as the average of three determinations per drop, making a total of fifteen contact angle determinations per test liquid, forty-five angles per test in total. Figure 3-9 below shows an image captured by the equipment of a water drop on the surface of a test specimen.

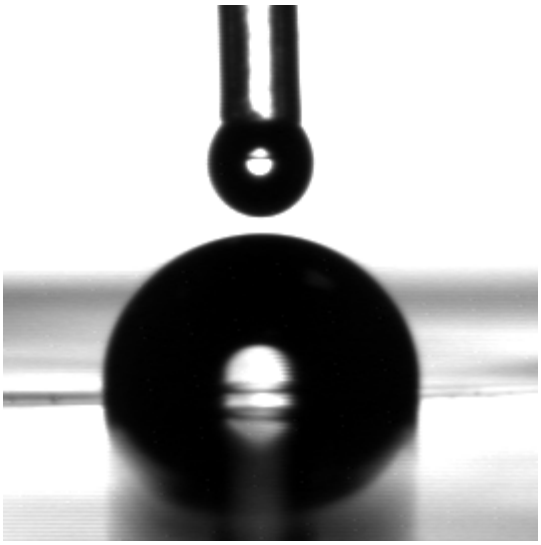

Figure 3-9: Image taken from contact angle measurements on bitumen

Once the contact angles are derived for each test liquid, for each bitumen, the surface energy components, γ^{LW}, γ^{+} and γ^{-} can be calculated as follows. The following procedure can be found in full elsewhere (Bhasin, 2006).

The Good Van Oss Chaudury equation can given as:

$$\gamma_{Liquid}(1+\cos\theta) = \left(2\sqrt{\gamma_{Liquid}^{LW}}\right)x + \left(2\sqrt{\gamma_{Liquid}^{-}}\right)y + \left(2\sqrt{\gamma_{Liquid}^{+}}\right)z \quad (38)$$

Where

γ_{Liquid} = total surface energy of the liquid

γ_{Liquid}^{LW} = LW surface energy of the liquid

γ_{Liquid}^{-} = base surface energy of the liquid

γ_{Liquid}^{+} = acid surface energy of the liquid

$\cos_{\theta}$ = contact angle (radians)

and

x = square root of bitumen surface energy γ^{LW}

y = Square root of bitumen surface energy γ^{-}

y = Square root of bitumen surface energy γ^{+}

As three test liquids were used, three linear equations (39-41), can be derived and solved as a matrix.

$2.5 = 1.5x + 0.4y + 0.5z$ (39)

$3 = 1.2x + 1y + 0.8z$ (40)

$5 = 2.1x + 2.2y + 0.3z$ (41)

Forming the matrix:

$$\left[\begin{array}{ccc|c} 1.5 & 0.4 & 0.5 & 2.5 \\ 1.2 & 1.0 & 0.8 & 3.0 \\ 2.1 & 2.2 & 0.3 & 5.0 \end{array}\right] \quad (42)$$

Solving the matrix obtains x, y and z, which represent the square root of the individual surface energy components, γ^{LW}, γ^{+} and γ^{-}. These surface energy components can then be calculated as the square of the constants, x^2, y^2, z^2 and finally, γ^{AB} and γ^{TOTAL} can then be calculated using Equations 43 and 44 below

$$\gamma^{AB} = 2\,(\gamma^{-}\gamma^{+})^{0.5} \quad (43)$$

$$\gamma^{TOTAL} = \gamma^{LW} + \gamma^{AB} \quad (44)$$

The test results for the three bitumens are given in Table 3-15.

Table 3-15: Surface energy of bitumens used in the study, determined using sessile drop technique

	γ^{TOTAL}	γ^{LW}	γ^{AB}	γ^{+}	γ^{-}
B1	31.66	29.55	2.11	3.52	0.32
B2	46.43	43.20	3.29	3.59	0.76
B3	40.46	37.86	2.60	1.85	0.91

Some researchers (Cheng 2002, Hefer 2004, Bhasin 2006) have used different methods to calculate the surface energy of bitumen, namely the Wilhelmly plate method, which allows for the calculation of an advancing and receding contact and angle, and researchers have published two sets of surface energy data referred to as wetting and dewetting surface energy. The values obtained in this study are consistent with published data for bitumens of adhesive energies from wetting experiments.

The three bitumens have similar values of surface energy, but Bitumen B2 has both the highest surface energy and the highest polar component γ^{AB} of surface energy. In all three bitumens, the Lifshitz-Van Der Waals forces are significantly higher than the acid-base components of surface energy, again this is consistent with published literature relating to surface energy of bitumens.

TESTING REGIME FOR THE MASTICS

The experimental plan was drawn up to examine and model the effects of a set of ten fillers in one bitumen type, and secondly to examine and model the effects of a single filler in three bitumen types. By investigating the effects of a single filler type in three bitumen types, many of the index properties of the fillers, such as particle shape, density and particle size distribution remain essentially the same, which allows the surface interactions to be more easily isolated.

The rheological testing was carried out in two stages. Firstly a simple rheological test was carried out using the Delta Ring and Ball procedure. Each filler was tested in each of the three different bitumen types in accordance with BS EN 13179-1:2000. The second stage involved the testing of the fillers in creep compliance tests using the Dynamic Shear Rheometer. The mastics were tested over a range of temperatures from 45°C to 69°C at 4°C increments and the relative creep compliance, $J(t)_{rel}$, calculated.

Analysis of rheological behaviour over a range of temperatures gives rise to an insight into the behaviour of a mastic system. It has been suggested that for a given system, three possibilities exist (Rigden, 1947). If the change in relative viscosity η_{rel} (or in this case relative creep compliance ($J(t)_{rel}$)) changes in the same way as viscosity of the liquid phase, then the mastic behaviour is dependent wholly on the properties of the liquid phase. If η_{rel} increases as a result of temperature, then Brownian motion effects and increase randomness with temperature are prevalent. Conversely, if the relative viscosity reduces with temperature, this could be considered the result of a physical or chemical bond which becomes progressively weaker as the temperature is increased. These effects were examined using the creep compliance data.

In summary, the testing of the mastics in creep conditions was intended to examine:

- The effect of filler concentration on relative recovery compliance.
- The relative creep compliance for each filler in the three bitumens at three solid volume fraction addition levels.
- A potential correlation with the Delta Ring and Ball testing carried out in stage one of the experiments.
- The change in relative creep compliance with respect to temperature for each mastic combination.

These results are discussed in Chapter IV.

Following this work, rheological models, proposed by Mooney, Krieger and Dougherty and Chong were applied to the data obtained from the creep compliance experiments. The following tasks were then undertaken:

- Establish the suitability of the three chosen models for bitumen-filler mastics.
- Determine η_{rel} and φ_{max}, and subsequently determine intrinsic viscosity,$[\eta]$, for each filler and bitumen combination using the four selected rheological models.
- To examine the change in η_{rel} and φ_{max} with temperature for each filler and bitumen combination.
- To investigate if any index property of the filler is responsible for any parameter used in the rheological models, i.e. φ_{max} and $[\eta]$ and their product (the MPK Coefficient).

The results of this work are outlined and discussed in Chapter V.

Finally, once all these stages were completed, an analysis of rheological modelling was undertaken to better understand the contribution of surface effects to the behaviour of bitumen: filler mastics. A comparison of the relative creep compliance, maximum packing fraction and intrinsic viscosity with the level of bond energy was carried out. Chapter VI outlines the calculations of interactive adhesive energy and their implications for the rheology of bitumen-filler mastics.

CHAPTER IV

TESTING OF THE MASTICS

INTRODUCTION

This chapter describes the test results of mastics produced from the reference materials described in the previous chapter. The rheological testing was carried out in two stages. Firstly, simple measurements using the Delta Ring and Ball procedure (BS EN 13179-1:2000) were taken. The fillers were tested in each of the three different bitumen types and the increase in softening point reported and examined against index properties of the mastic constituents.

Following this, creep compliance of the mastics was measured using a Dynamic Shear Rheometer (DSR). The mastics were tested over a range of temperatures from 45^{o}C to 69^{o}C at three levels of solid volume addition, 0.3, 0.4 and 0.5. Relative creep compliance and relative creep compliance rate were derived for each mastic. Further to this, an analysis of the change in relative creep compliance over the temperature range of the test was undertaken.

The maximum packing fraction of each bitumen-filler combination, φ_{max}, was calculated at each temperature using a two point projection technique based on the relative creep compliance recorded at 0.4φ and 0.5φ. Again, an analysis was made of the changes in maximum packing fraction with respect to temperature. Finally, normalizing the solid volume fraction by the maximum packing fraction, φ/φ_{max}, master curves of stiffening were derived for the fillers in each bitumen type.

In summary, the aim of the testing outlined in this chapter is to:

- Measure simple stiffening effects of fillers in different bitumen types using a standard test method – Delta Ring and Ball.
- Determine relative creep compliance, $J(t)_{rel}$, over a range of solid volume fractions and temperatures using a Dynamic Shear Rheometer in creep compliance mode.
- Calculate the maximum packing fraction for each filler type in each Bitumen, B1-B3, using a simple two-point projection technique.
- To examine the changes in $J(t)_{rel}$ and φ_{max} with temperature for each filler and bitumen combination.
- To investigate if any index property of the filler is responsible for the level, or change in level with temperature, of $J(t)_{rel}$ and $\varphi_{max.}$
- To derive master curves of filler stiffening for each bitumen type by normalising solid volume fraction to the maximum packing fraction, $\varphi/\varphi_{max.}$

SIMPLE TESTING – DELTA RING AND BALL TESTS

Background

The softening point test, commonly used for many years to determine the consistency of bitumen, is standardised in Europe in BS EN 13179-1:2000, BSI, London. In the test two brass rings filled with bitumen are prepared and placed in a beaker with liquid, usually water (although glycerol can be used for materials with softening points higher than 80^{o}C). A steel

ball is placed on each ring and the samples are heated at a rate of 5°C per minute until the bitumen is soft enough to allow the ball to drop through the bitumen and touch a plate mounted 25mm below the rings. The softening point of the bitumen is defined as the temperature at which this occurs.

Delta Ring and Ball tests follow exactly the same procedure, but are tested with mastics prepared to a standard volumetric composition of 0.375 filler to 0.625 bitumen. The Delta Ring and Ball value is recorded as the difference in softening point between the bitumen and the mastic. Figure 4-1 shows the ring and ball softening point equipment.

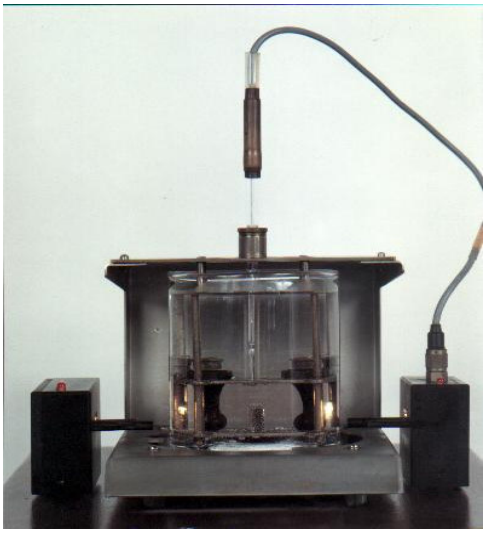

Figure 4-1: Softening Point Ring and Ball Apparatus

Theoretically, as the mastic produced in Delta Ring and Ball tests is manufactured at a fixed volumetric ratio, i.e. solid volume fraction, φ, is fixed, the Delta Ring and Ball value should be related to the maximum packing fraction of the filler as the effects of solid volume are scaled by maximum packing fraction. Fillers with lower maximum packing fraction would result in higher ratios of φ/φ_{max} and should result in larger increases in softening point.

In the UK there are no specified limits for Delta Ring and Ball tests of fillers, although with the recent introduction of EME-2 (an asphalt base material originally developed in France) into the UK, a limit of 16 has recently been proposed (Sanders and Nunn, 2005).

Test Results

The softening point of the three bitumens was determined and the change in softening point recorded for each bitumen-filler combination was calculated in accordance with BS EN 13179-1:2000. The test results are given in Table 4-1.

Table 4-1: Delta (Δ) Ring and Ball values for each filler in three bitumen types

	Δ Ring and Ball B1 (^{o}C)	**Δ Ring and Ball B2 (^{o}C)**	**Δ Ring and Ball B3 (^{o}C)**
C1	15.0	14.0	8.6
C2	14.4	14.5	7.6
C3	11.0	12.0	4.0
C4	11.2	11.2	4.2
C5	14.0	15.0	5.8
AVERAGE C1-5	**13.1**	**14.1**	**6.0**
S1	14.4	16.0	8.0
S2	11.6	12.5	8.8
S3	14.4	14.0	9.0
S4	13.6	11.8	10.0
S5	14.0	16.5	7.8
AVERAGE S1-5	**13.6**	**14.2**	**8.7**
RANGE (ALL) ^{o}C	**4.0**	**5.8**	**6.0**

Discussion of test results

The values obtained for all combinations ranged from 4°C to 17°C. All fillers had the lowest value of Delta Ring and Ball when tested in Bitumen B3, the polymer-modified resin. In general, the change in softening point in this bitumen is around half of that for the fillers in Bitumens B1 and B2. With the exception of two combinations (Fillers C2 and Filler S4 mixed with Bitumen B2 (10/20 penetration bitumen), all bitumen-filler combinations tested would conform to the suggested maximum increase of 16°C proposed in the UK for EME-2.

On average, Fillers C1-5, stiffen the bitumens to a lesser extent than Fillers S1-5, however the difference is small, less than 1°C in Bitumens B1 and B2, and 2.7°C in Bitumen B3. Fillers C3 and C4, manufactured from dolomitic aggregates, have the lowest values of Delta Ring and Ball in all three bitumens which suggests an intrinsic property in dolomitic aggregates which gives a tendency to low stiffening in bitumen.

Filler S4 has unusual results in that this filler has the highest value of Delta Ring and Ball with Bitumen B3 and the second lowest with Bitumen B2.

Bitumens B1 and B2 are chemically similar and derived from the same source of crude oil. Figure 4-2 shows that there is a reasonable correlation between the two sets of Delta Ring and Ball values obtained in these bitumens.

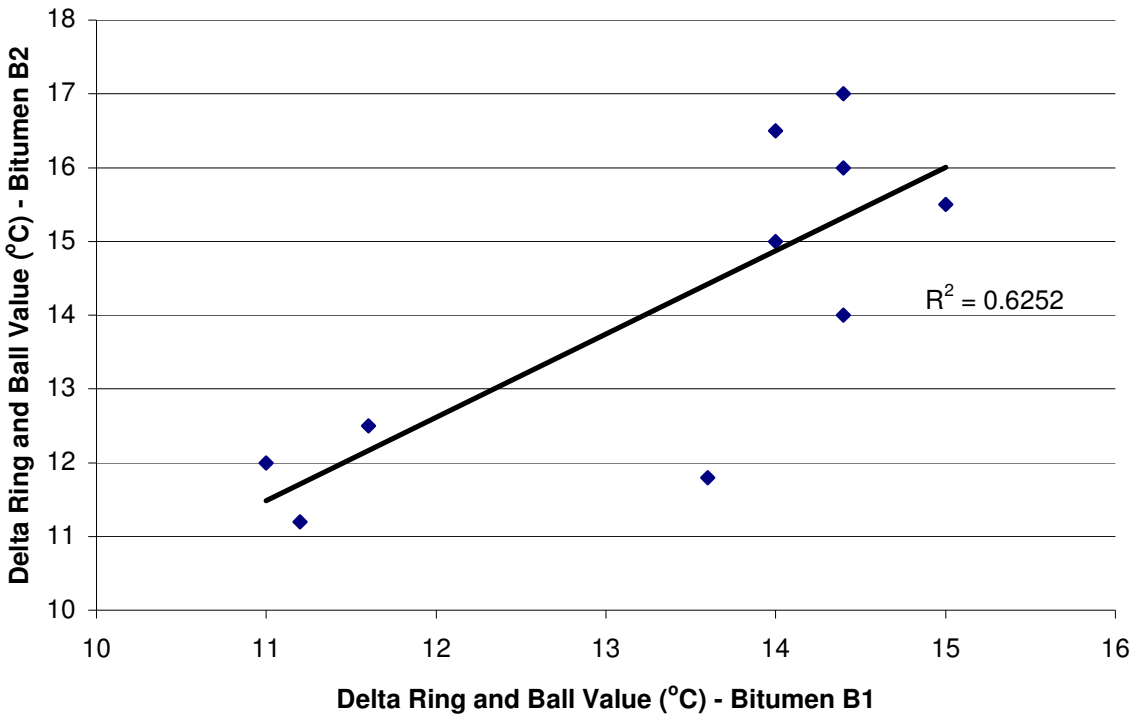

Figure 4-2: Correlation between Delta Ring and Ball measured in Bitumens B1 and B2

Bitumens B1 and B3 are chemically dissimilar, but rheologically similar in that the starting softening points are close together. A poor correlation (See Figure 4-3) exists between the two bitumens. These observations would suggest that chemical similarity is more important than rheological similarity in the Delta Ring and Ball test for different mastics. Bitumens B2 and B3 are neither rheologically or chemically similar and no correlation exists between the two sets of Delta Ring and Ball data, see Figure 4-4.

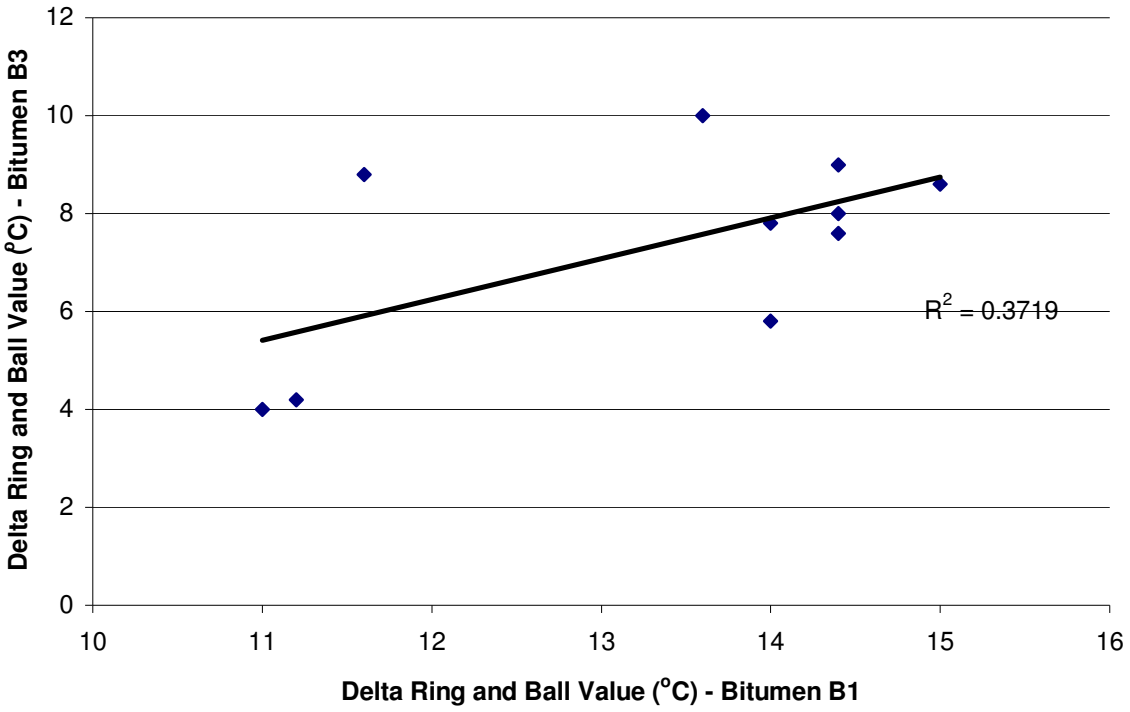

Figure 4-3: Correlation between Delta Ring and Ball measured in Bitumens B1 and B3

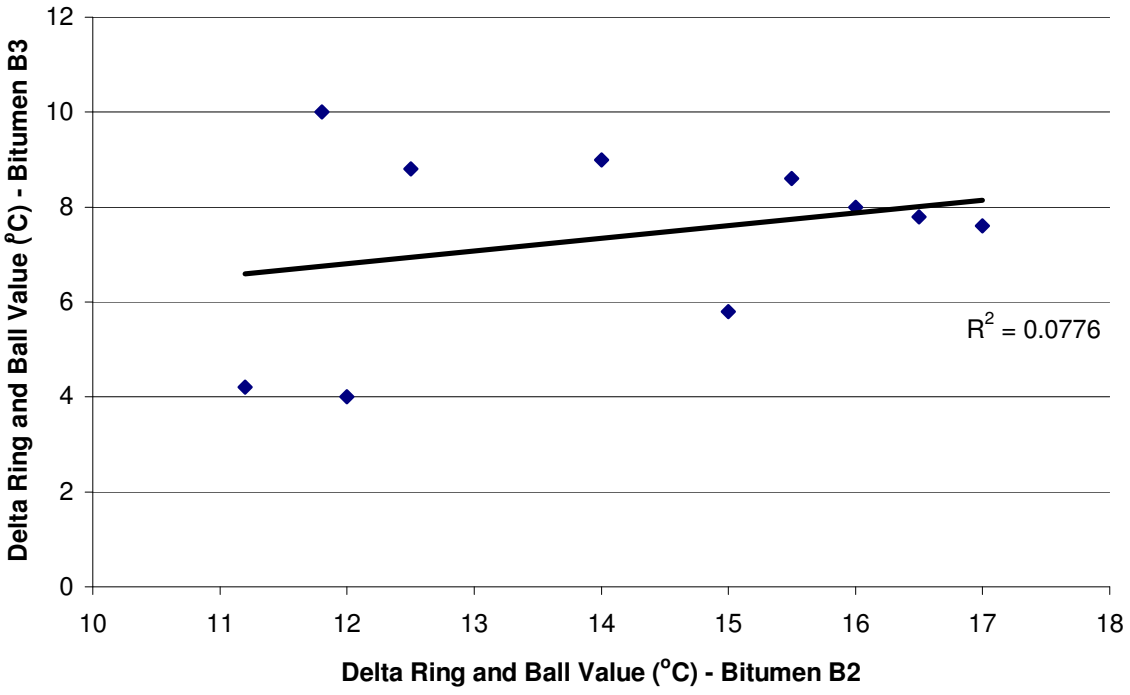

Figure 4-4: Correlation between Delta Ring and Ball measured in Bitumens B2 and B3

Delta Ring and Ball and index properties of the filler

There were no significant correlations between any index property of the fillers and the Delta Ring and Ball Values of the mastics. This is not surprising giving the relatively narrow range of values for Delta Ring and Ball obtained for the fillers in each bitumen type. Changes in Delta Ring and Ball Values for a single filler type in three bitumen types with respect to bond energy are discussed in Chapter VI.

If we consider the fillers in their subsets based on broad petrologic type, C1-5 and S1-5, there are some correlations between index properties and the Delta Ring and Ball Values (See Tables 4-2 and 4-3).

In all three bitumens, Fillers C1-5 correlated only to the maximum packing fraction estimated from tap density tests. This property is a measure similar to Rigden Voids and hence this finding is in line with other researchers observations that Delta Ring and Ball is loosely related to the packing characteristics of the filler (Kandhal, 1980; Cooley et al., 1998, Harris and Stuart, 1998).

Whereas, for Fillers S1-5 there is evidence that surface interactions come into play, with a strong correlation between the basic component of surface energy γ^- of the siliceous fillers and the Delta Ring and Ball Value with increasing levels of γ^- being related to increasing values of Delta Ring and Ball Value in B1 and B2. Interestingly, the correlation is reversed in B3 polymer modified and which is chemically dissimilar to B1 and B2. Increasing values of γ^- in the filler when mixed with B3 give lower levels of Delta Ring and Ball Value. This observation was also true in the creep compliance tests and is discussed further in Chapter V.

Table 4-2: Correlation between index properties of the filler and Delta Ring and Ball values

ALL FILLERS	B1	B2	B3
φ_{max}(Air)	-0.09	-0.00	-0.10
γ^{LW}	-0.15	-0.13	-0.03
γ^{+}	0.15	0.05	0.01
γ^{-}	0.08	0.10	-0.05
SSA BET (m²/g)	0.03	0.03	-0.10
MBV	0.05	0.01	-0.03
FM	0.01	0.02	-0.38
Aspect Ratio	0.01	0.01	0.12

Table 4-3: Correlation between index properties of the filler and Delta Ring and Ball values by subsets C1-5 & S1-5

C1-5	B1	B2	B3
φ_{max}(Air)	-0.49	-0.49	-0.55
γ^{LW}	-0.08	-0.08	-0.04
γ^{+}	0.04	0.04	-0.01
γ^{-}	0.08	0.08	-0.00
SSA BET (m²/g)	0.06	0.06	-0.01
MBV	0.06	0.06	-0.01
FM	0.05	0.05	-0.01
Aspect Ratio	0.08	0.08	-0.25
S1-5	**B1**	**B2**	**B3**
φ_{max}(Air)	0.10	0.84	-0.94
γ^{LW}	-0.43	0.00	-0.06
γ^{+}	0.38	0.15	-0.07
γ^{-}	0.53	0.94	-0.66
SSA BET (m²/g)	0.24	0.19	0.08
MBV	0.26	0.00	0.05
FM	0.69	0.15	0.00
Aspect Ratio	0.04	0.01	0.00

Summary

Thirty Delta Ring and Ball tests were carried out in accordance with BS EN 13179-1:2000, representing ten filler types in three different bitumens. Twenty-eight out of thirty of the values of Delta Ring and Ball were below the 16 proposed in the UK as an acceptable level in EME-2 mixtures.

Bitumens B1 and B2 are derived from the same source and are chemically similar. The test results for the mastics in these two bitumens were similar, with averages of around 13-14^{o}C, and reasonable correlation was found between Delta Ring and Ball values obtained by the fillers in these two bitumens. This occurred despite B2 having a much higher starting softening point than B1 (B1 softening point is 53^{o}C compared to 68^{o}C for B2).

Bitumen B3 is not true bitumen, but a polymer modified resin, and gave markedly different Delta Ring and Ball results compared to the fillers in Bitumens B1 and B2. The change in softening point was around half of that recorded in the other two bitumen, with an average of around 7^{o}C. This sample is rheologically similar to Bitumen B1 and results correlated reasonably between these two bitumens despite the chemical dissimilarity. The general observation can be made that in the case of these mastics, chemical similarity appears to have a stronger influence on Delta Ring Ball values than rheological similarity.

Delta Ring and Ball results did not correlate to any individual index property of the fillers. However, when the fillers were considered according to their broad petrologic type, either C1-5 (calcium carbonate type aggregates) or S1-5 (silica type aggregates) some interesting correlations were found.

For fillers derived from limestone, as discussed in the previous chapter, can be considered “inert” and in the case of Fillers C1-5 the level of Delta Ring and Ball related only to the packing characteristics of these fillers and the estimation of maximum packing fraction determined for fillers in air.

For fillers S1-5, which contain a proportion of silica, surface characteristics appear to influence the change in softening point, with γ^-, being well correlated to Delta Ring and Ball values. However, it appears that siliceous fillers do not behave in the same manner in all bitumen types, with inverse relationships being found in the polymer modified resin compared to the “traditional” bitumens.

Finally, with reference to individual filler types, the dolomitic Fillers C3 and C4 gave the lowest level of Delta Ring and Ball in all three bitumens, suggesting that dolomitic fillers have a fundamentally different behaviour to the other fillers. Fillers C1 and C2, both manufactured from pure calcium carbonate, have a tendency to be paired, with similar values in each bitumen type. The same is true for Fillers S1 and S3, which have the highest level of surface energy component γ^-. Filler S4 is worthy of special note as this filler has the highest value of Delta Ring and Ball of the set in Bitumen B3, whereas in Bitumen B2 it has the second lowest.

CREEP COMPLIANCE TESTING

Test set up and testing parameters

The creep compliance of Bitumens B1, B2 and B3, and the mastics were investigated over the temperature range of 45°C to 69°C. The test developed, as outlined in the previous chapter, examines the behaviour of the bitumen over the temperature range 45°C to 69°C using a Dynamic Shear Rheometer in creep mode. During the test, the creep compliance of the bitumen is measured after 1 second. Measurements are first taken at a temperature of 45°C, and the temperature is then increased at 4°C intervals and readings taken up to a final temperature of 69°C. A thermal equilibrium of 15 minutes was applied before the first, and for each subsequent measurement. A constant stress level of 2kPa is used throughout the test.

A Bohlin DSR 50 controlled stress rheometer was used for the testing (see Figure 4-5). The standard DSR test system consists of parallel metal plates, a temperature control chamber, a loading device and a control and data acquisition system. A water chamber controls the temperature of the test specimen. Water is pumped through the test chamber by a separate circulating bath temperature control unit. The water chamber and the temperature control unit can control the temperature of the specimen to an accuracy of ± 0.1°C (Airey, 1997).

The chamber completely encloses the top and bottom plates to minimise thermal gradients. Typically, the loading device applies a sinusoidal oscillatory torque to the specimen at various frequencies. When the load is strain controlled, the loading device applies a cyclic torque sufficient to cause an angular rotational strain accurate within 100

μrad of the specified strain. If the load is stress controlled, the loading device applies a cyclic torque accurate to within 10 mN.m of the specified torque.

The DSR can also be used to apply a constant level of torque to the specimen and monitor the accumulation of the resulting angular rotation i.e. shear creep test, which is the mode in which the experiments were carried out during this work.

Figure 4-5: The Dynamic Shear Rheometer used during the mastic testing

The selection of the testing geometry is based on the operational conditions with the 8 mm plate geometry generally being used at lower temperatures (-5°C to 20°C), or for stiffer bitumens, and the 25 mm geometry at intermediate to high temperatures (20°C to 80°C). As the mastics were likely to be significantly stiffer than pure bitumen, an 8mm plate was used during the experiments described in this work.

A 8mm diameter spindle was firmly mounted as the upper test plate of the DSR. A zero gap between the upper and lower test plates was established, by manually spinning the moveable top plate. Whilst the plate was spinning, the gap was closed until the movable plate touched the bottom fixed plate. The zero gap was reached when the plate stopped spinning completely. Finally, a gap setting of 1mm plus 50μm was established by moving the plates apart.

Testing of the bitumens

The bitumens were heated, stirring occasionally, to ensure homogeneity and to remove any air bubbles during the heating process, until it was sufficiently fluid to pour. The plates in the water chamber were heated to a temperature of 45^{o}C. The cover of the water chamber was removed and the loading mechanism was raised along with upper plate to provide enough room to pour the bitumen specimen. The surfaces of both the plates were dried to ensure that the bitumen specimen adheres to both the plates uniformly.

A sufficient amount of bitumen was weighed onto the centre of the bottom fixed plate to achieve the complete filling of a 1mm gap between the 8mm plates. The loading mechanism and the upper plate were lowered to the required gap width, squeezing the bitumen from between the two plates. A series of trials was conducted to achieve the correct filling between the plates, to ensure that the plates were neither under or over-filled with bitumen.

The cover of the water chamber was replaced, ensuring that both the upper and lower plates and the bitumen specimen were immersed in water. The test was started after the temperature had remained at 45°C ± 0.1°C for at least 15 minutes

The test results for the bitumens can be found in Table 4-4. The synthetic bitumen, B3, has the highest creep compliance of the three bitumens, whereas Bitumen B2 has very low creep compliance compared to the other two bitumens.

Table 4-4: Creep compliance of Bitumens B1, B2 and B3 over the temperature range 45-69°C

	Creep Compliance *J(t)*Pa (x 10^6) Pa		
Temperature (°C)	**B1**	**B2**	**B3**
45	254	29	515
49	515	37	1084
53	975	49	2219
57	1770	66	3917
61	3056	90	5691
65	4902	121	7213
69	6035	169	8360

The values in Table 4-4 were used to calculate relative creep compliance $J(t)_{rel}$ of the mastics as follows

$$J(t)_{rel} = \frac{J(t)bitumen}{J(t)mastic} \quad (44)$$

Where

J(t)mastic = the creep compliance of the mastic, as a function of time and temperature

J(t)bitumen = the creep compliance of the bitumen, as a function of time and temperature

All measurements in the following sections are taken as the creep compliance after 1 second loading and references to $J(t)_{rel}$ refer to the relative creep compliance after one second loading. The creep rate was also calculated over the final 0.35 seconds of the creep compliance curve and the relative creep compliance rate was also examined. For the mastics, there was a linear relationship between creep compliance at 1 second and the creep compliance rate of the mastic (see Figure 4-6). As a result, only the absolute creep compliance at 1 second is discussed in this work. Observations based on $J(t)_{rel}$ could be equally applied to the relative creep compliance rate of the mastics.

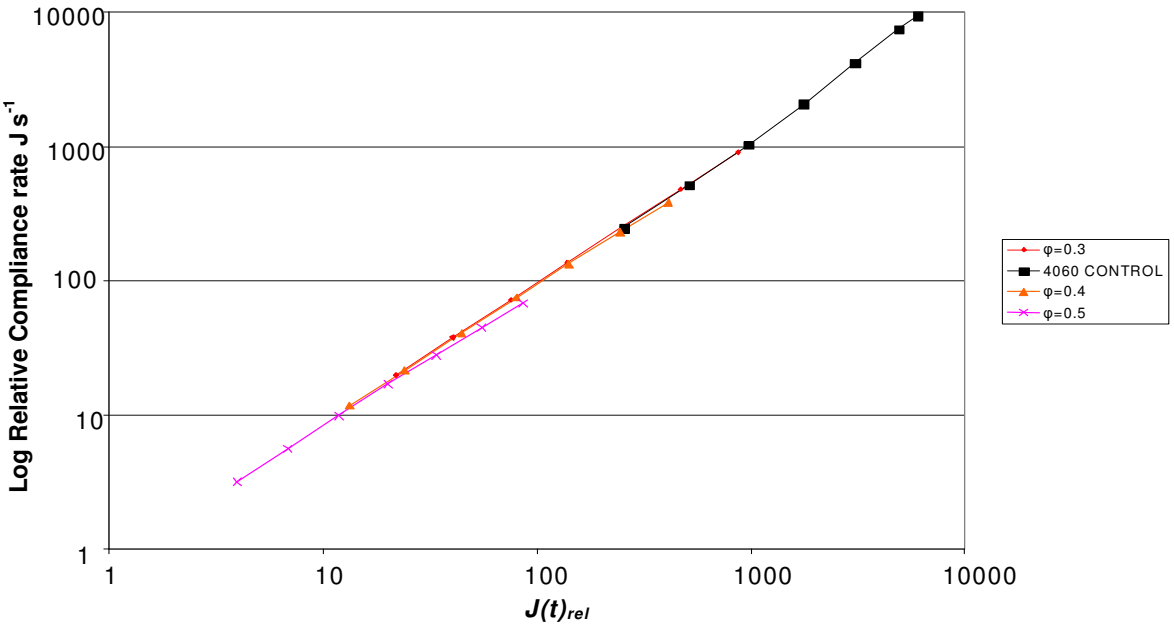

Figure 4-6: Relationship between creep compliance at 1 second and creep compliance rate over the final 0.35 seconds of the test

Preparation and testing of the mastics

The mixing procedure for the mastics was based broadly on the method outlined by Cooley et al. (1998). The procedure followed is summarised below

- Determine the specific gravity of the filler and bitumens.
- Dry filler to constant mass at 105^{o}C.
- Calculate the mass of bitumen and filler needed to give the correct value of φ based on volume of the mastic.
- Place 0.5 litre of bitumen in an oven at 170^{o}C (subdivided from bulk bitumen to avoid reheating).
- Weigh correct quantity of bitumen and filler.
- On a hot plate, blend using a spatula until mixture appears homogenous.
- Prepare DSR plate in the manner described above.

The mastics were tested in the DSR in creep mode under the same test conditions as the bitumens at three levels of solid volume addition 0.3, 0.4 and 0.5.

Mastic Test Results

$J(t)_{rel}$ as function of solid volume fraction

For each bitumen-filler combination at each level of solid volume, φ, the average relative creep compliance over the temperature range 45°C-69°C after one second loading was calculated using Equation 44. In the following sections, the average level of $J(t)_{rel}$ is discussed. Changes in $J(t)_{rel}$ with respect to temperature are discussed later in this chapter.

Results for relative creep compliance of mastics manufactured with Bitumen B1 are given in Table 4-5 below. The average creep compliance, up to a solid volume fraction of 0.4φ, are consistently higher for Fillers S1-5 than for C1-5, but as the solid volume increases to 0.5φ there is less distinction between the two petrographic subsets as the solid volume fraction approaches the maximum packing fraction. The relatively low stiffening recorded for the two dolomitic fillers, C3 and C4 is consistent with the Delta Ring and Ball data outlined previously.

Table 4-5: Relative creep compliance of mastics in Bitumen B1

Bitumen: B1	$J(t)_{rel}$, 0.3φ	$J(t)_{rel}$, 0.4φ	$J(t)_{rel}$, 0.5φ
Filler			
C1	11.4	20.1	79.8
C2	11.2	19.8	77.7
C3	10.4	12.5	29.0
C4	9.7	13.6	31.4
C5	8.3	17.5	49.9
S1	15.6	26.4	82.9
S2	17.1	27.6	66.8
S3	15.3	35.2	102.7
S4	16.5	22.4	157.0
S5	14.8	21.4	55.2

With regards to the levels of stiffening recorded at 0.3φ, the fillers reduce creep compliance by a factor of between 8.3 and 16.5, i.e. some fillers reduce the creep compliance much more effectively than others, this is in contrast to the Delta Ring and Ball measurements which recorded a relatively small range of increase in softening point in Bitumen B1. The stiffening of the bitumen as the solid volume increase to 0.5φ is over 100 fold for Fillers S3 and S4, whereas the level is around 30 for Fillers C3 and C4.

The level of relative creep compliance in Bitumen B2 is lower than in Bitumen B1 at solid volume levels 0.3φ and 0.4φ, approximately half of the reduction in creep compliance of Bitumen B1 based mastics. At high levels of solid volume addition the relative creep compliance is similar to the levels recorded for Bitumen B1. Again, the relatively low stiffening of Fillers C3 and C4 is noteworthy. Filler S1 gave very low creep compliance and is indicative of filler close to it's maximum packing fraction at 0.5φ.

Table 4-6: Relative creep compliance of mastics in Bitumen B2

Bitumen: B2	$J(t)_{rel}$, 0.3φ	$J(t)_{rel}$, 0.4φ	$J(t)_{rel}$, 0.5φ
Filler			
C1	6.6	9.5	50.6
C2	4.5	17.3	47.2
C3	2.6	9.0	24.4
C4	4.2	12.3	26.2
C5	4.6	15.8	38.9
S1	4.9	16.2	347.7
S2	4.6	23.7	49.9
S3	6.0	7.6	87.8
S4	3.3	14.3	50.5
S5	5.1	6.9	22.3

Finally, for mastics manufactured with Bitumen B3, the polymer-modified resin, a very wide range of behaviours were found (Table 4-7). Although, at high levels of solid volume, the majority of the fillers stiffen to a similar level as in the other two bitumens (around the level of 50-100 times lower creep compliance). Two fillers C3 and S3 have very low levels of relative creep compliance, with Filler C3 having just a 16 fold difference. To put this into context, five out of the ten fillers in Bitumen B1 have values close to 16 at just 0.3φ.

Table 4-7: Relative creep compliance of mastics in Bitumen B3

Bitumen: B3	$J(t)_{rel}$, 0.3φ	$J(t)_{rel}$, 0.4φ	$J(t)_{rel}$, 0.5φ
Filler			
C1	6.9	16.3	60.7
C2	5.0	24.2	101.8
C3	4.1	7.5	16.0
C4	2.5	4.6	44.2
C5	12.4	28.2	51.3
S1	4.8	9.5	36.3
S2	5.6	22.1	53.6
S3	4.5	9.1	22.9
S4	16.6	28.8	99.6
S5	10.6	19.3	60.4

$J(t)_{rel}$ as function of bitumen type

The level to which a filler type can reduce creep compliance is different in different bitumen types. For example, the relative creep compliance of Filler C3 at 0.3φ ranged from just 2.6 in Bitumen B2 to 4.1 in Bitumen B3 to as high as 10.4 in Bitumen B1. In all three of these mastics, the particle shape, particle size distribution, fineness modulus etc. are constant, as is the solid volume fraction, yet the level of stiffening is four times greater in one bitumen type than another. This indicates that some form of interaction between the filler and bitumen

is at work. Table 4-8 shows the different levels of relative creep compliance recorded for the same solid volume fraction, 0.3φ, of filler in different bitumen types.

Table 4-8: Levels of creep compliance for same volume fraction ($0.3\ \varphi$) of filler in different bitumen types

	$J(t)_{rel}$, 0.3φ (B1)	$J(t)_{rel}$, 0.3φ (B2)	$J(t)_{rel}$, 0.3φ (B3)
Filler			
C1	11.4	6.6	6.9
C2	11.2	4.5	5.0
C3	10.4	2.6	4.1
C4	9.7	4.2	2.5
C5	8.3	4.6	12.4
S1	15.6	4.9	4.8
S2	17.1	4.6	5.6
S3	15.3	6.0	4.5
S4	16.5	3.3	16.6
S5	14.8	5.1	10.6

There are significant differences between Bitumens B1 and B2 in creep compliance testing, whereas the values were very similar in the Delta Ring and Ball tests. Bitumen B3, which caused the smallest change in softening point (in general), reduces creep compliance more effectively than Bitumen B2.

Although most fillers stiffen Bitumen B1 the most effectively, fillers do not consistently stiffen the bitumen types in the same order (See Table 4-9 below). This observation is further examined and discussed in detail in Chapter VI.

Table 4-9: Order of reduction in relative creep compliance for the same filler in different bitumen types

	Order of reduction in relative creep compliance		
Filler	Highest	Middle	Lowest
C1	B1	B3	B2
C2	B1	B3	B2
C3	B1	B3	B2
C4	B1	B2	B3
C5	B3	B1	B2
S1	B1	B2	B3
S2	B1	B3	B2
S3	B1	B2	B3
S4	B3	B1	B2
S5	B1	B3	B2

Relative creep compliance as a function of temperature

Analysis of rheological behaviour over a range of temperatures gives rise to an insight into the behaviour of a mastic system. It has been suggested that for a given system, three possibilities exist (Rigden, 1947).

- If the change in relative viscosity changes in the same way as viscosity of the liquid phase, then the mastic behaviour is dependent wholly on the properties of the liquid phase.
- If η_{rel} increases with temperature, then effects caused by increasing randomness with increasing temperature are prevalent.
- If the relative viscosity reduces with temperature, this could be considered the result of a physical or chemical bond that becomes progressively weaker as the temperature is increased.

During the tests, relative creep compliance was derived across the temperature range 45°C to 69°C. In this section the temperature-dependence of relative creep compliance is discussed.

For mastics manufactured using Bitumen B1, as temperature increased there was a increase in $J(t)_{rel}$ up to a temperature of 65°C, after this temperature there is a fall in $J(t)_{rel}$. The peak occurs at a temperature very close to the Delta Ring and Ball value of the mastics. According to the rationale outlined above, increasing $J(t)_{rel}$ as a function of temperature is a result of temperature acting against the stability of the suspension, increasing temperature leading to increasing randomness and an increase in relative viscosity. This peak occurs close to the softening point of the mastic (see Figure 4-7)

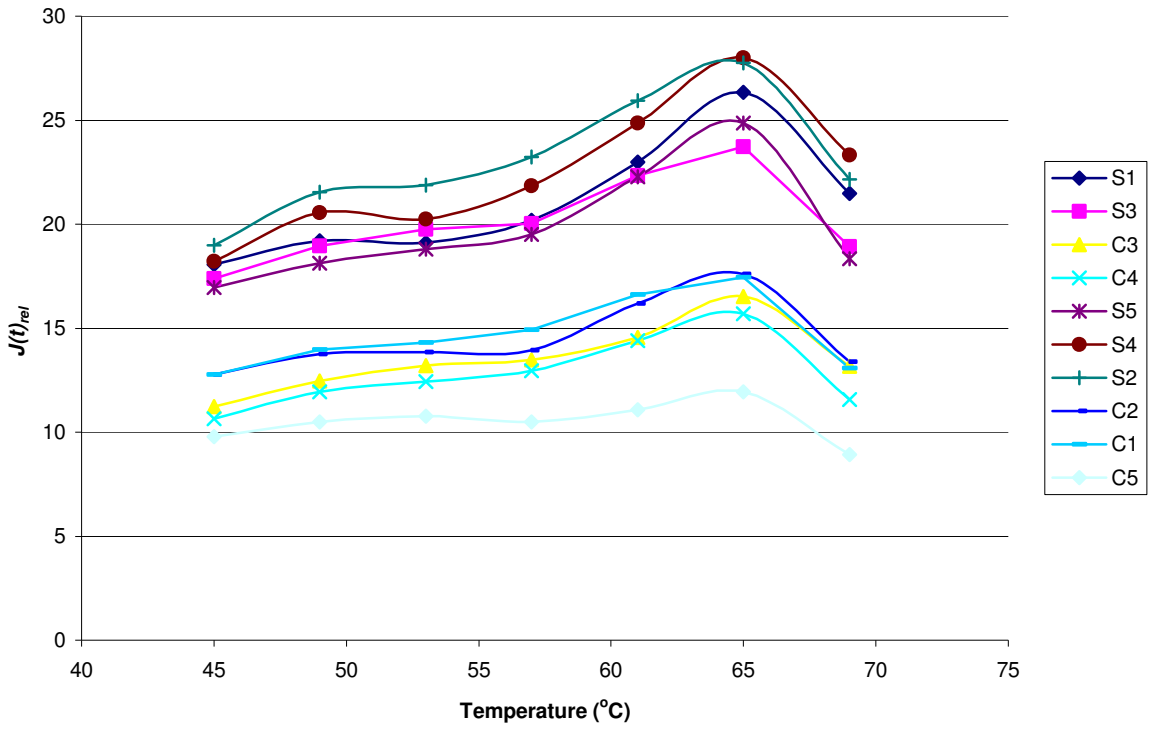

Figure 4-7: Change in relative creep compliance versus temperature, Fillers at 0.3 solid volume fraction, Bitumen B1

At 0.3φ (a relatively low volume concentration of filler) there are two clear groups of fillers. Fillers C1-5 have lower values of *J(t)rel* than Fillers S1-5. At 0.3φ there will be relatively limited inter-particle interactions and the fact that there are two distinct groups based on petrographic type suggests a chemical type reason for the splitting of the two groups. It should be noted that all ten fillers show the same trends with regard to temperature in Bitumen B1. At 0.4φ, there is still a differentiation between the two groups at higher temperatures, but at lower temperatures one filler (S4) has much lower $J(t)_{rel}$ than expected, followed by a relatively sharp rise in $J(t)_{rel}$ compared with the other fillers.

At high concentration of filler in the mastic there will be considerable inter-particle interactions this has lead to a loss in there being two distinct groups (C1-5 and S1-5). However, there are still notable pairings. The two dolomitic fillers, C3 and C4, show very similar behaviours, as do the two pure calcium carbonate fillers C1 and C2. Although less pronounced than at lower concentrations, there is still a small drop in $J(t)_{rel}$ after 65^{o}C, which is close to the Delta Ring and Ball temperature (See Figure 4-8).

Bitumen B3 also shows an increasing $J(t)_{rel}$ with respect to temperature, but there are however two distinct behavioural groups. Four fillers, C3, C4, S1 and S3 have significantly lower values of $J(t)_{rel}$, additionally these four fillers possess a peak $J(t)_{rel}$ within the temperature range of 45^{o}C to 69^{o}C (See Figure 4-9). The grouping effect in Bitumen B3 is even more pronounced at 0.4φ, with two very distinct behavioural groups being formed. At 0.5φ, the behaviour is very consistent across the range of fillers tested with no peaks of *J(t)*rel within the temperature range tested. It is still the case the same four fillers stiffen the bitumen to a lower extent.

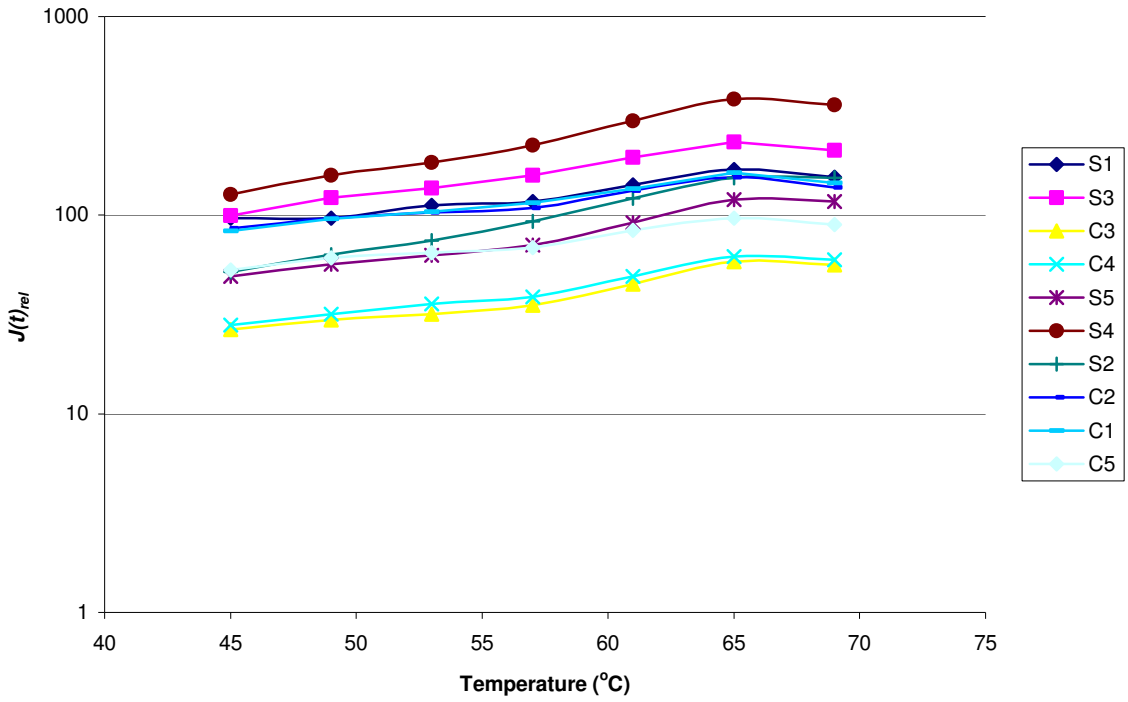

Figure 4-8: Change in relative creep compliance versus temperature, fillers at 0.5 solid volume fraction, Bitumen B1

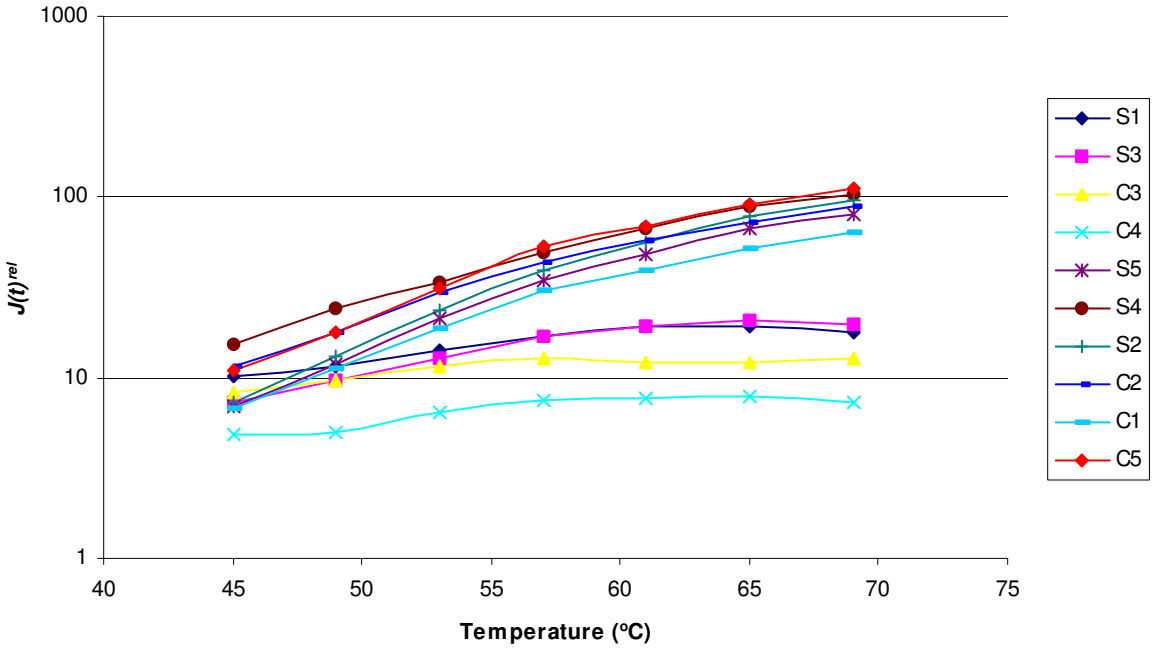

Figure 4-9: Change in relative creep compliance versus temperature, fillers at 0.4 solid volume fraction, Bitumen B3

Again, Fillers C3 and C4 have shown a tendency to be poor stiffeners of bitumen, regardless of bitumen type. The Delta Ring and Ball value of Fillers C3 and C4 in Bitumen B3 are the lowest of the fillers tested and the low stiffening in creep tests is consistent with this observation. The increase in $J(t)_{rel}$ only peaks for the four fillers with the lowest reduction in creep compliance, the other fillers do not have a peak $J(t)_{rel}$, even though the temperature range passes through the Delta Ring and Ball softening point of the mastics produced with Bitumen B3. It is not clear why this happens with Bitumen B3, whilst in Bitumen B1 all fillers possess a similar trend for relative creep compliance with temperature.

Fillers S1 and S3 however have relatively high Delta Ring and Ball values in Bitumen B3 and it is not clear why these two fillers stiffen the polymer-modified resin to such a low extent in the creep recovery tests. Fillers S1 and S3 have the highest γ^- values of the ten fillers and there could be two possible explanations for the low level of stiffening in Bitumen B3. One possibility is the high level of γ^- makes the filler very effective at attracting polymer from the bitumen. Fillers in polymer-modified bitumens can be viewed as a three-phase system of filler, bitumen and polymer. There will be a competing tendency between the filler and the bitumen for the polymer. If the filler is effective at attracting polymer to its surface, the bitumen phase will become depleted in polymer, lowering the viscosity of the liquid phase and hence lowering the overall viscosity of the mastic. The polymer adhered to the surface of the aggregate would form part of the solid phase, but the effect of this minor increase in size of the filler particles would not compensate for the decrease in viscosity of the bitumen phase due to loss of polymer (see Chapter VII: Further Work). However, this does not explain why the effect is evident in creep testing but not in the Delta Ring and Ball tests.

In Bitumen B2, for all of the mastics tested, the Delta Ring and Ball value was greater than 69^{o}C and hence outside of the temperature range tested in the creep compliance tests. For fillers in B2, there is general tendency for relative creep compliance to decrease with temperature. This, according to Rigden, could be the result of a bond being formed between the fillers and bitumen that is progressively weakened with temperature. This may suggest a fundamentally different behaviour for hard bitumens with fillers. Alternatively, Bitumen B2 has a very low creep compliance compared to Bitumens B1 and B3. The effect of the constant shear applied at the lowest temperatures may not have much effect on the filler particles and as temperature increases the filler particles may be moved more by the shear and cause better dispersion, lowering the relative creep compliance.

At 0.3φ there is not a clear trend with increasing temperature. Also, there is a much narrower range of relative creep compliance for the ten fillers than with Bitumen B1. There is not a clear trend between C1-5 and S1-5 and interestingly, the filler that caused the most stiffening in Bitumen B1 caused the least in B2 (S4). Fillers S3 and C4 did show a clear reduction in $J(t)_{rel}$ with respect to temperature.

At 0.4φ the relative creep compliance remains relatively constant across the temperature range of the tests. Several fillers have a reduction in $J(t)_{rel}$ followed by an increase in $J(t)_{rel}$**.** At 0.5φ most fillers have a downward trend in $J(t)_{rel}$ with respect to temperature (See Figure 4-10). Filler C4 has unusual behaviour and exhibits a strong increase in $J(t)_{rel}$ at higher temperatures after a fall in the relative creep compliance at lower temperatures.

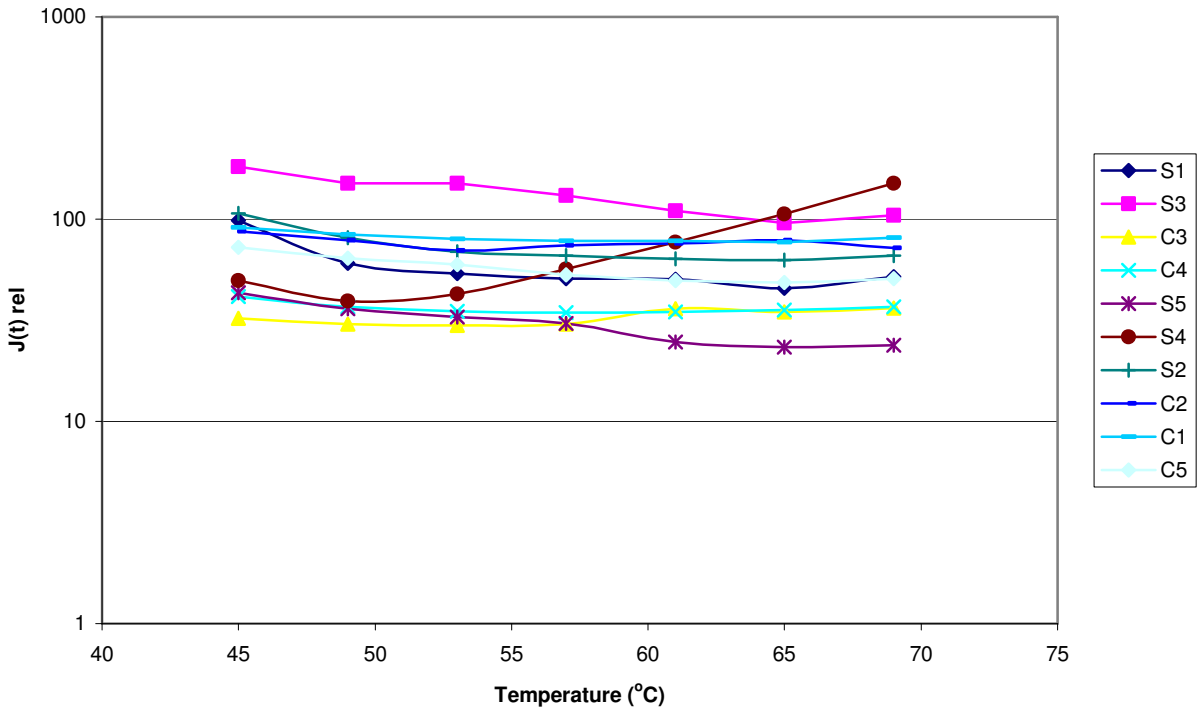

Figure 4-10: Change in relative creep compliance versus temperature, fillers at 0.5 solid volume fraction, Bitumen B2

Summary of relative creep compliance tests

In this section we have seen that relative creep compliance can be used to describe the behaviour of bitumen-filler mastics. A series of tests have been carried out at three levels of solid volume fraction addition, in three bitumen types, over a range of temperatures.

The reduction in creep compliance, caused by a single filler type, varies according to the type of bitumen in which it is dispersed. The order of stiffening from bitumen to bitumen is not consistent across the ten fillers and different fillers are more effective at stiffening different bitumen types. There tends be some pairing amongst the fillers based on chemical similarity, with Fillers C3 and C4 (dolomitic), Fillers C1 and C2 (pure calcium carbonate)

and Fillers S1 and S3 (highest level of γ^- component of surface energy) having similar behaviour in the three bitumen types.

In the Delta Ring and Ball tests, Bitumens B1 and B2 gave similar results, whereas B3 had changes in softening point around half that of the other two bitumens. This was not the case in the creep compliance tests where the general order of stiffening was B1>B3>B2.

The behaviour of fillers in Bitumen B2 was very different to Bitumens B1 and B3. In Bitumens B1 and B3 there is general tendency for $J(t)_{rel}$ to increase with increasing temperature. In Bitumen B1, the mastics had a defined peak in $J(t)_{rel}$ within the temperature range at a temperature close to the softening point of the mastic determined in the Delta Ring and Ball tests. In Bitumen B3, which has a very similar softening point, but is chemically different, some fillers have a defined peak in stiffening, but these fillers are confined to those that stiffen the bitumen to the lowest extent. This observation is not confined to a single petrologic group, but consists of the two dolomitic Fillers C3 and C4 and the two siliceous fillers with the highest surface energy component γ^-.

Determination of φ max from two-point projection test

Maximum packing fraction, φ_{max}, is defined as the solid volume fraction at which viscosity of a suspension becomes infinite, i.e. the point at which there is no flow. In terms of creep compliance, φ_{max} would relate to the solid volume fraction at which relative creep compliance becomes infinite – i.e. $1/J(t)_{rel}$ approaches zero. As stated previously, the value of φ_{max} is related to the packing density of the filler, or expressed another way φ_{max} is related to the void content of the filler, as proposed by Rigden (Rigden 1947, 1954). However, the determination of φ_{max} in air fails to account for important interactions between the two

phases. Additionally, the dispersal of the filler will differ in different bitumen types leading to a range of values for φ_{max}, whilst tap density, Rigden voids etc. are typically measured in a single medium, air.

Researchers have proposed a relative simple procedure to determine φ_{max} for ceramic pastes (Hurysz and Cochrane, 2004). The two-point projection method was originally developed to allow for rheological modelling from minimal experimentation. This procedure has been adapted to determine φ_{max} of bitumen filler mixtures in this thesis. The adapted method of determining φ_{max} is to plot the reciprocal of relative creep compliance against volume concentration and extrapolating to zero. This point represents the reciprocal infinite relative creep compliance, i.e. creep compliance of the mastic $J(t)$ approaching zero. At this point the volume of filler would be sufficient to reduce the creep compliance level to zero.

Taking the data from the creep recovery tests at 0.4φ and 0.5φ this procedure was carried out for each filler combination at each temperature (see previous example given in Chapter 2, Figure 2-4). The data points at the highest solid volume concentrations were used for the two-point projection method as these represent the measurements taken closest to the maximum packing fraction. One limitation of this approach is that to some extent the maximum packing fraction is dependent on the solid volume fractions from which the projections are made. A more accurate approach would be to make several measurements of relative viscosity (or other rheological measure) and derive a vertical asymptote from the exponential curve of solid volume fraction versus relative viscosity. This approach has been adopted by some asphalt researchers (Shashidar and Romero, 1998), but has the disadvantage of being time consuming.

For the determination of φ_{max} a linear relationship was assumed and the x intercept calculated from a straight line equation as followed:

$$y=mx + c \quad (45)$$

at x intercept, y = 0

therefore

$$0 = mx + c \quad (46)$$

rearranging gives

$$x = -c/m \quad (47)$$

Following this procedure, values for φ_{max} were calculated for each bitumen-filler combination.

The values obtained from the two-point projection method from creep testing are consistent with typical values recorded for $\varphi_{\max}$ of fillers in literature, however the first thing to note is that φ_{max} does not have the same value across the temperature range as a result of changes in $J(t)_{rel}$ from which the maximum packing fraction is derived.

The same filler has different values of φ_{max} in different bitumen types, a summary of the average value across the temperature range is given in Table 4-10 below.

Table 4-10: Maximum Packing Fraction of fillers in the three bitumens

	B1	B2	B3
C1	0.534	*0.523*	**0.547**
C2	*0.534*	**0.558**	*0.534*
C3	0.579	*0.558*	**0.604**
C4	0.578	**0.590**	*0.517*
C5	*0.555*	0.572	**0.624**
S1	**0.547**	*0.505*	0.537
S2	*0.576*	**0.604**	0.583
S3	0.554	*0.510*	**0.577**
S4	*0.517*	0.553	**0.565**
S5	**0.568**	*0.550*	0.553

No clear trend exists, and not all fillers have their highest values of φ_{max} in a single bitumen type. The highest value is given in bold type, the lowest in italics in Table 4-10 above. There are no correlations between the value of φ_{max} determined in one type of bitumen and the values of φ_{max} obtained in another bitumen types. Additionally, the values of φ_{max} are not well correlated to the single value of φ_{max} determined from the compacted bulk density of the filler as described in Chapter III.

Index properties and maximum packing fraction derived from rheological tests.

The correlation between index properties of the filler and φ_{max} determined in the creep tests is generally very poor. No clear trend exists to suggest that specific surface, shape, etc. have the major single influence on φ_{max}. This is not surprising as φ_{max} is a result of a complex set of factors encompassing particle size, particle size distribution, particle shape, surface area, etc.

In Bitumen B2, the strongest single correlation, is with the acid component of surface energy, where the two fillers with the highest γ^+ gave the lowest values of maximum packing fraction in the creep tests (See Figure 4-11)

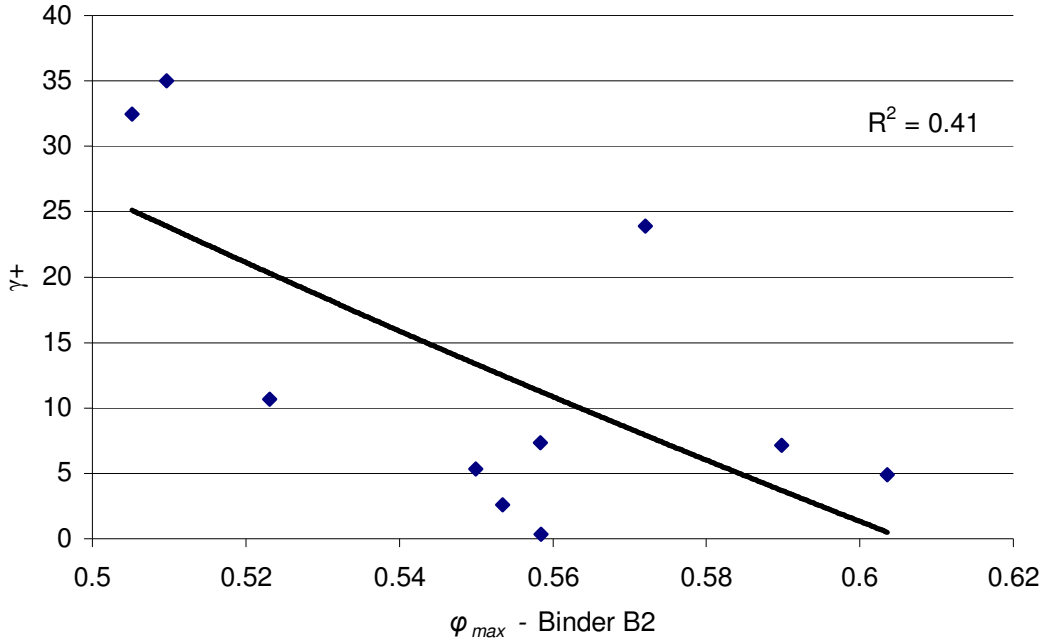

Figure 4-11: Relationship between γ^+ and maximum packing fraction determined rheologically in Bitumen B2

If we consider the two sub-groups of fillers separately, C1-5 (carbonate) and S1-5 (siliceous) the correlation with γ^+ is good for the siliceous fillers (see Figure 4-12). Fillers S1 and S3 have very high levels of γ^+ and have the lowest levels of φ_{max} for Fillers S1-5. Interestingly, Fillers S1 and S3 are the two fillers which stiffen Bitumen B3 to the lowest extent. As stated previously, the behaviour of these two fillers is often paired in the same way that Fillers C3 and C4, the dolomitic fillers, are paired.

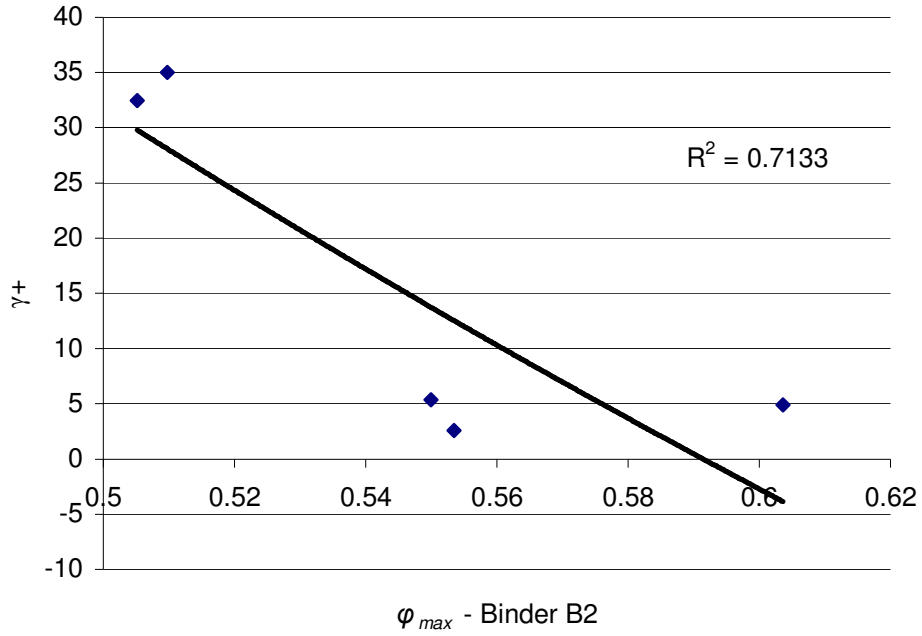

Figure 4-12: Relationship between γ+ and maximum packing fraction determined rheologically in Bitumen B2 for Fillers S1-5

The relationship between simple index properties and the maximum packing fraction determined using the two point projection technique for fillers in Bitumen B3 is a little better correlated than the "traditional" Bitumens B1 and B2. Increasing surface area and surface energy appear to result in higher value of φ_{max}. Although the correlation is still relatively poor (R^2 below 0.5)

Effect of temperature on maximum packing fraction determined using creep tests

Typically for the mastics, φ_{max} decreased with increase in temperature. This is counter-intuitive, as one would expect that as temperature increased and the viscosity of the liquid medium reduced, the dispersal of the solid particles would be more favourable, leading

to an increase in φ_{max}. Results for the mastics in the three bitumen types are given in Tables 4-11, 4-12 and 4-13.

The effects of increasing temperature on φ_{max} vary with bitumen type in a similar manner to that described above for changes in relative creep compliance. In Bitumen B1 and B3, φ_{max} reduces with increasing temperature. Whilst similar trends exist between B1 and B3 in that the values of φ_{max} reduce with temperature, with B2 the value of φ_{max} stay relatively constant with increasing temperature. The reduction in φ_{max} with temperature may be linked to viscosity of the bitumen as Bitumens B1 and B3 are rheologically similar whereas Bitumen B2 is considerable stiffer.

One explanation of the decreasing φ_{max} values is that the surface effects on the stiffening of the mastic are considerable and at higher temperatures, under shear, more surface is created as agglomerated filler particles are liberated, causing an increase in relative creep compliance. This is contrary to other research (Heukelom and Wijga, 1971) which proposed that increasing shear reduces volume by separating agglomerates causing a lowering of viscosity in the system.

Table 4-11: Changes in maximum packing fraction with temperature - Bitumen B1

Bitumen B1	Temperature (°C)							
	φ_{max} 45	φ_{max} 49	φ_{max} 53	φ_{max} 57	φ_{max} 61	φ_{max} 65	φ_{max} 69	AVERAGE φ_{max}
C1	0.543	0.540	0.536	0.534	0.532	0.529	0.526	**0.534**
C2	0.538	0.539	0.535	0.536	0.532	0.532	0.530	**0.534**
C3	0.611	0.599	0.593	0.583	0.566	0.557	0.548	**0.579**
C4	0.587	0.592	0.587	0.586	0.576	0.566	0.553	**0.578**
C5	0.612	0.602	0.584	0.569	0.562	0.557	0.549	**0.555**
S1	0.547	0.554	0.545	0.547	0.545	0.545	0.544	**0.547**
S2	0.612	0.602	0.584	0.569	0.562	0.557	0.549	**0.576**
S3	0.574	0.566	0.558	0.551	0.546	0.544	0.541	**0.554**
S4	0.523	0.519	0.518	0.517	0.515	0.514	0.513	**0.517**
S5	0.593	0.585	0.579	0.572	0.557	0.548	0.540	**0.568**

Table 4-12: Changes in maximum packing fraction with temperature - Bitumen B2

Bitumen B2	Temperature (°C)							
	φ_{max} 45	φ_{max} 49	φ_{max} 53	φ_{max} 57	φ_{max} 61	φ_{max} 65	φ_{max} 69	AVERAGE φ_{max}
C1	0.520	0.522	0.523	0.524	0.524	0.525	0.525	**0.523**
C2	0.548	0.553	0.558	0.556	0.562	0.563	0.570	**0.558**
C3	0.554	0.561	0.564	0.559	0.551	0.554	0.565	**0.558**
C4	0.571	0.578	0.589	0.589	0.602	0.606	0.593	**0.590**
C5	0.549	0.552	0.559	0.571	0.587	0.586	0.601	**0.572**
S1	0.508	0.506	0.505	0.505	0.504	0.504	0.504	**0.505**
S2	0.547	0.569	0.591	0.614	0.632	0.656	0.616	**0.604**
S3	0.508	0.508	0.508	0.509	0.511	0.513	0.512	**0.510**
S4	0.567	0.590	0.581	0.554	0.537	0.526	0.520	**0.553**
S5	0.527	0.534	0.540	0.546	0.561	0.565	0.576	**0.550**

Table 4-13: Changes in maximum packing fraction with temperature in Bitumen B3

Bitumen B3	Temperature (^{o}C)							
	φ_{max} 45	φ_{max} 49	φ_{max} 53	φ_{max} 57	φ_{max} 61	φ_{max} 65	φ_{max} 69	AVERAGE φ_{max}
C1	0.572	0.566	0.556	0.546	0.532	0.529	0.525	**0.547**
C2	0.538	0.543	0.541	0.534	0.531	0.524	0.525	**0.534**
C3	0.658	0.685	0.641	0.594	0.550	0.548	0.555	**0.604**
C4	0.546	0.522	0.516	0.511	0.509	0.507	0.505	**0.517**
C5	0.635	0.615	0.624	0.650	0.627	0.616	0.600	**0.624**
S1	0.553	0.546	0.541	0.536	0.533	0.525	0.523	**0.537**
S2	0.609	0.608	0.598	0.585	0.571	0.557	0.550	**0.583**
S3	0.616	0.618	0.591	0.576	0.553	0.544	0.538	**0.577**
S4	0.639	0.615	0.566	0.549	0.534	0.529	0.525	**0.565**
S5	0.569	0.568	0.561	0.554	0.545	0.541	0.535	**0.553**

Table 4-14 gives the range of values obtained using the two point projection method at each temperature. $\Delta\varphi_{max}$ is the absolute value of the change in φ_{max} over the range of temperatures tested, $\%\Delta\varphi_{max}$ gives the percentage change in φ_{max} with increasing temperature. As can be seen from Table 4-14, the value of φ_{max} can lower by as much as 20% over the temperature range 45^{o}C to 69^{o}C.

Bitumen B2, in keeping with the reduction in $J(t)_{rel}$ outlined in the previous section, has the inverse behaviour with $\Delta\varphi_{max}$ being positive. Two fillers, S1 and S4, show drops in φ_{max} and have the same behaviour in all three bitumens. There is wide range of behaviours though, with some fillers (C1, C2, C3, S1, S3) having relatively modest changes in φ_{max} and others (C5, S2 and S5) having relatively large increases in φ_{max} as temperature increases.

Table 4-14: Percentage changes in maximum packing fraction with temperature

	BITUMEN B1		BITUMEN B2		BITUMEN B3	
	Δφmax f(T)	*% Δφmax*	*Δφmax f(T)*	*% Δφmax*	*Δφmax*	*% Δφmax*
C1	-0.016	**-3.0%**	0.006	1.1%	-0.046	**-8.1%**
C2	-0.008	**-1.6%**	0.021	3.9%	-0.013	**-2.5%**
C3	-0.063	**-10.3%**	0.011	1.9%	-0.137	**-20.8%**
C4	-0.034	**-5.8%**	0.034	6.0%	-0.041	**-7.5%**
C5	-0.027	**-4.8%**	0.053	9.6%	-0.050	**-7.9%**
S1	-0.002	**-0.4%**	-0.004	***-0.8%***	-0.030	**-5.5%**
S2	-0.063	**-10.3%**	0.110	20.1%	-0.058	**-9.6%**
S3	-0.033	**-5.8%**	0.005	0.9%	-0.080	**-13.0%**
S4	-0.009	**-1.8%**	-0.047	***-8.3%***	-0.115	**-17.9%**
S5	-0.054	**-9.1%**	0.049	9.2%	-0.034	**-5.9%**

Summary of determination of φ_{max} using a two-point projection technique

A two-point projection technique has been used to calculate maximum packing fraction of a number of mastics. The values obtained appear realistic when compared with published data for maximum packing fractions of fillers (Barnes, 2000; Wypych, 1999). This technique, which requires minimal experimentation has the additional advantage of including interactions between the filler and the bitumen in the measurement, compared to estimating the maximum packing fraction from the volumetric properties of the filler in Rigden Void type tests.

The same filler has different maximum packing fraction values in different bitumen types. Furthermore, the value of maximum packing fraction can vary with test temperature. This indicates that estimating maximum packing fraction from the volumetric properties of the filler in air is unlikely to be useful in all situations.

Typically, φ_{max} decreased with increasing temperature, however for Bitumen B2 eight out of ten of the fillers showed increases in maximum packing fraction with increase in temperature.

Derivation of master curves of relative creep compliance

Researchers have long proposed that the effects of solid volume fraction φ are scaled by φ_{max} (Rigden 1947,1954; Heukelom and Wijga 1971) and Rigden referred to this relation as the "true volume fraction". The term φ/φ_{max} is a feature of several models used to describe the rheology of suspensions (Mooney 1957; Krieger and Dougherty 1959; Chong 1971). By normalizing relative creep compliance to φ_{max} calculated using the two-point projection method from the creep tests, a master curve of stiffening can be formed for each bitumen.

For fillers in Bitumen B1, there is a clear difference between the stiffening of calcium carbonate fillers C1-5 and siliceous fillers S1-5. The overall trend is good, showing stiffening to be scaled by φ_{max} with the data points fitting an exponential curve. Fillers in Bitumen B2 show a similar trend and again fit an exponential curve (see Figures 4-17 and 4-18).

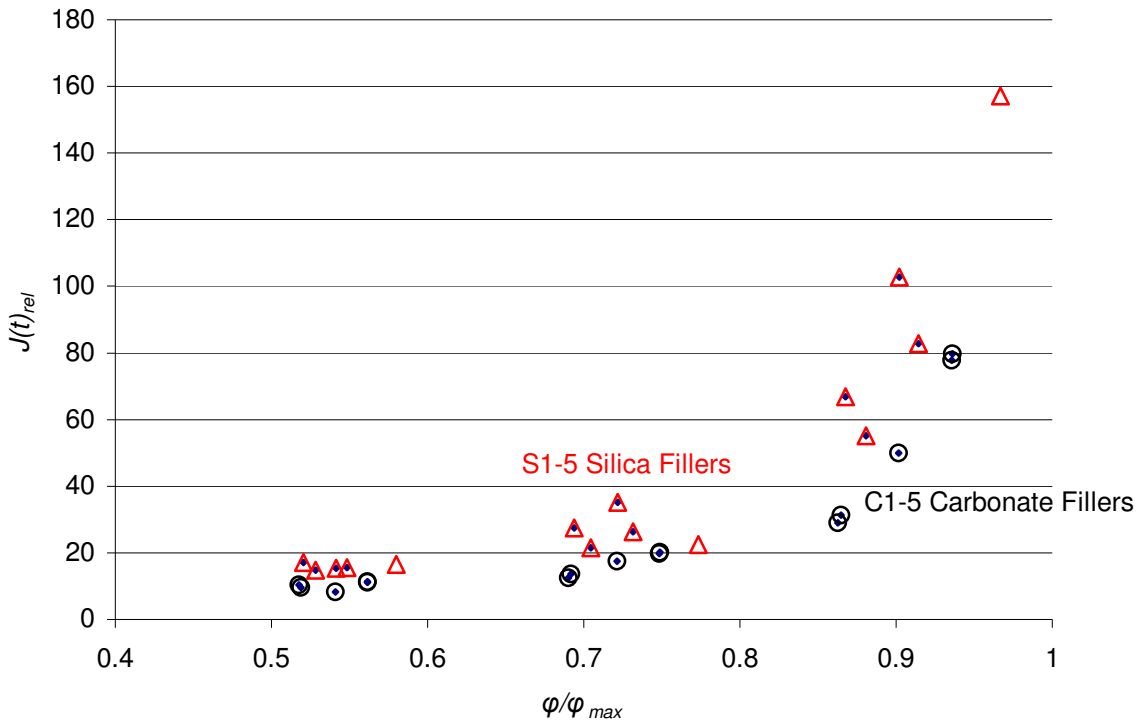

Figure 4-17: Stiffening of mastics in Bitumen B1 normalised for φ_{max}

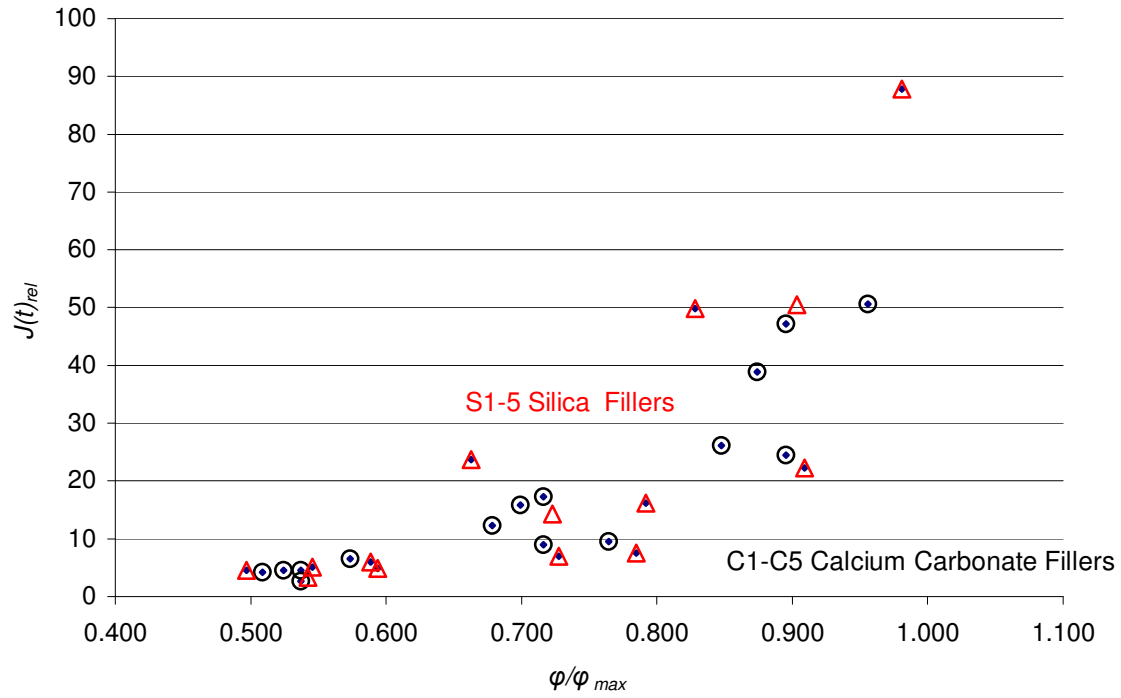

Figure 4-18: Stiffening of mastics in Bitumen B2 normalised for φ_{max}

If we compare the stiffening of the same set of fillers in the two different bitumens, bearing in mind that the bitumens are derived from the same crude oil source, the stiffening effect of the fillers in the 40/60 grade bitumen (B1) is much higher than in the 10/20 grade bitumen (B2). When you consider that the two curves are already normalised to account for differences in φ_{max}, this leads to the conclusion that there is a different level of interaction between the fillers in the 10/20 grade bitumen compared to the 40/60 grade.

Normalising the data to the true volume fraction, φ/φ_{max}, gives a very interesting curve for fillers in Bitumen B3 (see Figure 4-19). There appear to be two sets of distinct results. These relate to the four fillers outlined previously in this section, C3, C4, S1 and S3. These fillers also had peaks in their $J(t)_{rel}$ versus temperature curves as mentioned in the previous sections, whereas all of the other fillers increased $J(t)_{rel}$ with temperature across the range of temperatures tested.

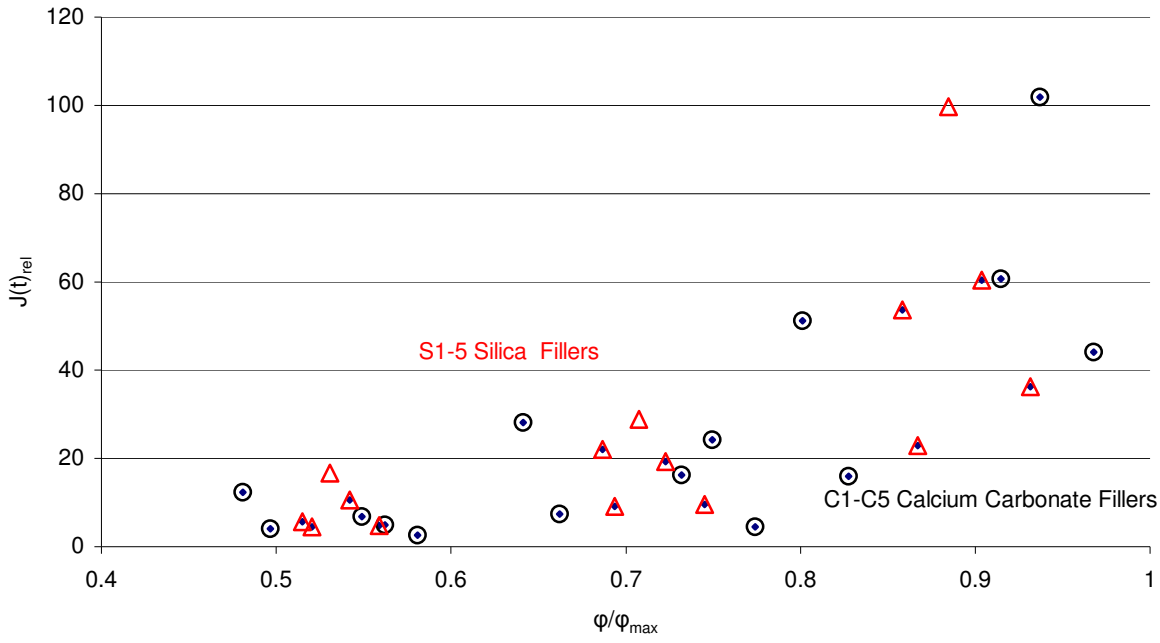

Figure 4-19: Stiffening of mastics in Bitumen B3 normalised for maximum packing fraction

If we consider the three master curves derived for the bitumen-filler mastics, the order of stiffening observed is B1>B3>B2 (See Figure 4-20). The synthetic Bitumen B3 stiffens to an intermediate extent compared to the two "traditional" bitumens, with the B3 curve being closer to the curve of the hard bitumen (B2) rather than the curve of Bitumen B1 with which B3 is rheologically closer.

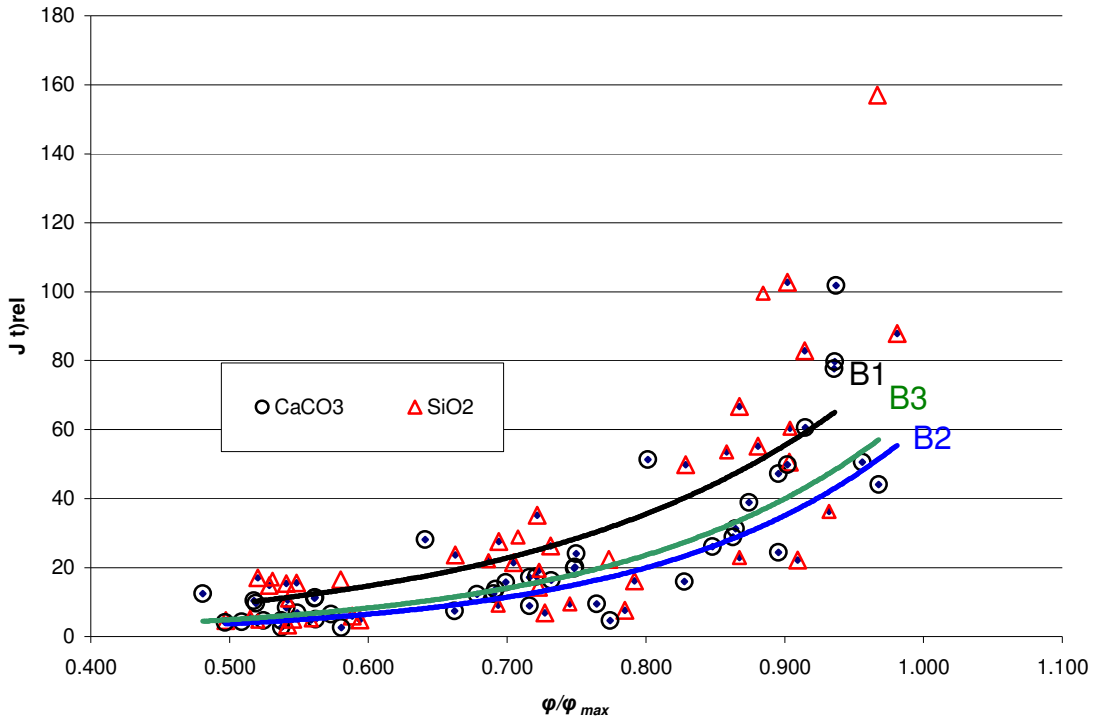

Figure 4-20: Stiffening of mastics in different bitumen types, normalised for maximum packing fraction

CHAPTER SUMMARY

In this Chapter, rheological tests have been carried out on different bitumen-filler combinations. The tests have showed that the same filler can stiffen different bitumen types to differing extents and that the order of stiffening is not consistent for all filler types. In Delta Ring and Ball tests, the two "traditional" bitumens, B1 and B2, gave very similar results, whereas the delta ring and ball values for the polymer modified resin B3 were around 50% lower. The vast majority of the mastic combinations were below 16^{o}C, the recently suggested increase in softening point for specific UK asphalts.

The index tests carried out on the fillers did not predict the level of Delta Ring and Ball for any bitumen type over the whole filler set. Separating the fillers into two sub-sets, C1-5 and S1-5, did provide some correlations of note. For the carbonate fillers, the maximum packing fraction as measured from the bulk properties of the filler in air did relate to the Delta Ring and Ball values, whereas for the siliceous fillers surface effects, in particular the γ^- component of surface energy, were correlated to the Delta Ring and Ball value, but not in a consistent way. Increasing γ^- lead to increasing Delta Ring and Ball Values in some bitumens and decreasing values in others.

Creep compliance testing using a DSR was used to determine the level of stiffening for each mastic at three solid volume fraction levels and seven temperatures ranging from 45^{o}C to 69^{o}C. The term relative creep compliance $J(t)_{rel}$ was introduced to describe the change in creep compliance after 1 second of applied stress 2kPa.

In common with the Delta Ring and Ball tests, the level of relative creep compliance, $J(t)_{rel}$, differed from bitumen to bitumen, with different fillers stiffening different bitumens to different extents. In the creep tests, the general order of stiffening was dissimilar to the Delta Ring and Ball results, with fillers in Bitumen B3 stiffening to a higher extent than the same filler set in B2. Bitumen B1 gave the highest stiffening when filled.

The level of relative creep compliance changes with temperature. For fillers in Bitumens B1 and B3, the relative creep compliance increases with increasing temperature. According to Rigden, this is a result of increasing randomness of the system as temperature increases. For all fillers in B1 and four of the fillers in B3, there was a peak $J(t)_{rel}$. For all fillers in Bitumen B1 this peak occurred close to the softening point of the mastic as measured in the Delta Ring and Ball test. For the fillers in B3, only the four fillers with the lowest values of $J(t)_{rel}$ gave a peak value and in this case the peak was higher than the softening point of the mastic.

A two-point projection method was used to determine the maximum packing fraction. This method gave reasonable values of maximum packing fraction as compared to value obtained from literature (Barnes, 2000; Wypych 1999). The φ_{max} value varied for the same filler in different bitumens. Again, the order of maximum packing fraction in different bitumen types was not consistent for all fillers.

The measured φ_{max} for the fillers in bitumen did not relate to the value of φ_{max} measured in air using bulk properties of the filler. Additionally, the values of φ_{max} in one bitumen type did not correlate to the values of φmax in another bitumen type. Maximum packing fraction decreases with temperature in Bitumens B1 and B3, whilst for most fillers it

remains relatively constant or moderately decreases in Bitumen B2. Two fillers, S1 and S4 showed increases in maximum packing fraction in all bitumen types

Finally, the value of relative creep compliance at each solid volume fraction was normalised to the maximum packing fraction derived using the two-point projection method. Master-curves of fillers in each bitumen type were produced. These follow an exponential relationship with respect to φ/φ_{max}. After normalising for the maximum packing fraction, the stiffness master curves of the bitumens follow the order: B1>B3>B2.

In the next chapter the average relative creep compliance and maximum packing fraction are used to derive the intrinsic viscosity and the Marron-Pirece-Kitano (MPK) Coefficient of the fillers using the three rheological models proposed by Chong, Krieger and Dougherty, and Mooney.

CHAPTER V

RHEOLOGICAL MODELLING OF THE MASTICS

INTRODUCTION

Several models have been proposed to describe the behaviour of suspensions of solid particles in liquids. Einstein considered the case of dilute solutions of rigid spheres, where the particles are widely spaced, i.e. unaware of each other's existence. The Einstein equation yields a linear relationship with respect to concentration and the equation does not include the term φ_{max}. Thus, according to the Einstein equation, the viscosity of the suspension can carry on increasing indefinitely. In reality, this is not the case. As the concentration of solid particles is increased there is increasing interaction in the liquid phase close to the surface of neighbouring solid particles and further energy is dissipated. Additionally, inter-particle interactions become increasingly important as the solid phase volume increases.

Several later models (Mooney, 1957; Krieger and Dougherty, 1959; Chong, 1971) introduced the term φ_{max}, the maximum packing fraction which represents the solid phase volume at which the viscosity of the suspension becomes infinite.

In the previous chapter, the term $J(t)_{rel}$, relative creep compliance was introduced to describe the behaviour of mastics at varying levels of solid volume fraction (φ). The Mooney, Chong and Krieger-Dougherty equations (Equations 8-10) can be rewritten to include this term:

The modified Mooney equation

$$J(t)_{rel} = \exp\left(\frac{[\eta]\phi}{1-\frac{\phi}{\phi_{\max}}}\right) \tag{48}$$

The modified Krieger-Dougherty equation

$$J(t)_{rel} = \left(1-\frac{\phi}{\phi_{\max}}\right)^{-[\eta]\phi_{\max}} \tag{49}$$

and the modified Chong equation

$$J(t)_{rel} = \left[1+\frac{[\eta]\phi}{2}\left(\frac{\frac{\phi}{\phi_{\max}}}{1-\frac{\phi}{\phi_{\max}}}\right)\right]^2 \tag{50}$$

Where

$J(t)_{rel}$ = relative creep compliance of the mastic

$[\eta]$ = the intrinsic viscosity of the solid phase

φ = the solid phase volume

φ_{max} = the solid phase maximum packing volume determined from two-point projection of zero reciprocal relative creep compliance.

As the terms $J(t)_{rel}$, φ and φ_{max} are known, each equation can be solved to give a value for $[\eta]$, the intrinsic viscosity of the filler. Intrinsic viscosity has classically been related to particle shape. Einstein proposed that for spheres with perfect adhesion $[\eta]$= 2.5. Spheres are proposed to have the lowest intrinsic viscosity, increasing as the shape turns to grains, cubes, plates and rods (fibres). The intrinsic viscosity of other geometries has also been proposed (Barnes, 2000).

$$[\eta] = \frac{7}{100} p^{\frac{5}{3}} \tag{51}$$

for rod-like particles

and

$$[\eta] = \frac{3}{10} p \tag{52}$$

for disc like particles

Where: p is the axial ratio (greater than unity)

The effect of increasing irregularity of shape manifests itself in a lowering of φ_{max}, so the two terms $[\eta]$ and φ_{max} are proposed to move in concert. Equation 49 outlined above includes the term $[\eta]\varphi_{max}$, which is intended to normalise the effects of changing values of $[\eta]$ and φ_{max}. This term is often close to the value of 2 and is sometimes referred to as the MPK Coefficient (Rides, 2005).

For each of the three models, $[\eta]$ was calculated for each filler-bitumen combination, at each concentration and using the average $J(t)_{rel}$ and φ_{max} as determined from the creep experiments described in the previous chapter. Additionally, the MPK Coefficient was calculated for each of the mastics.

As mentioned previously, Einstein calculated that the value of $[\eta]$ for spheres, with perfect adhesion (no slip) was 2.5. As the filler particles in these experiments are non-spherical, typically with an aspect ratio of 1.5 it should be expected that the intrinsic viscosities of fillers used in asphalt should be in excess of 2.5 (even taking into account the potential less than perfect adhesion). If a model returns unrealistically high (or unrealistically low values) of $[\eta]$ then this indicates that the model is not well suited to describing the behaviour of filler-bitumen mastics. This was the approach taken when assessing the suitability of each model.

In summary, the aim of the testing outlined in this chapter is to:

- Determine $[\eta]$, and the MPK Coefficient, for each filler and bitumen combination using the selected rheological models.
- To establish the suitability of the three chosen models for bitumen-filler mastics.
- To investigate if any index property of the filler is responsible for the values of $[\eta]$, and the MPK coefficient.

MODELLING AND DETERMINATION OF *[η]* FOR THE TEN FILLERS

Fillers in Bitumen B1

Intrinsic Viscosity

At low volume concentration, 0.3φ, the two groups of fillers have different intrinsic viscosities, Fillers S1-5 have higher values of intrinsic viscosity than Fillers C1-5. This could be explained as a function of shape as Group S has on average, higher aspect ratios than Group C.

The Mooney and Krieger-Dougherty equations give realistic values for *[η]*, whilst the Chong equation predicts unrealistically high values, indicating that this model underestimates the level of stiffening by the filler (Table 5-1).

Table 5-1: Intrinsic viscosity of fillers in Bitumen B1, 0.3 solid volume fraction

INTRINSIC VISCOSITY B1, 0.3φ					
	Average $J(t)_{rel}$	φ_{max}	MOONEY	CHONG	KRIEGER-DOUGHERTY
C1	11.36	0.534	3.42	12.34	5.52
C2	11.17	0.534	3.39	12.20	5.48
C3	10.39	0.579	3.60	13.78	5.54
C4	9.68	0.578	3.46	13.04	5.36
C5	8.34	0.555	3.05	10.70	4.91
S1	15.56	0.547	4.03	16.16	6.31
S2	27.55	0.576	4.44	19.24	6.70
S3	15.30	0.554	4.07	16.45	6.32
S4	16.54	0.517	3.84	14.80	6.25
S5	14.77	0.568	4.12	16.93	6.31

At 0.4φ the Krieger Dougherty equation still gives meaningful values for intrinsic viscosity, albeit a little lower than for mastics at 0.3φ. The Mooney equation however has intrinsic viscosities below 2.5 as a result of over-predicting the stiffening effect of the filler. The Chong equation returns values that are reasonable, if a little high for some fillers. Again, in general, Fillers C1-5 have lower intrinsic viscosities than Fillers S1-5.

Table 5-2: Intrinsic viscosity of fillers in Bitumen B1, 0.4 solid volume fraction

INTRINSIC VISCOSITY B1, 0.4φ					
	Average $J(t)_{rel}$	φ_{max}	MOONEY	CHONG	KRIEGER-DOUGHERTY
C1	20.13	0.534	1.89	5.85	4.07
C2	19.84	0.534	1.85	5.80	4.05
C3	12.46	0.579	1.88	5.66	3.71
C4	13.63	0.578	1.95	5.99	3.84
C5	17.48	0.555	1.96	6.16	4.04
S1	26.38	0.547	2.17	7.60	4.55
S2	27.55	0.576	2.51	9.37	4.86
S3	35.23	0.554	2.46	9.52	5.02
S4	22.40	0.517	1.73	5.47	4.05
S5	21.43	0.568	2.23	7.62	4.43

The Krieger-Dougherty model is the only model that gives realistic values for intrinsic viscosity at the highest level of solid addition (Table 5-3). Furthermore, it can be seen from the all of the data calculated for fillers in Bitumen B1 that the Krieger-Dougherty model is the only model which consistently predicts a realistic value for intrinsic viscosity of asphalt fillers across the range of solid volume fractions.

Table 5-3: Intrinsic viscosity of fillers in Bitumen B1, 0.5 solid volume fraction

INTRINSIC VISCOSITY B1, 0.5φ					
	Average $J(t)_{rel}$	φ_{max}	MOONEY	CHONG	KRIEGER-DOUGHERTY
C1	79.79	0.534	0.56	2.17	2.98
C2	77.72	0.534	0.56	2.15	2.97
C3	28.99	0.579	0.91	2.77	2.92
C4	31.35	0.578	0.92	2.87	2.98
C5	49.90	0.555	0.77	2.67	3.05
S1	82.87	0.547	0.76	3.04	3.29
S2	66.78	0.576	1.11	4.38	3.61
S3	102.69	0.554	0.91	3.97	3.60
S4	157.05	0.517	0.33	1.58	2.87
S5	55.21	0.568	0.96	3.50	3.33

Derivation of the MPK Coefficient – *Fillers in Binder B1*

As stated previously, the value of the MPK Coefficient ($\varphi_{max}[\eta]$) is often in the region of 2. In the case of bitumen-filler mastics produced using Bitumen B1, the values of MPK Coefficient fall with increasing solid volume fraction. The average values for each mastic are quite consistent within each subgroup C1-5 and S1-5, with Fillers S1-5 having higher Coefficients than C1-5. Results are given in Table 5-4 below.

Table 5-4: Average MPK Coefficient of fillers in Bitumen B1

Bitumen B1	**MPK *0.3φ***	**MPK *0.4φ***	**MPK *0.5φ***	**Average**	***Sub-group average***
C1	2.95	2.17	1.59	**2.24**	
C2	2.93	2.16	1.59	**2.23**	
C3	3.21	2.15	1.69	**2.35**	
C4	3.10	2.22	1.72	**2.35**	
C5	2.73	2.24	1.69	**2.22**	***2.28***
S1	3.45	2.49	1.80	**2.58**	
S2	3.86	2.80	2.08	**2.91**	
S3	3.50	2.78	1.99	**2.76**	
S4	3.23	2.09	1.48	**2.27**	
S5	3.58	2.52	1.89	**2.66**	***2.64***

Equation 49, the modified Krieger-Dougherty model, can be simplified for the case of fillers in Bitumen B1 as follows.

General (all fillers)

$$J(t)rel = \left(1 - \frac{\phi}{\phi_{\max}}\right)^{-2.46} \quad (53)$$

For calcium carbonate fillers C1-5

$$J(t)_{rel} = \left(1 - \frac{\phi}{\phi_{\max}}\right)^{-2.28} \quad (54)$$

For siliceous fillers S1-5

$$J(t)_{rel} = \left(1 - \frac{\phi}{\phi_{\max}}\right)^{-2.64} \quad (55)$$

where

$J(t)_{rel}$ = relative creep compliance

φ_{max} = maximum packing fraction determined using two point projection method.

Fillers in Bitumen B2

Intrinsic Viscosity

The results obtained for intrinsic viscosity followed similar patterns to the fillers in Bitumen B1 with only the Krieger-Dougherty model predicting realistic values for the fillers at the three solid volume levels. In general, the intrinsic viscosities of the fillers are lower in Bitumen B2 than in Bitumen B1, which mirrors the reduction in relative creep compliance

for the mastics. The intrinsic viscosities of fillers in Bitumen B2 are given in Tables 5.5 to 5.7. For the fillers in 10/20 grade bitumen the values of intrinsic viscosity are lower and the level of stiffening with respect to φ/φ_{max} also lower.

Table 5-5: Intrinsic viscosity of fillers in Bitumen B2, 0.3 solid volume fraction

INTRINSIC VISCOSITY B2, 0.3φ					
	Average $J(t)_{rel}$	φ_{max}	MOONEY	CHONG	KRIEGER-DOUGHERTY
C1	6.58	0.523	2.44	7.76	4.23
C2	4.55	0.558	1.95	6.50	3.52
C3	2.60	0.558	0.73	3.52	2.22
C4	4.21	0.590	1.91	6.77	3.43
C5	4.56	0.572	2.01	6.86	3.57
S1	4.86	0.505	1.83	5.49	3.47
S2	4.59	0.604	2.15	7.72	3.68
S3	6.01	0.510	2.21	6.76	3.96
S4	3.35	0.553	1.30	4.67	2.80
S5	5.07	0.550	2.13	6.95	3.74

Table 5-6: Intrinsic viscosity of fillers in Bitumen B2, 0.4 solid volume fraction

INTRINSIC VISCOSITY B2, 0.4φ					
	Average $J(t)_{rel}$	φ_{max}	MOONEY	CHONG	KRIEGER-DOUGHERTY
C1	9.48	0.523	1.26	3.20	2.97
C2	17.30	0.558	1.98	6.24	4.05
C3	8.98	0.558	1.47	3.95	3.12
C4	12.29	0.590	1.95	5.95	3.75
C5	15.81	0.572	2.03	6.40	4.02
S1	16.18	0.505	1.41	3.97	3.51
S2	23.69	0.604	2.63	9.84	4.83
S3	7.56	0.510	1.01	2.40	2.58
S4	14.27	0.553	1.79	5.31	3.74
S5	6.92	0.550	1.21	3.06	2.71

Table 5-7: Intrinsic viscosity of fillers in Bitumen B2, 0.5 solid volume fraction

INTRINSIC VISCOSITY B2, 0.5φ					
	Average $J(t)_{rel}$	φ_{max}	MOONEY	CHONG	KRIEGER-DOUGHERTY
C1	50.64	0.523	0.35	1.13	2.41
C2	47.22	0.558	0.80	2.72	3.05
C3	24.45	0.558	0.66	1.84	2.54
C4	26.16	0.590	0.98	2.96	2.94
C5	38.87	0.572	0.92	3.02	3.09
S1	347.70	0.505	0.12	0.71	2.51
S2	49.86	0.604	1.34	5.03	3.68
S3	87.84	0.510	0.17	0.65	2.22
S4	50.54	0.553	0.75	2.59	3.02
S5	22.27	0.550	0.56	1.49	2.35

Derivation of the MPK Coefficient

In the case of both sets of fillers, C1-5 and S1-5, the average is similar 1.83 and 1.78 respectively, so a generalised version of the Krieger-Dougherty can be used for both sets of fillers. There is a significant overlap in the data sets for C1-5 and S1-5, unlike in Bitumen B1 where MPK values for all fillers in group S1-5 were higher than group C1-5. The $[\eta]\varphi_{max}$ calculations are given in Table 5-8 below.

Table 5-8: Average MPK Coefficient of fillers in Bitumen B2

Bitumen B2 (MPK)	**0.3φ**	**0.4φ**	**0.5φ**	**Average**	***Sub-group average***
C1	2.21	1.55	1.26	**1.68**	
C2	1.96	2.26	1.70	**1.98**	
C3	1.24	1.74	1.42	**1.47**	
C4	2.02	2.21	1.73	**1.99**	
C5	2.04	2.30	1.77	**2.04**	***1.83***
S1	1.75	1.77	1.27	**1.60**	
S2	2.22	2.92	2.22	**2.45**	
S3	2.02	1.32	1.13	**1.49**	
S4	1.55	2.07	1.67	**1.76**	
S5	2.06	1.49	1.29	**1.61**	***1.78***

The modified Krieger-Dougherty model can be simplified for the case of fillers in Bitumen B2 using the overall average MPK coefficient, 1.81.

$$J(t)_{rel} = \left(1 - \frac{\phi}{\phi_{\max}}\right)^{-1.81} \tag{56}$$

Fillers in Bitumen B3

Intrinsic Viscosity

Once again, the Krieger-Doughtery Equation was the only model that consistently gave sensible values of intrinsic viscosity for the bitumen filler mastics manufactured using Bitumen B3. The Chong equation on the whole gives reasonable values for intrinsic viscosity, but there are some very high and very low values indicating that this equation is not consistently appropriate for describing the behaviour of bitumen-filler mastics. The results are presented in Tables 5-9 to 5-11.

Table 5-9: Intrinsic viscosity of fillers in Bitumen B3, 0.3 solid volume fraction

INTRINSIC VISCOSITY B3, 0.3φ					
	Average $J(t)_{rel}$	φ_{max}	MOONEY	CHONG	KRIEGER-DOUGHERTY
C1	6.89	0.547	2.67	8.92	4.44
C2	5.00	0.534	2.07	6.67	3.69
C3	4.10	0.604	1.90	6.92	3.40
C4	2.54	0.517	0.60	2.86	2.08
C5	12.35	0.624	4.20	18.10	6.15
S1	4.81	0.537	1.97	6.27	3.57
S2	5.64	0.583	2.48	8.64	4.11
S3	4.54	0.577	2.02	6.96	3.57
S4	16.62	0.565	4.30	18.11	6.57
S5	10.55	0.553	3.45	12.67	5.45

Table 5-10: Intrinsic viscosity of fillers in Bitumen B3, 0.4 solid volume fraction

INTRINSIC VISCOSITY B3, 0.4φ					
	Average $J(t)_{rel}$	φ_{max}	MOONEY	CHONG	KRIEGER-DOUGHERTY
C1	16.31	0.547	1.83	5.58	3.88
C2	24.18	0.534	2.07	7.01	4.40
C3	7.46	0.604	1.58	4.43	3.07
C4	4.55	0.517	0.71	1.65	1.97
C5	28.18	0.624	2.96	12.07	5.22
S1	9.53	0.537	1.36	3.57	3.07
S2	22.08	0.583	2.39	8.47	4.58
S3	9.13	0.577	1.61	4.47	3.24
S4	28.84	0.565	2.43	9.01	4.83
S5	19.28	0.553	2.01	6.50	4.17

Table 5-11: Intrinsic viscosity of fillers in Bitumen B3, 0.5 solid volume fraction

INTRINSIC VISCOSITY B3, 0.5φ					
	Average $J(t)_{rel}$	φ_{max}	MOONEY	CHONG	KRIEGER-DOUGHERTY
C1	60.669	0.547	0.70	2.55	3.06
C2	101.838	0.534	0.73	3.13	3.36
C3	15.953	0.604	0.93	2.49	2.61
C4	44.170	0.517	0.24	0.75	2.13
C5	51.274	0.624	1.56	6.11	3.91
S1	36.291	0.537	0.49	1.48	2.49
S2	53.636	0.583	1.13	4.20	3.50
S3	22.930	0.577	0.82	2.33	2.69
S4	99.632	0.565	1.06	4.67	3.77
S5	60.351	0.553	0.79	2.89	3.17

Derivation of the MPK Coefficient

For Bitumen B3, there are, on average, higher MPK coefficients in fillers S1-5 compared to C1-5, however there is a wide range of values within each subgroup. As noted in the previous chapter, four fillers, C3, C4, S1 and S3 have values lower than 2 and have markedly different behaviour from the other fillers.

Table 5-12: Average MPK Coefficient of fillers in Bitumen B3

Bitumen B3 (MPK)	**0.3φ**	**0.4φ**	**0.5φ**	**Average**	***Sub-group average***
C1	2.43	2.12	1.67	**2.07**	
C2	1.97	2.35	1.79	**2.04**	
C3	2.05	1.85	1.58	**1.83**	
C4	1.08	1.02	1.10	**1.07**	
C5	3.84	3.26	2.44	**3.18**	***2.04***
S1	1.92	1.65	1.34	**1.63**	
S2	2.40	2.67	2.04	**2.37**	
S3	2.06	1.87	1.55	**1.83**	
S4	3.71	2.73	2.13	**2.86**	
S5	3.01	2.31	1.75	**2.36**	***2.21***

For Bitumen B3, using the overall average MPK coefficient, the modified Krieger-Dougherty equation can be written as

$$J(t)_{rel} = \left(1 - \frac{\phi}{\phi_{\max}}\right)^{-2.12} \quad (57)$$

Correlation between index properties and intrinsic viscosity of the filler

In this chapter we have seen that two primary factors can be used to describe the creep properties of bitumen-filler mastics, the solid volume fraction expressed as a percentage of the maximum packing fraction, φ/φ_{max}, and the intrinsic viscosity of the filler $[\eta]$ with intrinsic viscosity relating to any effects outside of the bulk volume filling relation φ/φ_{max}.

In the following section the relationship between intrinsic viscosity, according to the modified Krieger-Dougherty model, and index properties of the filler are examined.

In the case of fillers in Bitumen B1, intrinsic viscosity is strongly correlated with fineness modulus, measured by laser diffraction at low volume concentration (0.3φ). In general, fillers in this bitumen have a regular behaviour, with subset C1-5 stiffening to a lesser extent than Fillers S1-5 and also having lower values for intrinsic viscosity than S1-5. The only single index property that splits the two filler sets into two subsets is fineness modulus (a property derived from particle size distribution and linked to specific surface area) measured by laser diffraction. The correlation with intrinsic viscosity is greater than 0.9 R^2. The BET value of surface area is also loosely correlated at a level of $0.38R^2$.

Interestingly, in both cases the finer fillers have lower intrinsic viscosity than the coarser fillers. Increasing aspect ratio does generally lead to increased values of intrinsic viscosity, but only at the level of $R^2 = 0.23$.

As solid volume concentration increases to 0.4φ the correlation for $[\eta]$ with the index properties is relatively poor. The correlation with specific surface (laser) is lower than at 0.3φ ($R^2 = 0.52$), conversely the correlation with aspect ratio is higher ($R^2 = 0.42$). This can be explained as an increase in particle-particle contact and an increased importance placed on particle shape as concentration increase. A summary of the correlations between index properties and intrinsic viscosity of fillers in Bitumen B1 is given in Table 5-13.

Table 5-13: Correlations (R^2 value) between index properties of the fillers and intrinsic viscosity of the fillers derived using the Krieger-Dougherty model, Bitumen B1

BITUMEN B1	**ALL**			**C1-5**			**S1-5**		
Solid Volume Fraction (φ)	0.3	0.4	0.5	0.3	0.4	0.5	0.3	0.4	0.5
φ_{max}	0.05	0.07	0.17	-0.06	-0.23	0.21	0.00	0.13	0.21
γ^{LW}	0.01	0.02	0.00	0.03	0.15	0.00	0.37	-0.03	0.00
γ+	0.01	0.25	0.20	-0.74	0.06	0.15	-0.08	0.30	0.15
γ-	-0.24	-0.00	-0.00	-0.95	0.15	0.03	-0.24	0.02	0.03
BET	-0.38	-0.02	-0.01	-0.97	0.13	0.20	-0.09	0.20	0.20
MBV	-0.22	0.00	0.00	-0.98	0.13	0.11	-0.12	0.23	0.10
Aspect Ratio	0.23	0.04	0.01	-0.64	-0.00	-0.82	-0.25	-0.93	-0.82
FM	-0.91	-0.43	-0.35	-0.92	0.09	-0.01	-0.63	-0.00	-0.01

Examining the subgroups separately gives interesting results. For Subgroup S1-5, the siliceous fillers, the fineness of the filler is well correlated to intrinsic viscosity at 0.3φ, whereas aspect ratio is the dominant factor at higher concentrations, 0.4φ and 0.5φ. Again this appears sensible, as at low level of solid volume fraction surface effects are likely to be

more prevalent as particle-to-particle interactions are lower. At high levels of solid volume fraction, inter-particle interactions are likely to be high; in such cases particle shape may become a significant factor.

For Fillers C1-5, at low solid volume concentrations, a strong correlation is found between the level of surface interaction and intrinsic viscosity. The surface energy component responsible for the level of intrinsic viscosity is γ^{AB}, the Lewis acid-base interactions. At high levels of solid volume fraction, 0.5φ, as with Fillers S1-5, particle shape expressed as aspect ratio has the strongest correlation.

Again, the behaviour of the fillers appears to be better explained by their subgroups rather than considering all fillers together. There consistently appears to be fundamental differences in the behaviour of calcium carbonate fillers and siliceous fillers.

For fillers in Bitumen B2, the relationship between index properties and intrinsic viscosity (calculated from the Krieger Dougherty equation) is very poor with no significant correlations found. However, again the correlation between the values of $[\eta]$ derived from the Krieger-Dougherty equation and the index properties of the fillers gives very interesting results when considering the two sets of fillers separately. In Bitumen B2, it was found that the behaviour of the fillers, with respect to the Lifshitz Van der Waals component of surface energy were inverse for the two filler groups (see Figures 5-1 and 5-2). Siliceous fillers have higher values of $[\eta]$ as these forces increase, whereas for C1-5 the inverse is true (See Figure 5-1)

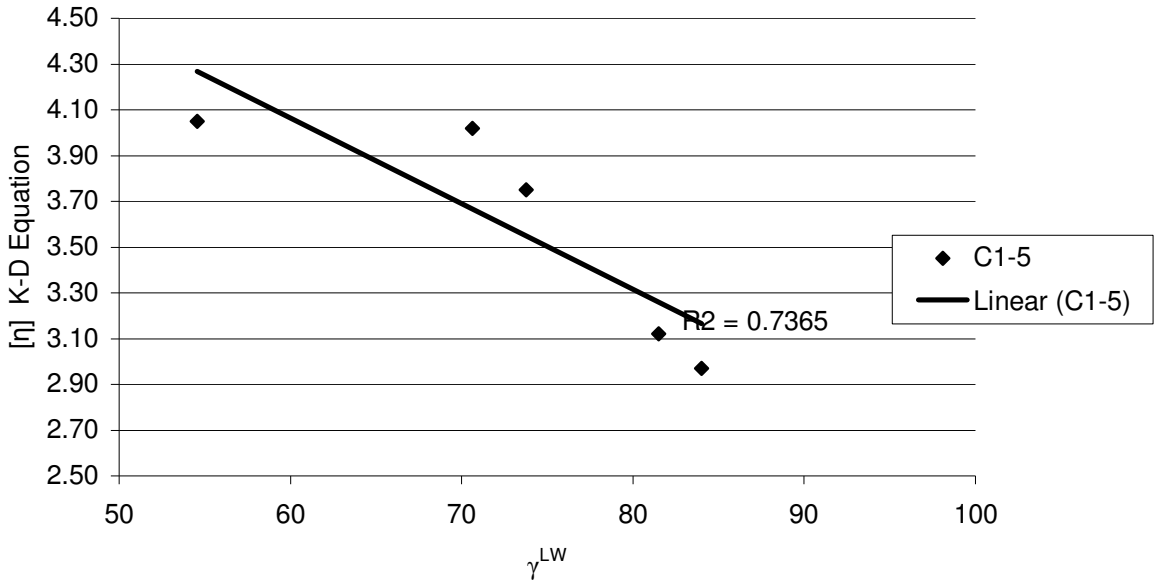

Figure 5-1: Intrinsic Viscosity versus Lifshitz Van Der Waals component of surface energy of the Fillers C1-5, Bitumen B2

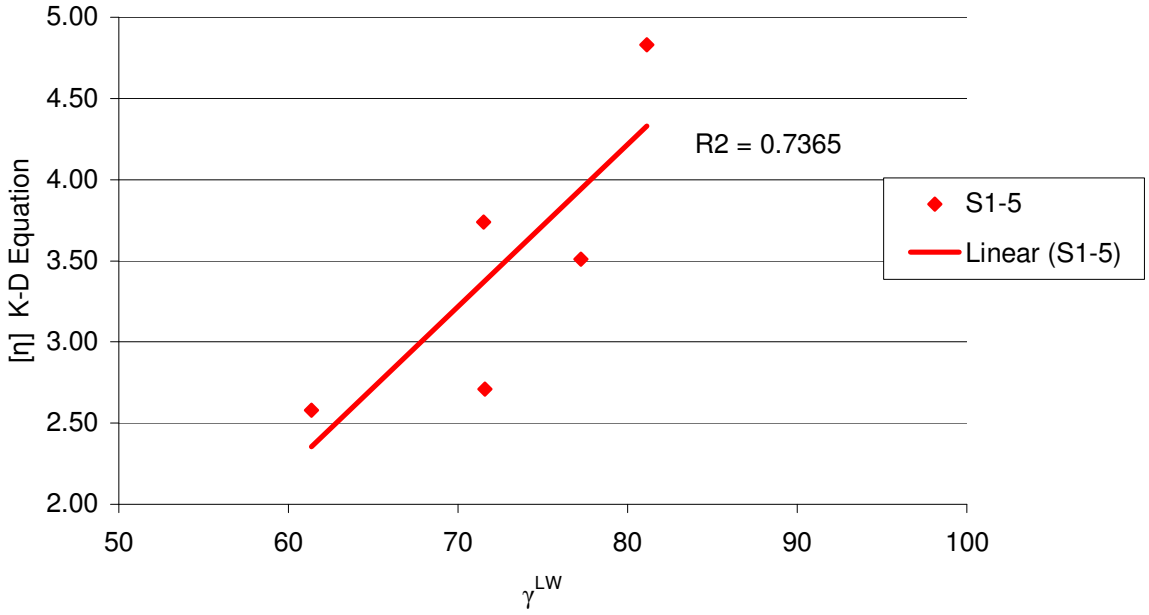

Figure 5-2: Intrinsic Viscosity versus Lifshitz Van Der Waals component of surface energy of the Fillers S1-5, Bitumen B2

For siliceous fillers, at low concentrations, the aspect ratio has the strongest correlation with intrinsic viscosity; this confirms classical thinking as proposed by Barnes (2000). At higher concentrations, there is a significant increase in inter-particle interactions and the role of the surface appears more important than the shape of the particles. This is the inverse of the behaviour noted for the same filler set in Bitumen B1. The correlation with fineness modulus follows the same trend with increasing fineness leading to lower intrinsic viscosities (see Table 5-14).

Table 5-14: Correlations between index properties of the fillers and intrinsic viscosity of the fillers derived using the Krieger-Dougherty model, Bitumen B2

BITUMEN B2	C1-5			S1-5		
	0.3φ	0.4φ	0.5φ	0.3φ	0.4φ	0.5φ
φ_{max}	0.0286	0.1939	0.2524	-0.2242	-0.0966	-0.2242
γ^{LW}	0.0319	-0.725	-0.6527	0.5359	0.6978	0.5359
γ^{+}	0.036	0.0108	0.0203	-0.3912	-0.2046	-0.3912
γ^{-}	0.0387	0.2973	0.3204	-0.7267	-0.5624	-0.7267
BET	0.053	0.2531	0.2811	-0.5885	-0.7774	-0.5885
MBV	0.0603	0.2716	0.302	-0.3959	-0.4942	-0.3959
Aspect Ratio	0.0204	0.3423	0.4157	0.0045	0.0144	0.0045
FM	0.0143	0.2108	0.2364	-0.8011	-0.929	-0.8011

For Fillers C1-5 there is also a strong correlation with γ^{LW} component of surface energy, but the relationship is the inverse of that with Fillers S1-5. This once again points to fundamental differences in the way carbonate based fillers behave in bitumen compared to siliceous fillers. Also the aspect ratio has an increasing influence as concentration increases, again this is the inverse of the situation with siliceous fillers in Bitumen B2.

For the fillers in Bitumen B3, the overall correlation of the whole set is relatively poor. The correlation with φ_{max} measured in air is the strongest, followed by aspect ratio.

There is an influence of the surface factors, with both surface area measured using the BET technique and γ^- having a minor correlation with $[\eta]$, see Table 5-15.

Table 5-15: Correlations between index properties of the fillers and intrinsic viscosity of the fillers derived using the Krieger-Dougherty model, Bitumen B3

BITUMEN B3	ALL			C1-5			S1-5		
	0.3φ	0.4φ	0.5φ	0.3φ	0.4φ	0.5φ	0.3φ	0.4φ	0.5φ
φ_{max}	-0.20	-0.32	-0.33	-0.30	-0.39	-0.31	-0.38	-0.47	-0.59
γ^{LW}	0.00	-0.03	-0.03	0.00	-0.14	-0.15	0.00	0.12	0.08
γ^+	-0.10	-0.04	0.07	0.60	0.24	0.29	-0.61	-0.92	-0.85
γ^-	0.20	0.18	0.18	0.65	0.48	0.56	-0.10	-0.50	-0.59
BET	0.15	0.14	0.16	0.61	0.39	0.47	-0.05	-0.17	-0.17
MBV	0.18	0.15	0.17	0.57	0.36	0.44	-0.09	-0.23	-0.16
Aspect Ratio	0.24	0.04	0.04	0.01	-0.00	0.00	0.52	0.13	0.12
FM	0.00	-0.00	0.00	0.66	0.44	0.51	0.02	0.15	-0.13

Once again, dividing the fillers into their petrologic subsets gives some very strong correlations between $[\eta]$ for some of the index properties. For the siliceous fillers there is a very strong correlation between the surface energy factors and $[\eta]$, in particular there is a very strong correlation with γ^{AB} and γ^+. As this factor becomes larger the intrinsic viscosity falls (See Figure 5-3).

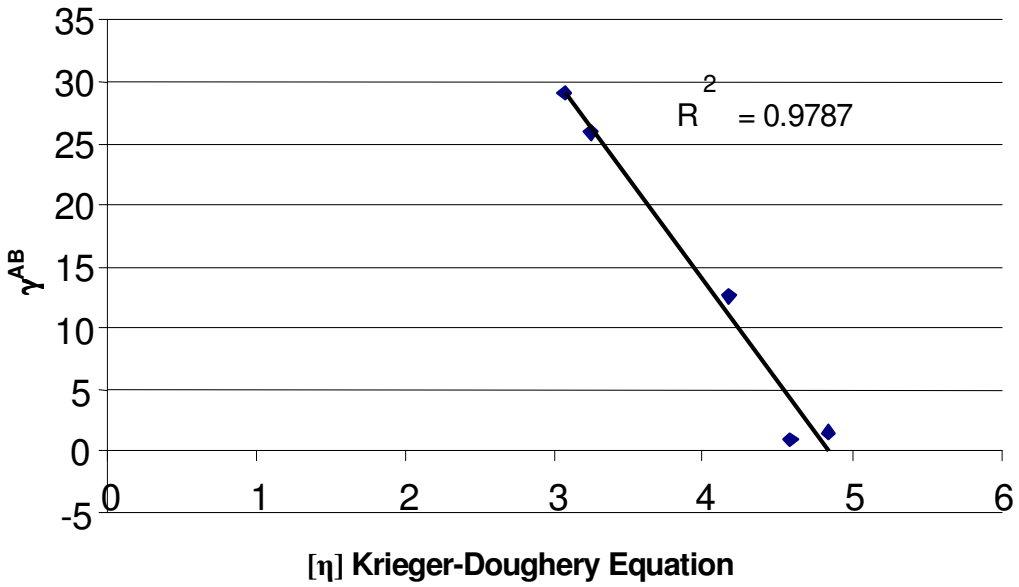

Figure 5-3: Correlation between *[η]* determined by the Krieger-Dougherty Equation and γ^{AB} component of surface energy (Van Oss Approach) for Fillers S1-5

For fillers C1-5 the opposite is found. Although there is still a strong correlation between *[η]* and surface energy, with these fillers higher values of γ^{AB} lead to higher values of *[η]* (Figure 5-4).

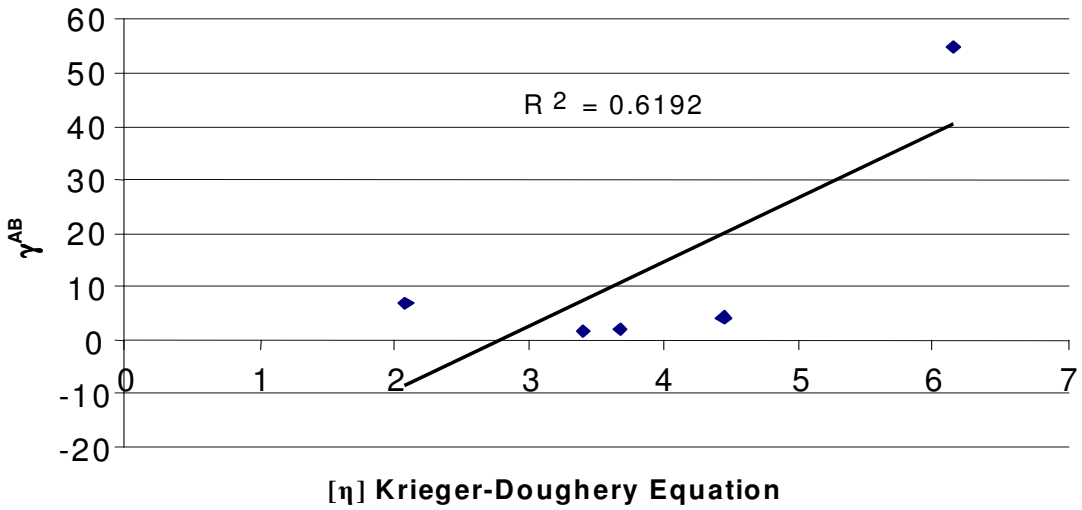

Figure 5-4: Correlation between *[η]* determined by the Krieger-Dougherty Equation and γ^{AB} component of surface energy (Van Oss Approach) for Fillers C1-5

CHAPTER SUMMARY

In this section intrinsic viscosity of asphalt fillers has been calculated using three models proposed by Chong, Mooney and Krieger and Dougherty. Consistently, the Krieger-Dougherty equation produced the most realistic values of intrinsic viscosity for asphalt fillers in bitumen. The range of intrinsic viscosity changes with volume concentration, with a tendency for intrinsic viscosity to fall as solid volume concentration increases. Table 5-16 below summarise the values for asphalt fillers in bitumen.

Table 5-16: Summary of average intrinsic viscosities and MPK Coefficients

ALL FILLERS	**B1**		**B2**		**B3**	
	[η]	**MPK**	***[η]***	**MPK**	***[η]***	**MPK**
Average	4.43	2.46	3.26	1.81	3.74	2.12
Maximum	6.70	3.86	4.83	2.92	6.57	3.84
Minimum	2.87	1.48	2.22	1.13	1.97	1.02
Standard Deviation	1.21	0.68	0.66	0.41	1.13	0.70
C1-5	**B1**		**B2**		**B3**	
	[η]	**MPK**	***[η]***	**MPK**	***[η]***	**MPK**
Average	4.09	2.28	3.13	1.74	3.63	2.06
Maximum	5.54	3.21	4.83	2.92	6.57	3.84
Minimum	2.92	1.59	0.66	0.41	1.13	0.70
Standard Deviation	1.03	0.57	0.88	0.54	1.32	0.78
S1-5	**B1**		**B2**		**B3**	
	[η]	**MPK**	***[η]***	**MPK**	***[η]***	**MPK**
Average	4.77	2.64	3.25	1.78	3.92	2.21
Maximum	6.70	3.86	4.83	2.92	6.57	3.71
Minimum	2.87	1.48	2.22	1.13	2.49	1.34
Standard Deviation	1.32	0.75	0.73	0.48	1.08	0.62

The modified Krieger-Dougherty equation can be simplified to include the MPK Coefficients for asphalt fillers and a set of equations can be proposed to describe the behaviour of asphalt fillers in different bitumen types as measured by relative creep compliance in Equations 58-62 below.

All Fillers in Bitumen B1

$$J(t)_{rel} = \left(1 - \frac{\phi}{\phi_{\max}}\right)^{-2.46} \tag{58}$$

Fillers C1-5 in Bitumen B1

$$J(t)_{rel} = \left(1 - \frac{\phi}{\phi_{\max}}\right)^{-2.28} \tag{59}$$

Fillers S1-5 in Bitumen B1

$$J(t)_{rel} = \left(1 - \frac{\phi}{\phi_{\max}}\right)^{-2.64} \tag{60}$$

Fillers in Bitumen B2

$$J(t)_{rel} = \left(1 - \frac{\phi}{\phi_{\max}}\right)^{-1.81} \tag{61}$$

Fillers in Bitumen B3

$$J(t)_{rel} = \left(1 - \frac{\phi}{\phi_{\max}}\right)^{-2.12} \tag{62}$$

In Bitumen B1 there are different coefficients for carbonate fillers and siliceous fillers, whilst in B2, a hard 10/20 penetration grade bitumen, and B3 a polymer modified resin, there is a wider range of behaviours.

The average MPK Coefficient for all experimental data, all bitumen-filler combinations at all concentrations, was 2.13, very close to the value of 2 proposed by Barnes. The MPK Coefficient reflects the order of the master curves derived from normalizing solid volume fraction for maximum packing fraction, φ/φ_{max} (Figure 5-5)

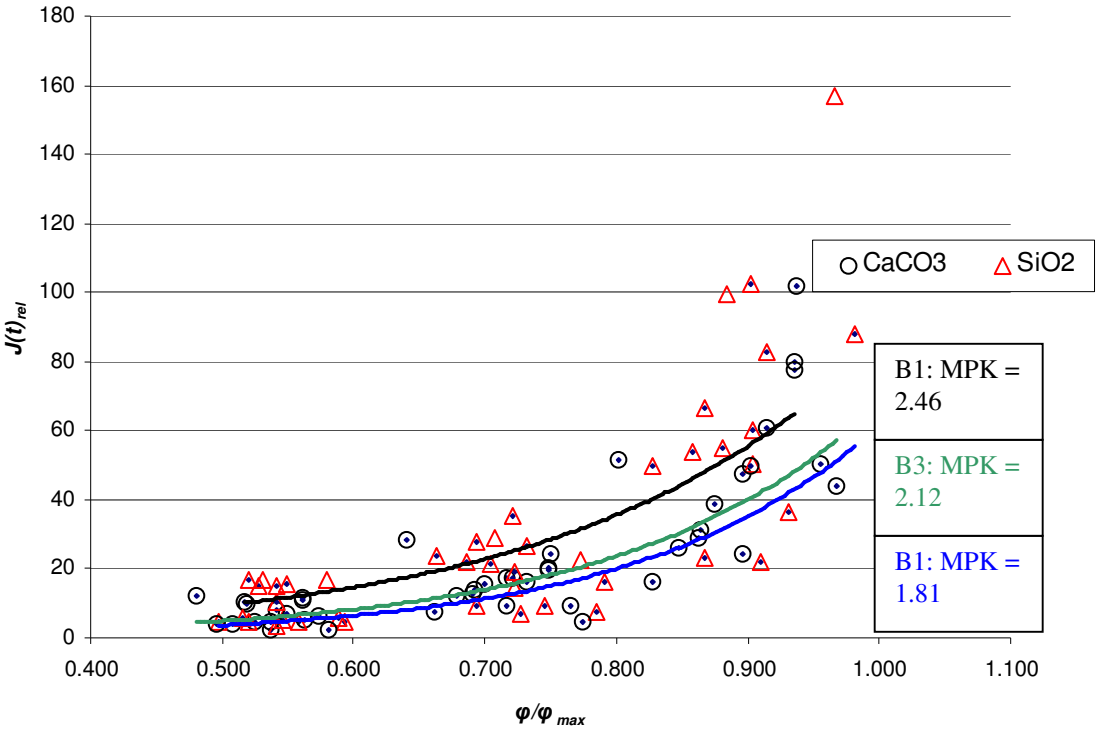

Figure 5-5: Stiffening master curves presented with their MPK Coefficients

It was not possible to relate intrinsic viscosity to a single index parameter of the filler. Aspect ratio, fineness modulus and surface energy were the three best correlated factors, although these could not be consistently applied to all filler types in all bitumen types. There

did appear to be fundamental differences in the behaviour of Fillers C1-5 and S1-5. Frequently, inverse relationships were found between the two subsets.

The position of the exponential curve is related to the MPK Coefficient for the three bitumen types as a function of the product of intrinsic viscosity and solid volume fraction. In Chapter VI, a possible explanation for the level of MPK, and the positioning of the exponential curves normalised for φ_{max} is given.

CHAPTER VI

SURFACE INTERACTIONS AND RHEOLOGY OF BITUMEN: FILLER MASTICS

INTRODUCTION

In the previous chapter rheological data obtained during creep compliance testing was fitted to three models and the intrinsic viscosity $[\eta]$ of the fillers calculated. The Krieger-Dougherty model was found to be the most consistent and gave realistic values of intrinsic viscosity for the asphalt fillers in bitumen. Multiplication of the term $[\eta]$ by the maximum packing fraction, φ_{max}, gives the MPK Coefficient, which has been found to be close to 2 for a variety of situations (Barnes, 2000; Rides, 2005). The average MPK Coefficient for the mastics tested ranged from 1.81 – 2.64, with an overall average value of 2.13.

The experiments conducted suggest that the Krieger-Dougherty equation is suitable for describing the behaviour of bitumen-filler mastics and that the MPK Coefficient for the mastics is in the region of 2 as predicted. It was not, however, possible to correlate intrinsic viscosity or MPK Coefficient to any single index parameter of the fillers measured during the characterisation stage of the testing outlined in Chapter III.

The ten fillers gave different levels of relative creep compliance and different MPK coefficients in different bitumen types, even when the solid volume fraction was normalised to the maximum packing fraction. For the tests conducted, the average order of stiffening, and MPK coefficient (given in brackets) are as follows:

Binder B1 (2.46) > Binder B3 (2.12)> Binder B2 (1.81)

According to rheological modelling, the interfacial changes could alter the properties of the mastic in two possible ways. The dispersion of the filler could be effected by the interfacial properties and the maximum packing fraction value could shift with changing interfacial energy, leading to differences in the scaling of solid volume fraction and changes in observed stiffening. For example, if the dispersion was very poor φ_{max} would fall, causing greater stiffening for the same solid volume fraction, due to shift upwards in the value of φ/φ_{max}.

Alternatively, the interaction between the filler and the bitumen could lead to a change in the creep compliance of the liquid phase (bitumen). The viscosity of suspensions is in the first instance governed by the viscosity of the liquid phase and any change in the viscosity of the liquid phase leads to a proportionate increase in the viscosity of the mastic (Barnes, 2000).

When considering a set of fillers in a single bitumen type, the resultant properties of the mastic are the combination of several complex effects, including particle shape, packing characteristics, fineness of the filler and surface interactions between the liquid bitumen phase and the solid filler particles.

As many of the index properties of the fillers remain constant when only bitumen type is changed, for example properties such as shape, density and surface area, such factors are unlikely to account for observed differences in stiffening in different binder types. Examining a single filler type in three different bitumen types cancels out several of the index properties and focuses the attention on the interaction between the two phases as the physical properties of the filler remain essentially unchanged in different bitumen types.

In this chapter the bond energy between the filler and bitumen of each mastic is derived using thermodynamic equations, and the level of bond is compared to the rheological behaviour of the ten fillers in each bitumen type. In addition, individual fillers are assessed in three bitumen types. Specifically, the level of bond energy between the two phases is related to the MPK Coefficient for the fillers in bitumen.

SURFACE FREE ENERGY OF ADHESION

Background

Surface energy characterisation gives rise to the ability to quantify the level of bond energy between two (or more) materials. Surface energy of asphalt components has been the subject of significant study in the United State in recent years and several measurement approaches have been developed (Cheng, 2004; Hefer, 2005; Bhasin, 2006). This thermodynamic approach allows for the calculation of the bond energy between two (or more materials) through the use of the surface free energy of adhesion concept.

Derivation of bond energy for the mastics

The surface energy of the fillers and bitumens used in this study were measured and modelled according to the approach developed by Van Oss as outlined in Chapter III. The free energy of adhesion between two materials was given in Chapter II, Equation 1, the Dupré equation (Dupré, 1869).

In the case of bitumen-filler mastics, γ_1 represents the surface energy of the filler, γ_2 represents the surface energy of the bitumen and γ_{12} represents the bond energy between the bitumen and the filler.

According to the Van Oss approach (Good and Van Oss, 1992; Good 1992), the strength of the bond between two materials, γ^{12}, is made up of two components, a non-polar component termed *the Lifshitz-van der Waals component*, and a polar component referred to as the *Acid-Base component*. The total interactive energy is given as the sum of these two components

$$\gamma_{12}{}^{TOTAL} = \gamma_{12}{}^{LW} + \gamma_{12}{}^{AB} \tag{63}$$

The non-polar LW energy, $\gamma_{12}{}^{LW}$, between two materials is given by

$$\gamma_{12}{}^{LW} = (\sqrt{\gamma_1{}^{LW}} - \sqrt{\gamma_2{}^{LW}})^2 \tag{64}$$

And the polar AB adhesive surface energy component, $\gamma_{12}{}^{AB}$ is given by:

$$\gamma_{12}{}^{AB} = 2(\sqrt{\gamma_1{}^{+} - \gamma_2{}^{-}})(\sqrt{\gamma_1{}^{-} - \gamma_2{}^{+}}) \quad (65)$$

Equations 64 and 65 can be combined as

$$\gamma_{12}{}^{TOTAL} = (\sqrt{\gamma_1{}^{LW}} - \sqrt{\gamma_2{}^{LW}}) + 2(\sqrt{\gamma_1{}^{+} - \gamma_2{}^{-}})(\sqrt{\gamma_1{}^{-} - \gamma_2{}^{+}}) \quad (66)$$

Having previously determined γ^{LW}, γ^{+} and γ^{-} for the bitumens and fillers (Chapter III) Equation 65 was used to calculate the interactive energy, γ_{12}, between the fillers and the bitumens and subsequently the free energy of adhesion for each bitumen-filler combination was derived. Additionally, the free energy of adhesion of the two components γ^{LW} and γ^{AB} were recorded separately using Equations 64 and 65 to assess which parameter was most closely related to the rheological behaviour of the mastics. The free energy of adhesion for the mastics is given in Table 6-1.

Table 6-1: Free energy of adhesion calculations for the mastics

	B1 – Bond Energy (mJ/m^2)			B2 – Bond Energy (mJ/m^2)			B3 – Bond Energy (mJ/m^2)		
	ΔG_{12}	$\Delta G_{12}{}^{LW}$	$\Delta G_{12}{}^{AB}$	ΔG_{12}	$\Delta G_{12}{}^{LW}$	$\Delta G_{12}{}^{AB}$	ΔG_{12}	$\Delta G_{12}{}^{LW}$	$\Delta G_{12}{}^{AB}$
C1	105.9	99.7	6.2	128.6	120.5	8.1	120.9	112.8	7.6
C2	87.4	80.4	7.2	104.6	97.1	7.6	96.71	90.9	5.4
C3	102.4	98.1	4.3	124.5	118.7	5.9	117.2	111.1	5.6
C4	101.3	93.4	8.00	122.4	112.9	9.6	114.4	105.7	8.2
C5	117.9	91.3	26.6	140.1	110.4	29.6	128.0	103.4	24.1
S1	111.5	95.5	15.9	134.9	115.5	19.3	126.0	108.1	17.3
S2	101.3	98.0	3.4	123.1	118.5	4.7	115.7	110.9	4.4
S3	100.0	85.2	14.9	121.3	103.0	18.4	113.6	96.4	16.8
S4	95.5	91.9	3.6	115.7	111.2	4.5	108.4	104.0	3.9
S5	104.8	92.0	12.8	125.5	111.2	14.3	115.9	104.1	11.3
Average	102.8	92.6	10.3	124.1	111.9	12.2	115.7	104.8	10.5

CORRELATION BETWEEN BOND ENERGY AND RHEOLOGICAL CHARACTERISATIONS

Delta Ring and Ball tests

It was not possible to correlate any surface energy parameter to the Delta Ring and Ball values of the fillers. The values of Delta Ring and Ball fell into a very narrow range for Bitumens B1 and B2, with an average of 13.7^{o}C and a standard deviation of 1.76^{o}C. Bitumen B3 recorded the lowest set of results with an average value of 7.4^{o}C, standard deviation 1.9^{o}C. The low value of Delta Ring and Ball was not reflected in any of the bond energy values, with Bitumen B3 typically having an intermediate value for ΔG_{12} and its components. The relatively low values for fillers recorded in Bitumen B3 were not reflected in the surface free energy calculations.

Creep compliance testing

For the creep compliance testing, a selection of key rheological parameters was chosen for comparison with the interactive parameters calculated for the mastics. As discussed in the previous chapter, the Krieger-Dougherty model was found to be the most appropriate model for describing the behaviour of bitumen-filler mastics and gave the most realistic values of intrinsic viscosity for the fillers. In the following discussions only the intrinsic viscosity and MPK Coefficient derived from the Krieger-Dougherty equation are considered.

The following rheological parameters were chosen:

- $J(t)_{rel}$ *at 0.3, 0.4 and 0.5*φ
- φ_{max} at 45°C, 57°C and 65°C
- $[\eta]$ at 0.3, 0.4 and 0.5φ
- Average MPK Coefficient for the mastic

The values for these rheological factors were compared with the bond energy parameters

- ΔG_{12}^{TOTAL}
- ΔG_{12}^{LW}
- ΔG_{12}^{AB}

The results were examined in two ways, firstly the group of ten fillers in a single bitumen type (followed by sub-grouping by C1-5 and S1-5 if appropriate) and secondly, by single filler types in three different bitumen types.

The MPK Coefficient *and surface interactions*

In Chapter IV, we saw that the same ten samples of filler gave rise to different levels of stiffening in different bitumen types. The modified Krieger-Dougherty equation can be simplified to include the MPK Coefficients for asphalt fillers. The average MPK Coefficient

for all experimental data (all bitumen-filler combinations at all concentrations) was 2.13, very close to the value of 2 proposed by Barnes (2000).

Equations 58 to 62 were proposed in the previous chapter to describe the behaviour of asphalt fillers in different bitumen types. MPK Coefficients reflect the order of the master curves derived from normalizing solid volume fraction for maximum packing fraction, φ/φ_{max}. So we have seen how the position of the exponential curve is related to the MPK Coefficient for the three bitumen types as a function of the product of intrinsic viscosity and solid volume fraction.

Taking the average bond energy for each mastic type manufactured with each filler type, we can see that the MPK Coefficient is closely related to the total level of bond energy, these results are presented in Table 6-2 and Figure 5-1. The relationship is equally as strong for the Lifshitz-Van der Waals forces but not as strong for the acid-base component of bond energy (Figures 5-2 and 5-3).

Table 6-2: Average MPK and bond energy for the mastics by bitumen type

		Bond Energy (mJ/m^2)		
	Average MPK Coefficient	**TOTAL**	**LW**	**AB**
B1	2.456	102.81	92.56	10.29
B2	1.806	124.07	111.90	12.20
B3	2.123	115.68	104.76	10.46

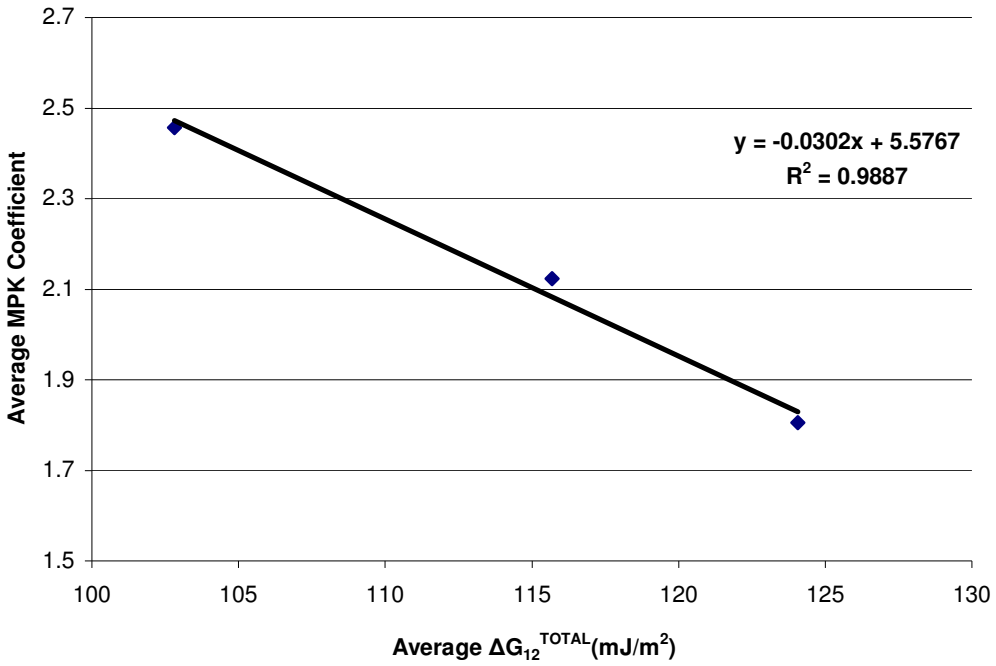

Figure 5-1: Average Marron-Pierce-Kitano Coefficient as a function of average total bond energy

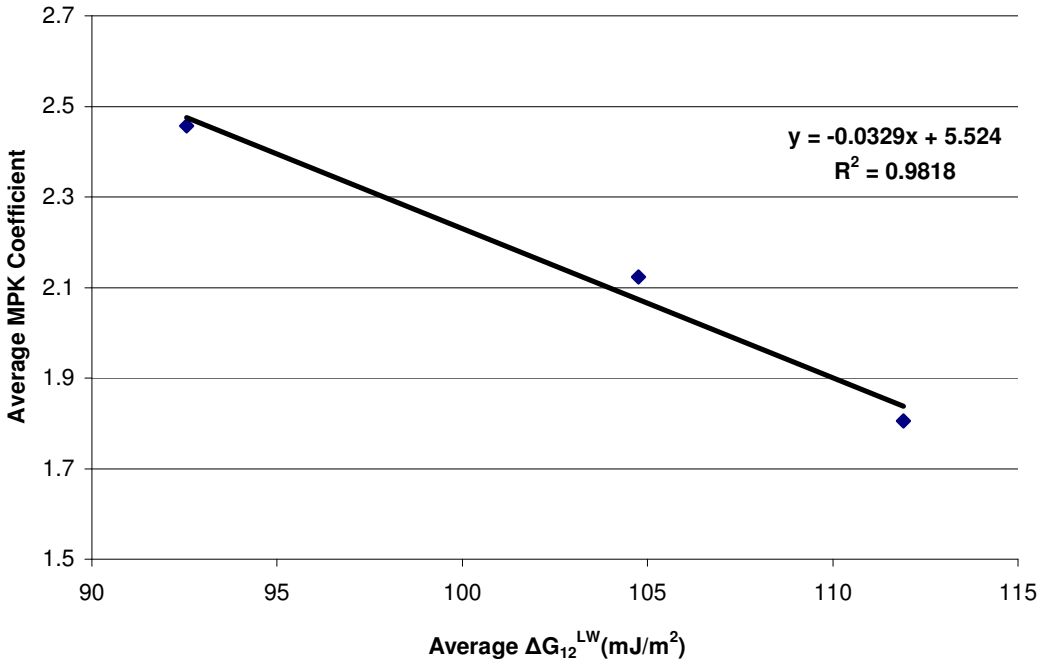

Figure 5-2: Average Marron-Pierce-Kitano Coefficient as a function of average LW component of bond energy

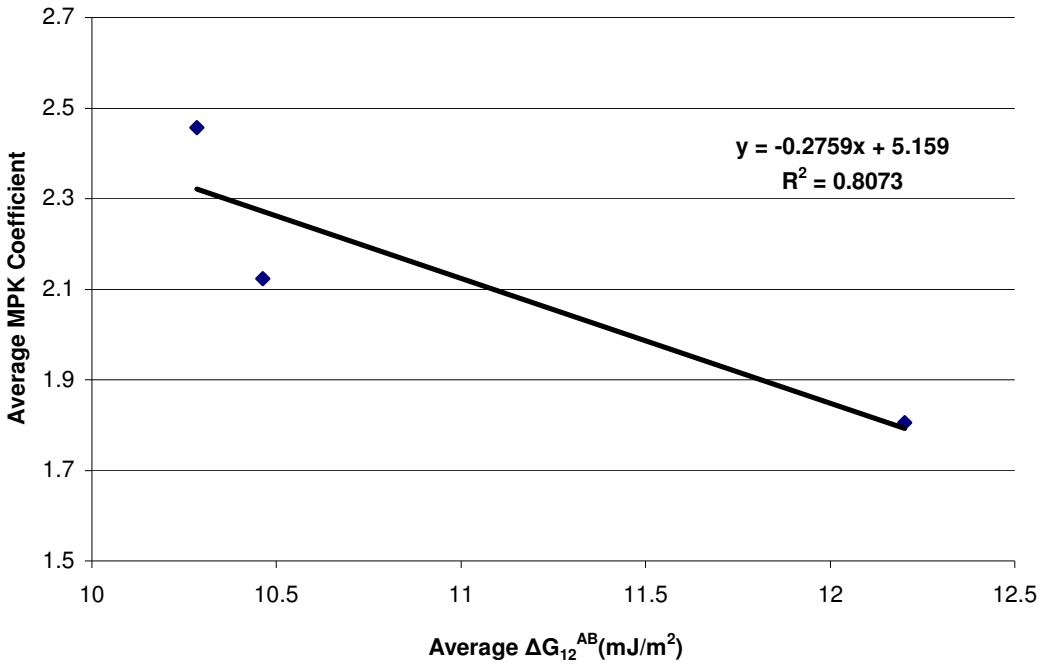

Figure 5-3: Average Marron-Pierce-Kitano Coefficient as a function of average acid-base component of bond energy

The above infers that bond energy could explain the shift in the curves of stiffening with different bitumen types. As the interactive energy, γ^{12}, between the two phases increases the overall, $\Delta G_{12,}$ bond energy falls and leads to higher levels of stiffening for the same ratio of φ/φ_{max}.

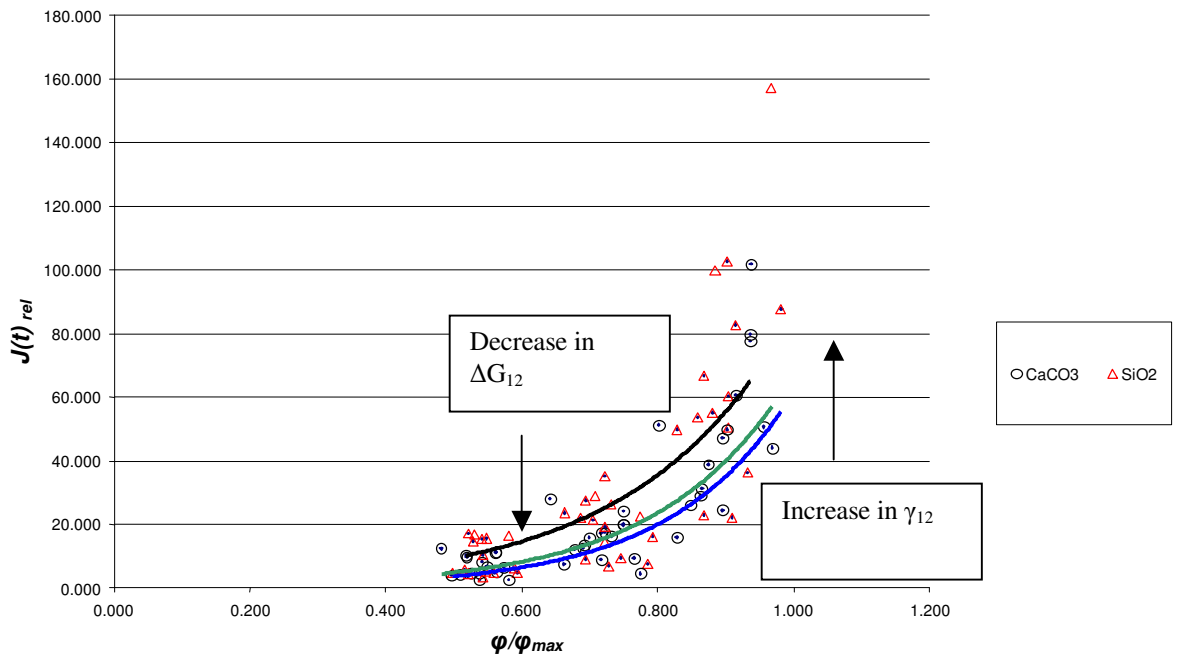

Figure 5-4: Shifts in master curves of filler stiffening by binder type – effects of bond energy

Different filler types in a single bitumen type – the role of surface interactions

In the situation where different filler types are considered in a single bitumen type, the physical properties such as shape, PSD, etc. have an influence on the rheological constants and it is difficult to isolate the surface effects from the other effects occurring simultaneously. It was not expected that the surface interactions would be easily detectable in such a scenario. Several previous studies have opted for this approach (Rigden 1947, 1954; Anderson et al., 1992; Kandhal, 1980) and have concluded that the packing fraction, a property relating to φ_{max} is the strongest single filler property responsible for the observed stiffening. We have already seen this effect in the previous chapter where dividing φ by φ_{max} to arrive at a true volume fraction collapses the data to a single exponential curve for a particular bitumen type (Figure 5-5)

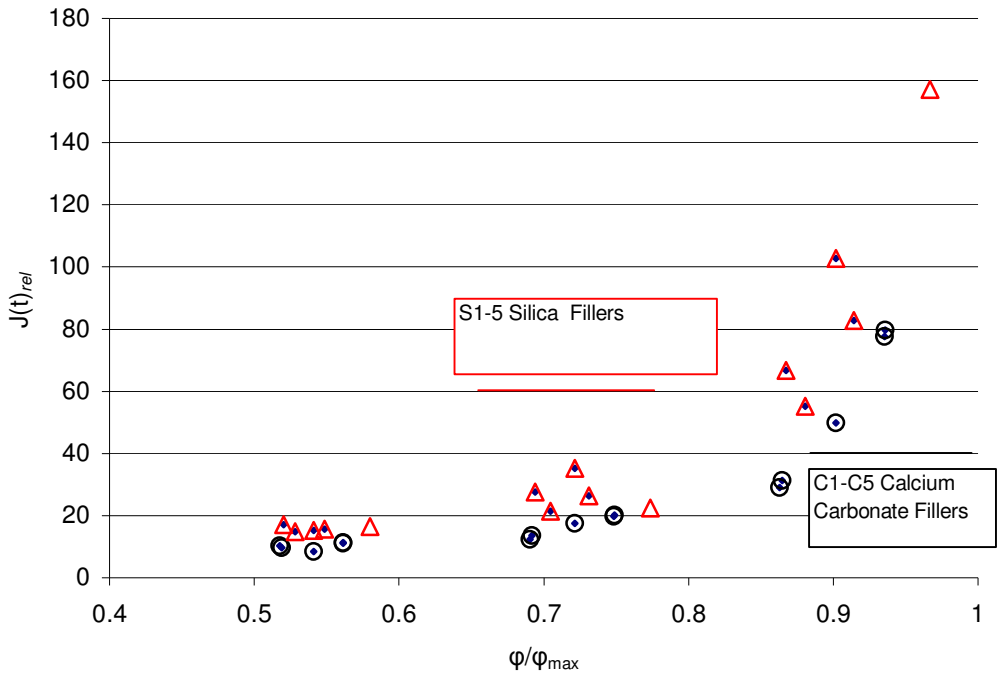

Figure 5-5: Stiffening of mastics in Bitumen B1 normalised for maximum packing fraction

To describe the behaviour of different fillers in a single bitumen type the interactive free energy parameters were not significant, as stated previously, there are different packing fractions and shape factors coming into play at the same time. In Bitumen B1 it was not possible to relate any Gibbs free energy parameter to any rheological constant examined.

Examining the subgroups C1-5 and S1-5 did give some indication of the importance of the interactive energy, but only at the lowest level of solid volume addition, 0.3φ. This is sensible, as at higher levels of solid volume fraction inter-particle factors such as shape and packing predominate.

At 0.3φ, the value of intrinsic viscosity, as determined by the Krieger-Dougherty equation, appears closely related to the Gibbs free energy parameter ΔG_{12}^{AB} (see Figures 5-6 and 5-7). This true for Filler sets C1-5 and S1-5, with the exception of Filler C4. Filler C4 has unusual behaviour has as been discussed previously (Chapter IV).

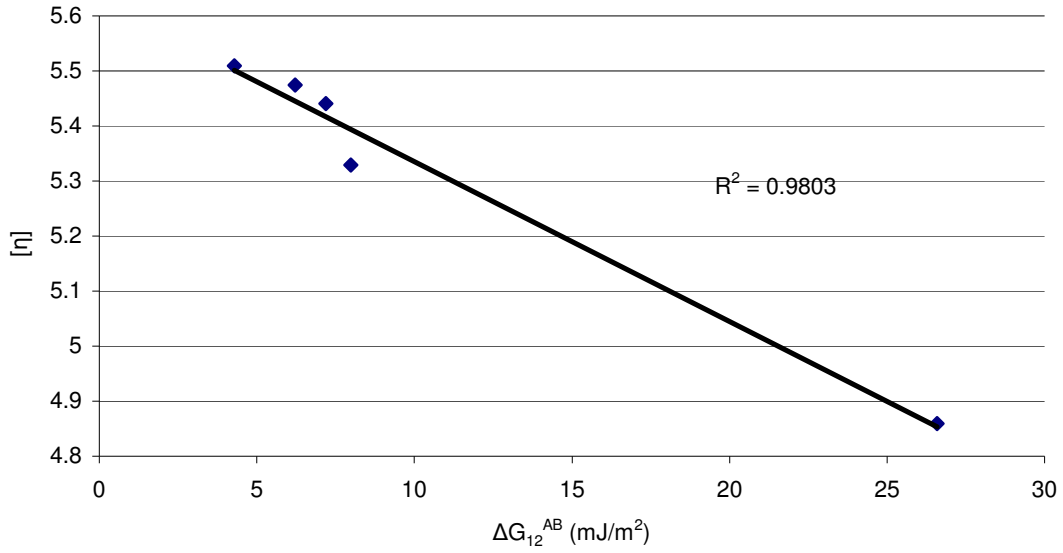

Figure 5-6: Intrinsic viscosity as a function of acid-base bond energy, Fillers C1-5, Bitumen B1

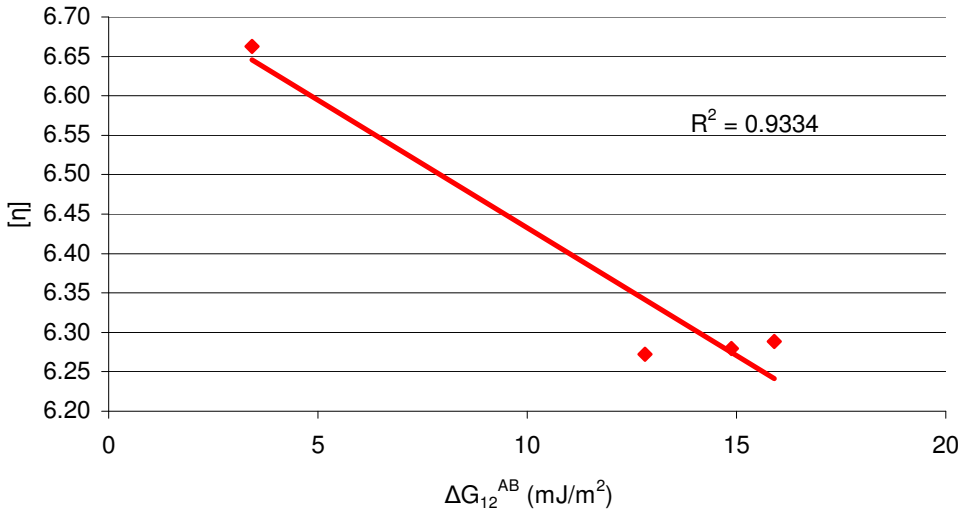

Figure 5-7: Intrinsic viscosity as a function of acid-base bond energy, Fillers S1-5, Bitumen B1

In Bitumen B2 there are no clear trends between the interactive parameters and the rheological parameters for the total filler set of sub-group C1-5. For Fillers S1-5, there are closer correlations between interactive parameters and the MPK coefficient, but only at R^2 level of 0.5.

Bitumen B3, the polymer modified resin, has relatively regular behaviour with respect to interactive parameters with correlations possible for several rheological factors with ΔG_{12}^{AB}. For Fillers C1-5, at low solid volume concentration (0.3φ), J $(t)_{rel}$ and $[\eta]$ and the MPK Coefficient are well correlated to ΔG_{12}^{AB}. The correlation is the inverse for the same filler set in Bitumen B1 (Figure 5-8).

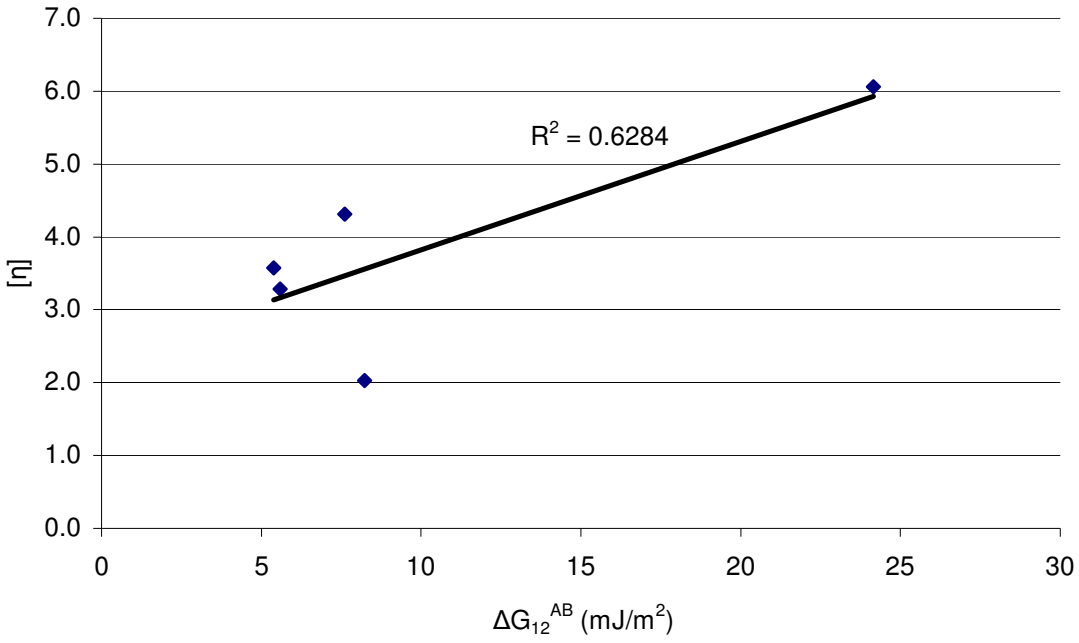

Figure 5-8: Intrinsic viscosity as a function of acid-base bond energy, Fillers C1-5, Bitumen B3

For Fillers S1-5 with Bitumen B3, the surface effects are very strongly correlated for almost all rheological constants, the exception being the maximum packing fraction. In particular, intrinsic viscosity and relative creep compliance are well correlated with the surface energy parameters (Figures 5-9 and 5-10).

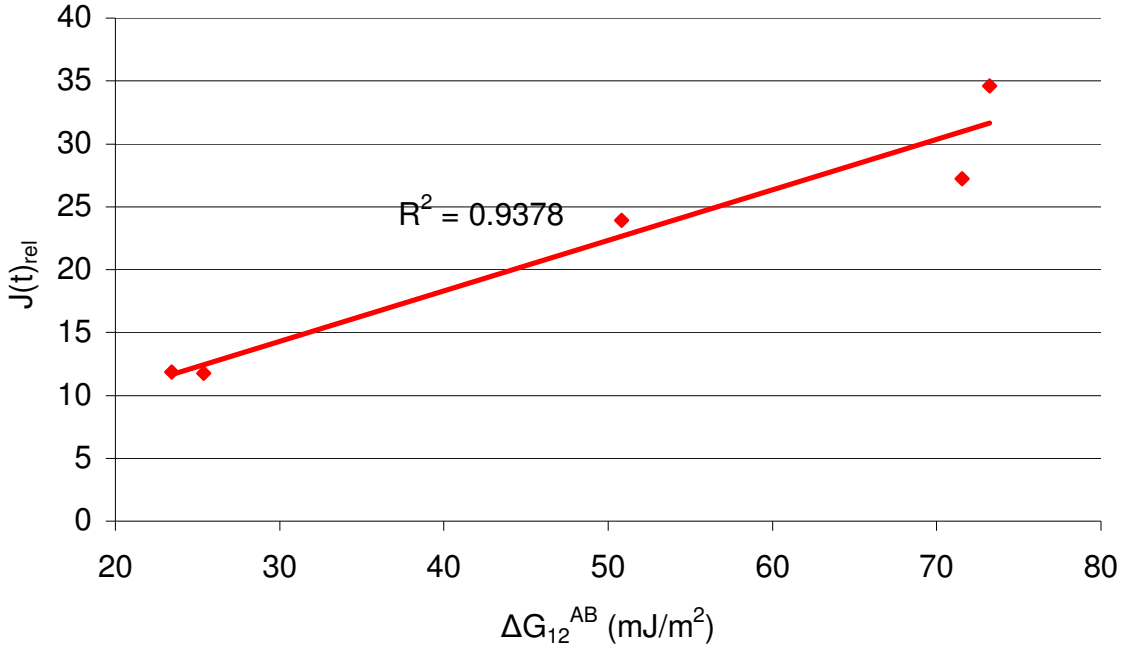

Figure 5-9: Relative creep compliance as a function of acid-base bond energy, Fillers S1-5, Bitumen B3

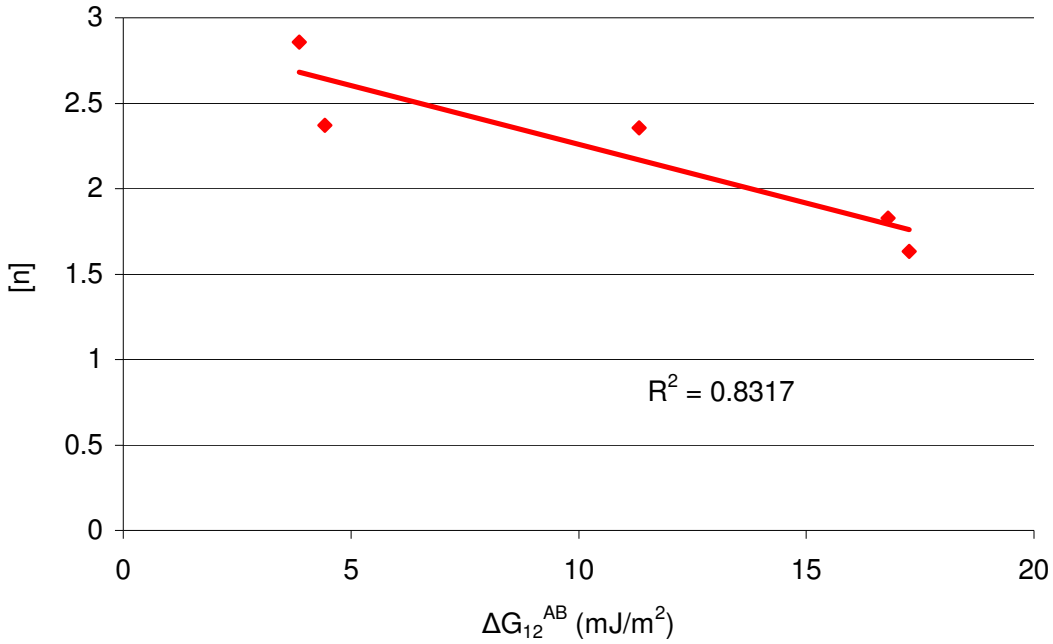

Figure 5-10: Intrinsic viscosity as a function of acid-base bond energy, Fillers S1-5, Bitumen B3

Summary - different filler types in a single bitumen type

When considering the behaviour of a set of different filler types in a single bitumen type, to some extent the surface interactions can be isolated under certain circumstances. For example, when the petrologic type of the aggregate is grouped, trends exist between the surface characteristics and the resulting rheological behaviour of the mastics. Understandably, these effects are best correlated at lower solid volumes fraction where the effects of scaling by the maximum packing fraction are lessened. It is the acid-base interactions ΔG_{12}^{AB} or the total level of interaction ΔG_{12}^{TOTAL}, which related closest to the rheological behaviour of the mastic.

In general, the bond energy has the closest relation to the intrinsic viscosity and MPK coefficient (derived from the product of the intrinsic viscosity and the maximum packing

fraction). For siliceous fillers, the MPK Coefficient can be reasonably related to the bond energy regardless of bitumen type. Figure 5-7 below shows the relationship between the MPK Coefficient derived from the Krieger-Dougherty equation and the total bond energy for Fillers S1-5 in all mastics produced. The relatively good correlation relates to the fact that for siliceous fillers, the bond energy effects often influence both the intrinsic viscosity and the maximum packing fraction, of which the MPK Coefficient is the product.

For calcium carbonate fillers, which can be considered as inert, the maximum packing fraction is not correlated to bond energy and hence, whilst showing the same general trend, the MPK coefficient is not as closely related to the interfacial conditions in Fillers C1-5 (see Figure 5-8). Additionally, whilst for siliceous fillers, the acid-base (and total) bond energy is the most strongly correlated, whilst for carbonate fillers, in general, the LW component of bond energy appears more closely related to the rheology of the mastics. When considering the stiffening effects of a filler there are two principle effects in evidence, the true solid volume fraction, expressed as ratio of the maximum packing fraction for the system, and other effects outside of this volumetric ratio, expressed as the MPK Coefficient, the product of the maximum packing fraction of the system and the intrinsic viscosity.

When considering a set of fillers in a single bitumen type, the factor φ/φ_{max} dominates the behaviour of the mastic, especially at solid volume fractions of 0.4φ and above (approximately greater than $\varphi/\varphi_{max} = 0.65$). At lower levels of solid volume fraction some surface interaction are discernable and relate closely intrinsic viscosity and MPK coefficient. Figures 5-11 and 5-12 show the relationship between MPK coefficient and bond energy for the two subgroups of fillers in all bitumen types.

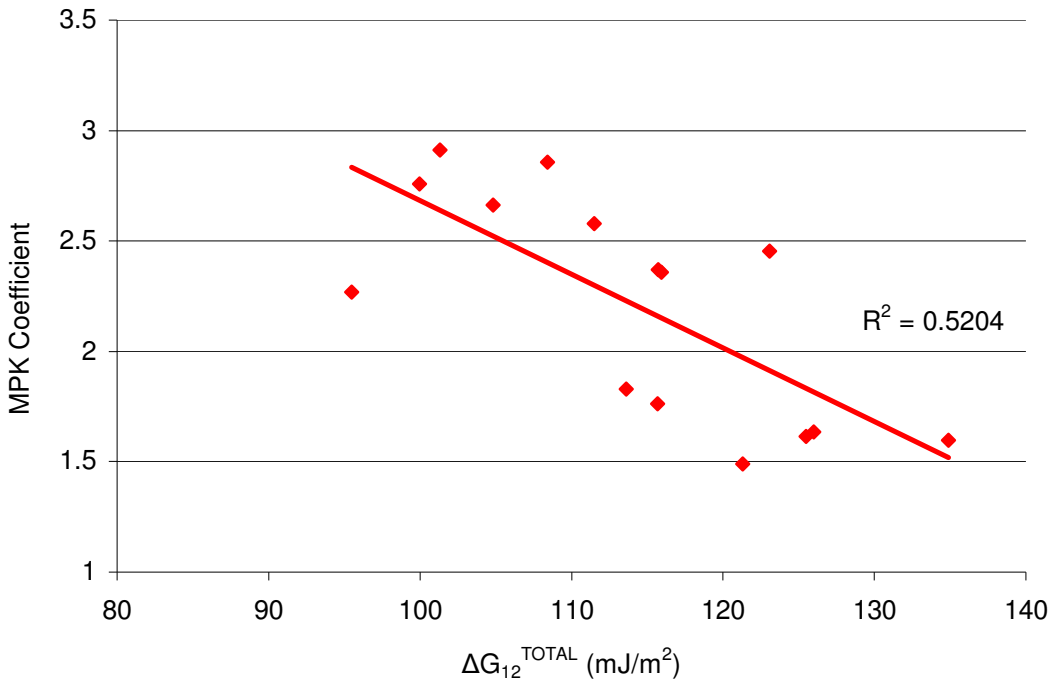

Figure 5-11: MPK Coefficient as a function of bond energy, Fillers S1-5

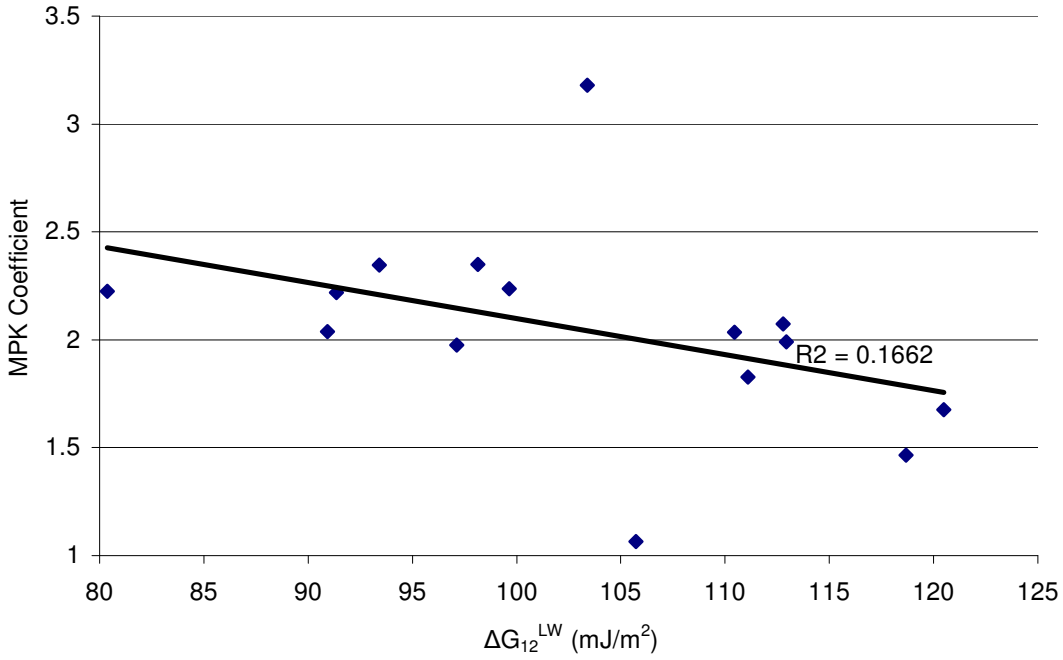

Figure 5-12: MPK Coefficient as a function of bond energy, Fillers C1-5

Individual fillers in different bitumen types

If a single filler type is rheologically modelled in different bitumen types, many of the index properties of the filler are effectively cancelled out. For example the shape and particle size distribution and surface area will remain unchanged (assuming similar levels of dispersion by the filler in the bitumen). The major change when examining a single filler type in different bitumen types would be expected to be differences in the interfacial properties of the bitumen-filler mixture. We have seen that we can calculate the magnitude of these changes, using a surface energy approach, earlier in this chapter.

In the following section the behaviour of each filler in the three bitumen types will be examined and observations of the rheological behaviour, in the context of changes in interfacial properties, calculated as bond energy, will be made.

In this section, the same selection of key rheological parameters derived from the creep compliance testing was chosen for comparison with the interactive parameters calculated for the mastics.

- $J(t)_{rel}$ at 0.3, 0.4 and 0.5φ
- φ_{max} at 45^{o}C, 57^{o}C and 65^{o}C
- $[\eta]$ at 0.3, 0.4 and 0.5φ
- Average MPK Coefficient for the mastic.

The values for these rheological factors were once again compared with the surface interactivity parameters

- ΔG_{12}^{TOTAL}
- ΔG_{12}^{LW}
- ΔG_{12}^{AB}

The MPK coefficient and intrinsic viscosity at higher concentrations correlated well to the bond energy calculations for Filler C1. The MPK coefficient correlated to all three bond energy components. There is a relationship between the level of maximum packing fraction and bond energy that may account for the level of dispersal, but this observation is not true for all fillers examined in this section.

For Filler C2, the MPK coefficient is very well correlated to the bond energy of the mastic, but the MPK coefficient does not correlate to the acid-base bond energy component. Additionally, the level of $J(t)_{rel}$ is closely correlated to the surface free energy at low volume concentrations (0.3φ).

Dolomitic Filler C3, shows behaviour very strongly correlated to surface effects. All rheological factors examined were related to changes in surface energy effects, with the exception of the maximum packing fraction, which was poorly correlated to surface effects.

Throughout the work contained in this thesis, the stiffening effects of Fillers C3 and C4 have been similar and the fillers frequently show similar trends when analysed. However, with respect to surface energy and its influence on a single filler type in different bitumen types, Filler C4 showed very little correlation between bond energy calculations and

rheological factors. The only significant correlation was between the relative creep compliance at 0.3φ. This was related to ΔG^{TOTAL} and ΔG^{LW}. No other relationships were evident.

Filler C5 has a significant quantity of clay within the matrix of the parent aggregate. This filler shows a strong link between the acid-base interactions between the filler and the bitumen and the resulting rheology of the mastic. In particular relative creep compliance of the filler at 0.3φ (Figure 5-13) and the MPK Coefficient are strongly linked to ΔG^{AB}.

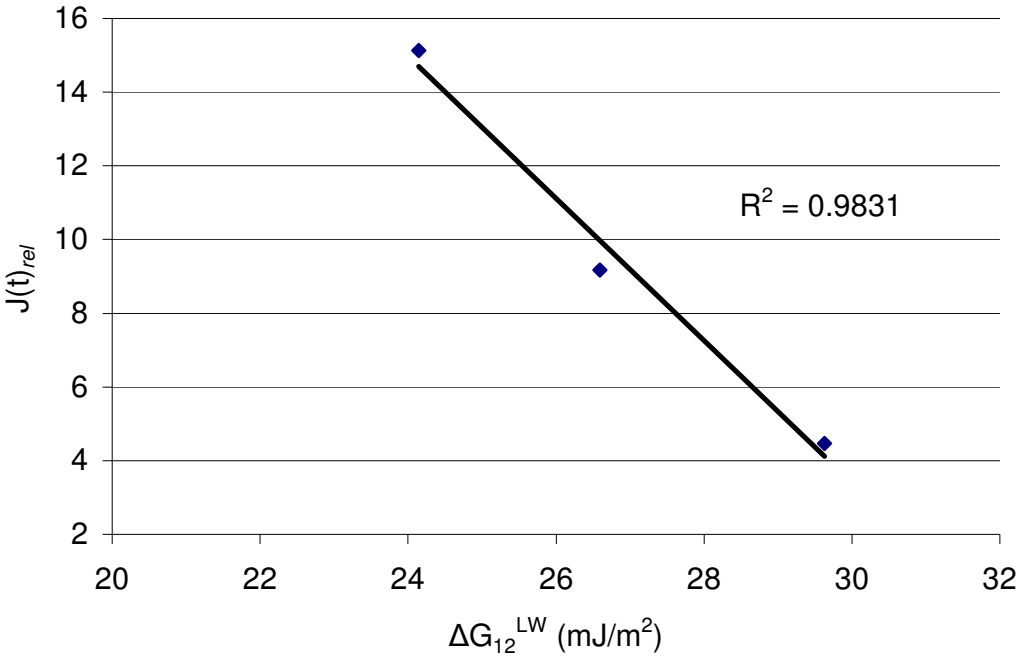

Figure 5-13: MPK coefficient as a function of LW bond energy, Fillers C5

For single filler types, the magnitude of the interaction with the bitumen plays an important role in the behaviour of the mastic. In almost all cases, increasing interaction between the filler and bitumen (decreasing bond energy) could be linked to an increase in relative creep compliance. Typically, this could be better related at low solid volume concentrations, however when the interactions are very strong, as in the case of Filler C5, the

effect can be observed even at high solid volume concentrations. At high level concentrations it appears to be the acid base component of bond energy which effects the level of *J(t)rel*.

A summary of correlations between the rheological factors and bond energy parameters for Fillers C1-5 is given in Table 6-3. The surface energy factors are given in bold if the correlation with the rheological parameter was greater than $0.7R^2$.

Table 6-3: Correlations between bond energy and rheological parameters – Fillers C1-5

	$J(t)_{rel}$ **0.3φ**	$J(t)_{rel}$ **0.4φ**	$J(t)_{rel}$ **0.5φ**	φ_{max} **45°C**	φ_{max} **57°C**	φ_{max} **65°C**	$[\eta]$ **0.3φ**	$[\eta]$ **0.4φ**	$[\eta]$ **0.5φ**	**MPK**
C1										
ΔG_{12}^{TOTAL}	0.39	**0.73**	-0.15	0.12	0.20	0.60	0.15	**1.00**	**0.92**	**0.83**
ΔG_{12}^{LW}	0.36	**0.76**	-0.17	0.13	0.23	0.63	0.13	**1.00**	**0.94**	**0.86**
ΔG_{12}^{AB}	0.46	0.67	-0.10	0.07	0.14	0.53	0.20	**0.99**	**0.88**	**0.78**
C2										
ΔG_{12}^{TOTAL}	**0.94**	0.13	0.22	-0.68	-0.61	-0.53	**0.81**	0.01	**-0.74**	**0.95**
ΔG_{12}^{LW}	**0.98**	0.07	0.14	-0.58	-0.51	-0.43	**0.88**	0.03	**-0.83**	**0.98**
ΔG_{12}^{AB}	0.01	**0.94**	**0.88**	-0.44	-0.51	-0.60	0.10	**0.96**	0.16	-0.01
C3										
ΔG_{12}^{TOTAL}	**0.99**	**0.95**	0.60	0.14	0.28	0.21	**1.00**	**0.75**	**0.86**	**0.99**
ΔG_{12}^{LW}	**0.99**	**0.93**	0.56	0.17	0.32	0.18	**1.00**	**0.72**	**0.83**	**1.00**
ΔG_{12}^{AB}	**0.99**	**1.00**	**0.76**	0.05	0.14	0.35	**0.98**	**0.88**	**0.95**	**0.94**
C4										
ΔG_{12}^{TOTAL}	**0.75**	0.25	0.02	0.25	0.01	-0.07	0.46	0.03	0.03	0.16
ΔG_{12}^{LW}	**0.76**	0.26	0.02	0.26	0.01	-0.07	0.45	0.03	0.03	0.17
ΔG_{12}^{AB}	0.25	0.00	0.38	0.00	-0.17	-0.51	0.05	-0.12	-0.12	-0.01
C5										
ΔG_{12}^{TOTAL}	0.24	0.05	0.50	0.07	-0.01	-0.26	0.31	0.00	0.00	0.04
ΔG_{12}^{LW}	0.09	0.00	0.31	0.00	-0.08	-0.45	0.15	0.02	0.04	0.00
ΔG_{12}^{AB}	**0.98**	**0.84**	**0.98**	**0.87**	0.55	0.15	**1.00**	**0.71**	0.66	**0.82**

In general, the level of interaction between the two phases does not appear to be linked to the dispersion of the filler in the different bitumen types through the term φ_{max}. Only one filler, C5, gave any correlation with surface interactions and only at one temperature.

Intrinsic viscosity, $J(t)_{rel}$ and MPK appear closely linked to the level of surface interaction with strong links between the MPK Coefficient and bond energy between the bitumen and filler. Filler C4 is the exception with very little of the rheological behaviour linked to surface effects.

Table 6-4: Summary of correlations between bond energy and rheological parameters – Fillers C1-5

Rheological Parameter	***J(t)$_{rel}$***	***φ_{max}***
C1	0.4 (ΔG_{12}, ΔG_{12}^{LW})	
C2	0.3 (ΔG_{12}, ΔG_{12}^{LW}), 0.4, 0.5 (ΔG_{12}^{AB})	
C3	0.3, 0.4 (ΔG_{12}, ΔG_{12}^{LW} ΔG_{12}^{AB}), 0.5 (ΔG_{12}^{AB})	
C4	0.4 (ΔG_{12}, ΔG_{12}^{LW})	
C5	0.3, 0.4, 0.5 (ΔG_{12}^{AB})	45^{o}C (ΔG_{12}^{AB})
Rheological Parameter	***[η]***	**MPK (φ_{max}*[η])**
C1	0.4, 0.5 (ΔG_{12}, ΔG_{12}^{LW}, ΔG_{12}^{AB})	ΔG_{12}, ΔG_{12}^{LW}, ΔG_{12}^{AB}
C2	0.3 (ΔG_{12}, ΔG_{12}^{LW}), 0.4 ($\Delta G_{12}^{AB,}$)0.5 (ΔG_{12}, ΔG_{12}^{LW})	ΔG_{12}, ΔG_{12}^{LW}
C3	0.3, 0.4, 0.5 (ΔG_{12}, ΔG_{12}^{LW}, ΔG_{12}^{AB})	ΔG_{12}, ΔG_{12}^{LW}, ΔG_{12}^{AB}
C4		
C5	0.3, 0.4 (ΔG_{12}^{AB})	ΔG_{12}^{AB}

The rheological behaviour of Filler S1 in different bitumen types is strongly linked to the surface interactions between the two phases. In the case of Filler S1 the dispersion of the filler and the maximum packing fraction also appear linked to the interactive energy between the two phases. Similarly, the rheology of Filler S2 in the three bitumens is strongly

influenced the magnitude of interaction between the bitumen and filler. In this case the surface effects do not appear to have a positive effect on the dispersion of the filler and φ_{max}.

Once again, for Filler S3 there are strong links between the bitumen-filler interactions and the mastic rheology. Again, the link between interfacial conditions and maximum packing fraction is not strong. The rheology of Filler S4 is not consistent with the other fillers. This fillers has consistently exhibited different behaviour to the other fillers. For example, in the Delta Ring and Ball tests this filler had the highest effect o f the ten fillers in B3**,** but with the second lowest in the hard Bitumen, B2. Additionally, the behaviour of filler S4 with change in temperature was very marked compared to the other fillers (See Chapter IV).

The dispersal of the Filler C4 at higher temperatures is inversely related to the interfacial energy between the bitumen and filler. The maximum packing fraction is closely related to the bond energy and in particular the LW component of bond energy but MPK Coefficient is not closely related to interfacial conditions. This is the only filler of the set of ten to not correlate the MPK Coefficient to the bond energy between the bitumen and filler.

In keeping with Fillers S1, S2 and S3, S5 has a strong link between rheology of the filler in different bitumen types and the interfacial conditions. The dispersion (φ_{max}), the relative creep compliance, intrinsic viscosity and MPK are also closely related to the total bond energy and LW component.

Table 6-5: Correlations between bond energy and rheological parameters – Fillers S1-5

	$J(t)_{rel}$ **0.3φ**	$J(t)_{rel}$ **0.4φ**	$J(t)_{rel}$ **0.5φ**	φ_{max} **45°C**	φ_{max} **57°C**	φ_{max} **65°C**	$[\eta]$ **0.3**	$[\eta]$ **0.4**	$[\eta]$ **0.5**	**MPK**
S1										
ΔG_{12}^{TOTAL}	**0.90**	**0.71**	-0.49	0.50	**0.85**	**0.97**	**0.86**	0.59	**0.83**	**0.88**
ΔG_{12}^{LW}	**0.91**	**0.72**	-0.48	0.49	**0.84**	**0.97**	**0.87**	0.60	**0.84**	**0.89**
ΔG_{12}^{AB}	**0.71**	0.47	**-0.73**	**0.74**	**0.98**	**0.99**	0.65	0.34	0.61	**0.68**
S2										
ΔG_{12}^{TOTAL}	**0.97**	**0.92**	**0.96**	0.03	**-0.88**	-0.58	**0.93**	0.06	0.13	**0.78**
ΔG_{12}^{LW}	**0.95**	**0.94**	**0.97**	0.04	**-0.90**	-0.61	**0.91**	0.04	0.11	**0.75**
ΔG_{12}^{AB}	**1.00**	**0.84**	**0.89**	0.00	**-0.79**	0.46	**0.98**	0.13	0.22	**0.87**
S3										
ΔG_{12}^{TOTAL}	**0.83**	**0.95**	0.19	0.06	0.24	0.60	0.73	**0.99**	**0.99**	**0.99**
ΔG_{12}^{LW}	**0.82**	**0.95**	0.19	0.07	0.25	0.61	**0.77**	**0.98**	**0.99**	**0.99**
ΔG_{12}^{AB}	**0.74**	**0.89**	0.12	0.12	0.34	0.70	0.63	**0.95**	**0.96**	**0.96**
S4										
ΔG_{2}^{TOTAL}	0.35	0.11	0.01	-0.27	**-0.94**	**-0.74**	0.63	0.06	0.05	0.10
ΔG_{12}^{LW}	0.35	0.12	0.01	-0.26	**-0.93**	**-0.73**	0.64	0.07	-0.05	0.11
ΔG_{12}^{AB}	**0.70**	0.43	0.19	0.03	**-0.67**	-0.38	**0.92**	0.34	0.02	0.40
S5										
ΔG_{2}^{TOTAL}	**0.96**	**0.74**	**0.97**	**0.96**	**0.97**	-0.43	**0.97**	**0.89**	**0.92**	**0.92**
ΔG_{12}^{LW}	**0.90**	0.64	**1.00**	**0.91**	**0.99**	-0.33	**0.92**	**0.81**	**0.85**	**0.86**
ΔG_{12}^{AB}	0.39	0.72	0.09	0.38	0.08	-0.94	0.37	0.53	0.48	0.46

The siliceous filler set shows very strong inter-relations between the surface interactions and the rheology of the mastics. Importantly, whereas in general the level of φ_{max} was not well correlated to the bond energy components of the mastic for Fillers C1-5, with Fillers S1-5, all of the rheological parameters appeared to be influenced by the interfacial properties. Table 6-6 gives a summary of the factors with strong (>0.7R^2) correlation for the mastics produced with Fillers S1-5

Table 6-6: Summary of correlations between bond energy and rheological parameters – Fillers S1-5

Rheological Parameter	$J(t)_{rel}$	φ_{max}
S1	0.3(ΔG_{12}, ΔG_{12}^{LW} ΔG_{12}^{AB}), 0.4 (ΔG_{12}, ΔG_{12}^{LW}), *0.5 (ΔG_{12}^{AB})*	45°C (ΔG_{12}^{AB}), 57°C, 65°C (ΔG_{12}, ΔG_{12}^{LW} ΔG_{12}^{AB})
S2	0.3, 0.4, 0.5 (ΔG_{12}, ΔG_{12}^{LW} ΔG_{12}^{AB})	*57°C (ΔG_{12}, ΔG_{12}^{LW} ΔG_{12}^{AB})*
S3	0.3, 0.4, (ΔG_{12}, ΔG_{12}^{LW} ΔG_{12}^{AB})	65°C (ΔG_{12}^{AB})
S4	0.3 (ΔG_{12}^{AB})	*57, 65°C (ΔG_{12}, ΔG_{12}^{LW})*
S5	0.3 (ΔG_{12}, ΔG_{12}^{LW}), 0.4 (ΔG_{12}, ΔG_{12}^{AB}), *0.5 (ΔG_{12}, ΔG_{12}LW)*	45, 57°C (ΔG_{12}, ΔG_{12}^{LW}), *65°C (ΔG_{12}^{AB})*
Rheological Parameter	$[\eta]$	**MPK**
S1	0.3 (ΔG_{12}, ΔG_{12}^{LW}, ΔG_{12}^{AB}), 0.5 (ΔG_{12}, ΔG_{12}^{LW})	ΔG_{12}, ΔG_{12}^{LW}
S2	0.3 (ΔG_{12}, ΔG_{12}^{LW}, ΔG_{12}^{AB})	ΔG_{12}, ΔG_{12}^{LW}, ΔG_{12}^{AB}
S3	0.3 (ΔG_{12}, ΔG_{12}^{LW}) 0.4, 0.5 (ΔG_{12}, ΔG_{12}LW, ΔG_{12}AB)	ΔG_{12}, ΔG_{12}^{LW}, ΔG_{12}^{AB}
S4	0.3 (ΔG_{12}^{AB})	
S5	0.3, 0.4, 0.5 (ΔG_{12}, ΔG_{12}^{LW})	ΔG_{12}, ΔG_{12}^{LW}

In the case of the Fillers S1-5, the interfacial conditions of the bitumen and filler mastic correlates to both intrinsic viscosity and maximum packing fraction. As the MPK Coefficient is the product of the two factors, there is a reasonable relationship between the bond energy and the MPK Coefficient (See Figure 5-11) indicating that the level of adhesion between the filler and bitumen manifests itself in changes in the rheology of the mastic.

Summary – single filler types in different bitumen types

Examination of single filler type in three bitumen types eliminates many of the index properties of the filler and allows and examination of the surface effects without undue interference from other factors such as particle shape and particle size distribution. In the previous chapters it has been stated that the same ten fillers gave rise to different levels of relative creep compliance in different bitumens. The position of the exponential curves can be expressed as the MPK Coefficient, which is the product of intrinsic viscosity and the maximum packing fraction.

In these experiments, on average, fillers gave the highest relative creep compliance in Bitumen B1 followed by Bitumen B3 and finally Bitumen B2. The MPK Coefficients were 2.46, 2.12 and 1.81 respectively.

Modified Krieger-Doughtery equations were derived for the asphalt fillers in three different bitumen types, with the general form

$$J(t)rel = \left(1 - \frac{\phi}{\phi_{\max}}\right)^{-k} \qquad (67)$$

Where:

k = the MPK Coefficient

Examining single filler types in three bitumen types showed that such surface effects were important in bitumen-filler mastics. Nine out of ten fillers had good correlations between their individual MPK Coefficients and the bond energy, with the Coefficient increasing with decreasing bond energy. The surface effects also were important when

considering relative creep compliance with all ten fillers having a close correlation with $J(t)_{rel}$ and bond energy, typically at lower levels of solid addition where particle-particle contacts are less prevalent. Sometimes however, the influence of bond energy of the mastic was strong enough to be evident at all solid volume concentrations. This is an important point as the interaction between the two phases, and changes in the viscosity of the liquid phase (bitumen) are significant enough to be detectable even taking into account the solid volume filling relationship of φ/φ_{max}.

For the Fillers C1-5, there was little influence of surface interactions on the dispersal of the filler in the bitumen and the value of maximum packing fraction. Only one Filler, (C5) which contained a quantity of clay within the matrix of the limestone, had a strong correlation between maximum packing fraction and bond energy. Conversely, the Siliceous Fillers S1-5 had much better correlations between the bond energy and the maximum packing fraction values. Because the bond energy affects both intrinsic viscosity and maximum packing fraction for Fillers S1-5 the MPK Coefficient (the product of φ_{max} and intrinsic viscosity) is fairly well correlated with bond energy for all mastics tested during this work. For Fillers C1-5, the maximum packing fraction is not related to the surface conditions and a lower level of correlation is found.

CHAPTER VII

SUMMARY, CONCLUSIONS AND RECOMMENDATIONS FOR FURTHER WORK

SUMMARY

Mastics manufactured using ten different fillers and three different bitumen types have been manufactured and tested using a traditional index test, Delta Ring and Ball, and in creep compliance tests at different levels of solid volume addition. The term relative creep compliance was introduced to describe the stiffening effects of the fillers at different solid volume fractions in different bitumens. A two-point projection technique was used to estimate the maximum packing fraction, φ_{max}, and mastercurves of stiffening were derived by normalising the solid volume fraction to the the maximum packing fraction, φ/φ_{max}.

Having determined relative creep compliance and maximum packing fraction, three models, those proposed by Chong, Krieger and Dougherty and Mooney, were used to calculate the intrinsic viscosity of the asphalt fillers in different bitumen types. Only the Krieger-Dougherty model provided reasonable values of intrinsic viscosity for asphalt fillers in all bitumen types and at all solid volume contents.

The product of the intrinsic viscosity and maximum packing fraction is known as the Marron-Pierce-Kitano (MPK) Coefficient and this, for a variety of situations, is close to the value of 2. For the 90 mastics tested during this work, the average MPK Coefficient was found to be 2.13, a value close to the proposed value of 2 for this Coefficient.

The MPK Coefficient changes for different fillers in different bitumen types. Overall, the order of the MPK Coefficient was Bitumen B1> Bitumen B3> Bitumen B2 and this order was reflected in the order of the master curves normalised for φ/φ_{max} thus the MPK Coefficient describes the level of stiffening outside of simple volume filling and solid volume filling as a ratio of maximum packing fraction.

Using a thermodynamic approach, the surface free energy of adhesion concept was used to calculate the bond energy of the mastic for each bitumen-filler combination. On average, the bond energy was strongly correlated to the MPK Coefficient and shifts in stiffness master curves could be linked to changes in the interfacial conditions of the mastics, with higher levels of interaction leading to higher levels of stiffening for the same ratio of φ/φ_{max}.

Finally, single filler types were considered in the three bitumen types. The bond energy of the mastics was strongly correlated to the rheology of the mastics in nine out ten of the fillers. One of the nine fillers, S4, was inversely correlated when compared to the other fillers and this observation was consistent with the unusual behaviour of this filler throughout this study.

CONCLUSIONS

The following conclusions were reached during the study

- The Krieger-Dougherty equation is an appropriate model choice for bitumen-filler mastics.

- The average intrinsic viscosity of asphalt fillers in bitumen, according to the Krieger-Dougherty equation, is between 3.3 and 4.4, dependent on bitumen type. The intrinsic viscosity is correlated to the bond energy of the mastic in most cases, and not to particle shape (same filler in different bitumen types means that particle shape effects are cancelled out).

- The average MPK Coefficient for the 90 mastics tested was found to be 2.13, and ranged from 1.5 - 2.5 dependent on bitumen type. Again this is, on average, related to the bond energy of the bitumen-filler interface of the mastic.

- Average bond energy for the mastics manufactured from each bitumen type was almost perfectly correlated to MPK/Intrinsic viscosity (effects outside of the solid volume relation) and the bond energy or the MPK Coefficient can be used to describe stiffening effects outside of the solid volume as a ratio of maximum packing fraction.

- Surface interactions are best isolated at low (0.3) solid volume contents where particle-particle contacts are minimised. However on many occasions, where the magnitude of the interfacial conditions is strong enough (for example in the case of Filler C5 which contained clay within it's matrix or in the case of some siliceous fillers) the interfacial effects can be distinguished at high (>0.9) φ/φ_{max} ratios.

- Delta Ring and Ball tests did not relate to bond energy of the mastics, or adequately to any index test performed on the filler or bitumens.

- Fillers often paired according to their petrologic type, for example, Fillers C1 and C2, (pure calcium carbonate), Fillers C3 and C4 (dolomitic) and Fillers S1 and S3 (siliceous fillers with the highest acid-base component of surface energy) often displayed similar rheological behaviours.

- Nine out of ten of the fillers, when tested in three bitumen types, had strong correlations between the MPK Coefficient and bond energy. Filler C4 was inversely correlated compared to the other fillers.

- For calcium carbonate fillers, using the Krieger-Dougherty equation, the bond energy relates to intrinsic viscosity only and does not appear to influence the maximum packing fraction.

- For siliceous fillers, surface energy related to both the maximum packing fraction and the intrinsic viscosity, hence is better related to their product, the MPK coefficient.

- Individual index properties of the fillers did not adequately predict the resulting rheological behaviour of the mastics

- The rheological properties, $J(t)_{rel}$, maximum packing fraction and intrinsic viscosity change with temperature. Not all bitumen-filler combinations change with temperature in the same way. For example, $J(t)_{rel}$ for fillers in Bitumen B1 increase and peak at a defined value (65^{o}C). Fillers in B3 increase and in the cases of the four fillers with the lowest stiffening peak at a defined temperature whereas six increase across the range of test temperatures. For fillers in Bitumen B2, most fillers show a decrease $J(t)_{rel}$ with increasing temperature.

RECOMMENDATIONS FOR FURTHER WORK

Binder-filler interaction analysis

To date, the technique of testing a single filler type in a series of different bitumen types has not been explored. The interaction between filler and bitumen can be considered as a "micro-asphalt" and changes in the rheological behaviour of mastics made from different bitumen and filler types may lead to a better understanding of the behaviour of asphalt mixture. For a single filler type in different bitumen types and using the Krieger-Dougherty

equation, the term $[\eta]^*\varphi$, the can be substituted for an interactive parameter of bond energy in the mastic. This relationship could be used in two ways.

Binder filler compatibility

The MPK coefficient could be used as an evaluation technique for filler-bitumen compatibility. For example, for three different bitumen types, the MPK and bond energy are closely linked, hence the bitumen with which the highest MPK value is obtained should be the bitumen to which the fillers is most strongly attracted.

In terms of durability several researchers have proposed a three-phase calculation based on the Dupré equation (Equation 1) as a predictor of asphalt durability (Cheng, 2002; Hefer, 2004; Bhasin, 2006). The parameter γ_{132} is introduced with water as the third component and the placement of γ_3 between γ_1 and γ_2 representing the water being present at the interface between the filler and the bitumen..

Simplistically, the level of interaction between the filler surface and the bitumen, and the filler surface and water are related, with high levels of interaction with bitumen by the surface, mirrored by high levels of interaction with water. Hence, a high level of interactive energy between filler and bitumen will be closely related to the calculation of γ_{132}. To this end, a low MPK Coefficient (low interaction between the bitumen and filler) could represent the combination with the most favourable combination with respect to durability of the mastic (and the asphalt) in the presence of water.

To summarise, the derivation of effects outside of the volume filling relationship of φ/φ_{max}, expressed as the MPK Coefficient is a potential measure of adhesivity between the bitumen and the filler and measurement of the filler in different types of bitumen may give

information relating to the durability of asphalt mixtures. A procedure to determine this interactive parameter is given below.

- Measure specific gravity of filler and bitumens.
- Calculate masses to produce three mastics with solid volume fractions of 0.3φ, 0.4φ and 0.5φ.
- Determine $J(t)_{rel}$ of each bitumen type.
- Measure $J(t)_{rel}$ for each mastic and calculate $J(t)_{rel}$ as $J(t)_{mastic}/J(t)_{bitumen.}$
- Plot $1/J(t)_{rel}$ at 0.4φ and 0.5φ, derive x axis intercept – and record as maximum packing fraction.
- Calculate intrinsic viscosity and MPK Coefficient for each bitumen filler combination using the Krieger-Dougherty equation.

Activity coefficient of the filler

Alternatively, testing filler in different bitumen types and calculating the MPK Coefficient is analogous to Zisman's derivation of surface energy by testing a solid in a series of related liquid types (Zisman, 1950) which gives rise to the possibility that an "intrinsic surface energy" of a filler could be derived from a series of rheological experiments using standard well characterised bitumen types.

Behaviour of filler-polymer modified bitumen systems

During this work, the behaviour of fillers in the polymer modified bitumen B3 has been noted as differing from the traditional penetration grade bitumens. A study of mineral filler- polymer modified bitumen interaction may give a useful insight into the performance and behaviour of polymer modified asphalts.

Behaviour of filler-binder systems with respect to changes in temperature

Finally, the change in behaviour over a range of temperatures, as partially examined in this work, may give valuable insights into fundamental differences in the behaviour of different filler types in different bitumens and should be explored further.

REFERENCES

Airey G.D., (1997) *"Rheological characteristics of polymer modified and aged bitumen",* PhD Thesis, University of Nottingham.

Anderson D.A., Bahia H. U., Dongre R, (1992a) *"Rheological properties of mineral filler – asphalt mastics and their relationship to pavement performance",* Effects of aggregates and mineral fillers on asphalt mixture performance: ASTM STP 1147, Richard C. Meininger, editor, American Society for Testing and Materials, Philadelphia.

Anderson D.A., Dongre R., Christensen D. W. III, and Dukatz, E.L, (1992b) *"Effects of minus 200-sized aggregate on fracture behaviour of dense-graded hot-mix asphalt",* Effects of aggregates and mineral fillers on asphalt mixture performance: ASTM STP 1147, Richard C. Meininger, editor, American Society for Testing and Materials, Philadelphia.

Anderson D. A. and Goetz W. H., (1973). *"Mechanical Behaviour and reinforcement of mineral filler – asphalt mixtures"*, Proceedings of the Association of Asphalt Paving Technologists Volume 42.

Anderson D. A., Tarris J. P., Brock J. D., (1982), *"Dust collector fines and their influence on mixture design."*, Report No: NAPA QIP 102.

Barnes H.A. (2000) *"A handbook of elementary rheology"*, Institute of Non-Newtonian Fluid Mechanics, University of Wales, ISBN 0-9538032-0-1.

Bhasin A., (2006), *"Development of methods to quantify bitumen-aggregate adhesion and loss of adhesion due to water"*, PhD Thesis, Texas A&M University.

Brunauer S., Emmett P. H., and Teller E., (1938), *"Adsorption of gases in multimolecular layers"*, Journal of the American Chemical Society Volume 60 pp309-319.

Cheng D., (2002), *"Surface free energy of aggregate-asphalt system and performance analysis of asphalt concrete based on surface energy"*, PhD Thesis, Texas A&M University.

Chong J.S., Christiansen E.B., and Baer A.D., (1971*), "Rheology of concentrated suspensions"* Journal of Applied Polymer Science, pp. 2007-2021.

Collop A.C., Airey G.D. and Khanzada S., (2002) *"Creep testing of bitumens using the dynamic shear rheometer",* International Journal of Pavement Engineering, Volume 3, Number 2, pp 107-116.

Cooley L. A., Stroup-Gardiner M., Brown E. R., Hanson D. I., and Fletcher M. O. (1998) *"Characterisation of asphalt-filler mortars with Superpave Bitumen tests"*, Association of Asphalt Paving Technologists.

Craus, J., Ishai I., and Sides A. (1978), *"Some Physico-Chemical Aspects of the Effect and the Role of the Filler in Bituminous Paving Mixtures"*. Proceedings of the Association of Asphalt Paving Technologists, Volume 47, p.558.

Craus J., Ishai I., and Sides A., (1981), *"Durability of bituminous paving mixtures as related to filler properties",* Proceedings of the Association of Asphalt Paving Technologists, Volume 50 , pp 291-318.

Delgadillo R., Dong D.W., Bahia H., (2006), "*Non-linearity of repeated creep and recovery binder test and the relationship with mixture permanent deformation"*, Paper 06-3016, 85th Transportation Research Board Meeting, Washington D.C.

Dukatz E.L., and Anderson D.A, (1980), "*The effect of various fillers on the mechanical behavior of asphalt and asphaltic concrete"*, Proceedings of the Association of Asphalt Paving Technologists Volume 49, pp 530-549.

Du Nuoy P.L., (1919) *" A new apparatus for measuring surface tension ",* The Journal of Physiology 1, p521-524.

Dupré A., (1869) *" Theorie Mecanique de la Chaleur ",* Université de France, Académie de Rennes.

Eilers, H., (1941), *"The viscosity of the emulsion of highly viscous substances as function of concentration",* Kolloid-Z., 97, p313.

Einstein A., (1906), *"On the movement of small particles suspended in stationary liquids required by the molecular-kinetic theory of heat."* Annalen der Physik 19, pp289-386.

Fowkes F.M., (1964), *"Predicting attractive forces at interfaces"*, Industrial & Engineering Chemistry Research Volume 56, p40-53.

Fowkes F.M., (1966*), "Surface Chemistry",* Chapter 9, pages 325-450 in "Treatise on Adhesives and Adhesion", New York.

Girifalco, L.A. and Good R.J., (1957), "A Theory for the estimation of surface and interfacial energies. I. Derivation and application to interfacial tension", J. Phys. Chem., 61, p. 904.

Good R.J, (1992), *"Contact angle, wetting and adhesion: A critical review*", Journal of Adhesion Science and Technology, Volume 6, pp 1269-1302.

Good R.J and van Oss C.J., (1992), *"The modern theory of contact angles and the hydrogen bond components of surface energies"*, Modern Approach to Wettability: Theory and Application, Plenum Press, New York.

Harris B. M., and Stuart K. D., (1998) *"Analysis of mineral fillers and mastics used in stone matrix asphalt*", Association of Asphalt Paving Technologists, Volume XXX.

Hefer W. H., (2004) *"Adhesion in bitumen-aggregate systems and quantification of the effects of water on the adhesive bond"*, PhD Dissertation, Texas A&M University.

Heukelom W., and Wijga P. W. O., (1971), *"Viscosity of dispersions as governed by concentration and rate of shear*", Proceedings of the Association of Asphalt Paving Technologists Volume 40.

Hurysz K.M. and Cochrane J.K., (2004), *"Modelling paste properties with minimum experimentation",* Journal of Ceramic Processing Research, Volume 5, No. 3, pp. 191-195.

Ishai I., Craus J., and Sides A., (1980) *"A model for relating filler properties to optimal behaviour of bituminous mixtures."* Proceedings of the Association of Asphalt Paving Technologists, Volume 49 , p 416.

Kandhal P. S., (1980), "*Evaluation of baghouse fines in bituminous paving mixtures*" Pennsylvania Department of Transport, Project No 79-23.

Kandhal P. S., Lynn C. Y., and Parker F., (1998) "*Characterization tests for mineral fillers relating to performance of asphalt paving mixtures*". NCAT Report No 98-2.

Kavussi A., and Hicks R. G., (1997), "*Properties of bituminous mixtures containing different fillers*", Proceedings of the Association of Asphalt Paving Technologists, Volume 66, p.153.

Kennedy T.W., Cominsky R.J., Harrigan E.T., Leahy R.B., (1990), "*SHRP Asphalt Research Program: 1990 Strategic Planning Document*", SHRP-A/ UWP-90-007, National Research Council, Washington D.C.

Kitano, T., Kataoka, T. and Shirota, T. (1981), "*An empirical equation of the relative viscosity of polymer melts filled with various inorganic fillers"* Rheol. Acta, 20 pp.207-209.

Krieger I. M., and Dougherty T. J., (1959) "*A mechanism for non-newtonian flow in suspensions of rigid spheres*." Trans. Soc. Rheol. 20, pp137–152.

Levoguer C. L. and Williams D. R., (2003) "*Dynamic Vapour Sorption Application Note 17, Measurement of the Surface Energies of Pharmaceutical Powders using a Novel Vapour Adsorption Method*" , Surface Measurement Systems Ltd., UK.

Little D.N. and Epps J.A., (2001), "*The benefits of hydrated lime in hot mix asphalt*", National Lime Association, US.

Mitchell J.G. and Lee A.R., (1939), *"The evaluation of fillers for tar and other bituminous surfaces",* Journal of the Society of Chemical Industries, 58-299.

Mooney M., (1957), "*The viscosity of a concentrated suspension of spherical particles*", Journal of Colloidal Science Volume 6, pp 162-170.

Owens D.K. and Wendt R.C., (1969), "*Estimation of surface free energy of polymers*". Journal of Applied Polymer Science 12, pp1741–1747.

Puzinauskas V. P., (1968), "*Filler in Asphalt Mixtures*", Proceedings of the Association of Asphalt Paving Technologists Volume 13.

Read J.M. and Whiteoak C.D, *"The Shell Bitumen Handbook",* Fifth Edition, ISBN 0-7277-3220-X, 2003.

Richardson C., (1907), *"The Modern Asphalt Pavement"*, John Wiley and Sons, New York

Rides M., (2005), *"Rheological characterisation of filled materials: a review"*, National Physical Laboratory Report DPEC-MPR 013, UK.

Rigden D. J., (1947), "*The use of fillers in bituminous road surfacings*", Journal of the Society of Chemical Industry, Volume 66.

Rigden D. J., (1954), "*Road Research Technical Paper No.28*.", Road Research Laboratory, Hammondsworth, Middlesex, HMSO, London 1954.

Sanders P. and Nunn M., (2005), *"The application of enrobé a module élevé in flexible pavements"*, Transport Research Laboratory Report 636, ISBN 1-84608-653-3.

Shashidhar N. and Romero P., (1998), *"Factors affecting the stiffening potential of mineral fillers"*, Transportation Research Record Volume 1638, Transportation Research Board of the National Academies, ISSN 0361-1991.

Taherkhani H., and Collop A.C., (2006), *"Creep and recovery testing of pure bitumen using dynamic shear rheometer"*, 7th International Congress on Civil Engineering, Tehran, Iran.

Tunnicliffe D. G., (1967), "*A Review of Mineral Filler*", Proceedings of the Asphalt Paving Technologists Volume 36.

Wilhelmy L., (1863), *"Uber die Abhangigkeit der Capillaritats-Constanten des Alkohols von Substanz und Gestalt des benetzten festen Korpers,"*Ann. Phys., Vol. 119, p. 177

Wypych G., (1999), *"Handbook of Fillers"*, ISBN 1-895198 19-4, ChemTec Publishing, Toronto, Canada

Young T., (1805), Phil. Trans. Royal Society (London), 95, 65

BIBLIOGRAPHY

Aggregates for bituminous mixtures and surface treatments for roads, airfields and other trafficked areas, BS EN 13043:2002, BSI, London.

Bitumen and bituminous binders - Determination of complex shear modulus and phase angle - Dynamic Shear Rheometer (DSR), BS EN 14770:2006, BSI, London

Determination of softening point of bituminous materials, BS EN 1427:2000, BS2000-58, BSI, London.

Determination of the specific surface area of powders, Part 1: BET method of gas adsorption for solids (including porous materials). BS 4359-1: 1996 (ISO 9277:1995) , BSI, London.

Determination of needle penetration of bitumen, BS EN 1426:2000, BS2000-49, BSI, London.

European Asphalt Pavement Association, (2004), *"Asphalt in figures, 2003"*, www.eapa.org.

NCHRP Report 459, (2001), "Characterization of modified asphalt binders in superpave mix design", Transportation Research Board, ISBN 0-309-06707-3.

Particle size analysis – Laser Diffraction Methods – Part 1: General principles BS ISO13320-1:1999, BSI, London.

Tests for Filler aggregate used in bituminous mixtures, Part 1: Delta Ring and Ball, BS EN 13179-1:2000, BSI, London.

Tests for Filler aggregate used in bituminous mixtures, Part 1: Delta Ring and Ball, BS EN 13179-1:2000, BSI, London.

Tests for Filler aggregate used in bituminous mixtures, Part 2: Bitumen number, BS EN 13179-2:2000, BSI, London.

Tests for geometrical properties of aggregates. Assessment of fines. Methylene blue test, BS EN 933-9 1999, BSI, London

Tests for geometrical properties of aggregates. Assessment of fines. Grading of fillers by air jet sieving, BS EN 933-10 2002, BSI, London.